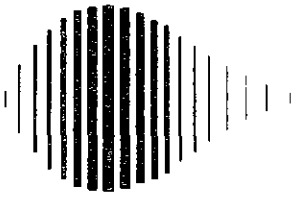

NATIONAL CENTER FOR EARTHQUAKE
ENGINEERING RESEARCH
State University of New York at Buffalo

NONNORMAL SECONDARY RESPONSE DUE TO YIELDING IN A PRIMARY STRUCTURE

by

D. C. K. Chen and L. D. Lutes
Department of Civil Engineering
Texas A&M University
College Station, Texas 77843-3136

Technical Report NCEER-90-0002

February 28, 1990

This research was conducted at Texas A&M University and was partially supported by the National Science Foundation under Grant No. ECE 86-07591.

NOTICE

This report was prepared by Texas A&M University as a result of research sponsored by the National Center for Earthquake Engineering Research (NCEER). Neither NCEER, associates of NCEER, its sponsors, Texas A&M University, nor any person acting on their behalf:

a. makes any warranty, express or implied, with respect to the use of any information, apparatus, method, or process disclosed in this report or that such use may not infringe upon privately owned rights; or

b. assumes any liabilities of whatsoever kind with respect to the use of, or the damage resulting from the use of, any information, apparatus, method or process disclosed in this report.

50272-101

REPORT DOCUMENTATION PAGE	1. REPORT NO. NCEER-90-0002	2. PB90-251976

4. Title and Subtitle
Nonnormal Secondary Response Due to Yielding in a Primary Structure

5. Report Date
February 28, 1990

6.

7. Author(s)
D.C.K. Chen and L.D. Lutes

8. Performing Organization Rept. No.

9. Performing Organization Name and Address

10. Project/Task/Work Unit No.

11. Contract(C) or Grant(G) No.
(C) 88-2013
ECE 86-07591
(G)

12. Sponsoring Organization Name and Address
National Center for Earthquake Engineering Research
State University of New York at Buffalo
Red Jacket Quadrangle
Buffalo, New York 14261

13. Type of Report & Period Covered
Technical Report

14.

15. Supplementary Notes

This research was conducted at Texas A&M University and was partially supported by the National Science Foundation under Grant No. ECE 86-07591

16. Abstract (Limit: 200 words)

Response nonnormality is investigated for a linear secondary system which is mounted on a yielding primary structure subjected to a normally distributed ground acceleration. The nonlinearity considered in the primary structure is bilinear hysteretic (BLH) yielding. The coefficient of excess (COE), which is a normalized fourth cumulant function, is used as a measure of the nonnormality in the current study. This work is a followup to an earlier study in which it was demonstrated that the response acceleration of the primary system can be significantly nonnormal in some situations. Linear substitute methods are used for analytically evaluating the nonnormality of secondary response. The basic concept is to use a linear model with nonnormal excitation to replace the nonlinear primary element with normal excitation, with the goal of matching the trispectrum for the acceleration of these two systems. A two filters model (with a more narrowband fourth cumulant filter) gives good approximations for the COE values of secondary response in most cases including both cascade and noncascade analysis. The probability of failure from either first-passage or fatigue is investigated for secondary response affected by nonnormality. It is shown that the nonnormality effect generally is more significant for first-passage failure than for fatigue failure based on the cases in this study, and both failure modes can be significantly affected by the nonnormality in some situations.

17. Document Analysis a. Descriptors

b. Identifiers/Open-Ended Terms
EARTHQUAKE ENGINEERING
LINEAR SECONDARY SYSTEMS
RESPONSE NONNORMALITY
STRUCTURAL RELIABILITY
FIRST PASSAGE FAILURE
FATIGUE FAILURE
GROUND ACCELERATION

c. COSATI Field/Group

Availability Statement
Release Unlimited

19. Security Class (This Report)	21. No. of Pages
Unclassified	130
20. Security Class (This Page)	22. Price

NONNORMAL SECONDARY RESPONSE DUE TO YIELDING IN A PRIMARY STRUCTURE

by

D.C.K. Chen[1] and L.D. Lutes[2]

February 28, 1990

Technical Report NCEER-90-0002

NCEER Project Number 88-2013

NSF Master Contract ECE 86-07591

1 Research Associate, Department of Civil Engineering, Texas A&M University
2 Professor, Department of Civil Engineering, Texas A&M University

NATIONAL CENTER FOR EARTHQUAKE ENGINEERING RESEARCH
State University of New York at Buffalo
Red Jacket Quadrangle, Buffalo, NY 14261

PREFACE

The National Center for Earthquake Engineering Research (NCEER) is devoted to the expansion and dissemination of knowledge about earthquakes, the improvement of earthquake-resistant design, and the implementation of seismic hazard mitigation procedures to minimize loss of lives and property. The emphasis is on structures and lifelines that are found in zones of moderate to high seismicity throughout the United States.

NCEER's research is being carried out in an integrated and coordinated manner following a structured program. The current research program comprises four main areas:

- Existing and New Structures
- Secondary and Protective Systems
- Lifeline Systems
- Disaster Research and Planning

This technical report pertains to the second program area and, more specifically, to secondary systems.

In earthquake engineering research, an area of increasing concern is the performance of secondary systems which are anchored or attached to primary structural systems. Many secondary systems perform vital functions whose failure during an earthquake could be just as catastrophic as that of the primary structure itself. The research goals in this area are to:

1. Develop greater understanding of the dynamic behavior of secondary systems in a seismic environment while realistically accounting for inherent dynamic complexities that exist in the underlying primary-secondary structural systems. These complexities include the problem of tuning, complex attachment configuration, nonproportional damping, parametric uncertainties, large number of degrees of freedom, and nonlinearities in the primary structure.
2. Develop practical criteria and procedures for the analysis and design of secondary systems.
3. Investigate methods of mitigation of potential seismic damage to secondary systems through optimization or protection. The most direct route is to consider enhancing their performance through optimization in their dynamic characteristics, in their placement within a primary structure or in innovative design of their supports. From the point of view of protection, base isolation of the primary structure or the application of other passive or active protection devices can also be fruitful.

Current research in secondary systems involves activities in all three of these areas. Their interaction and interrelationships with other NCEER programs are illustrated in the accompanying figure.

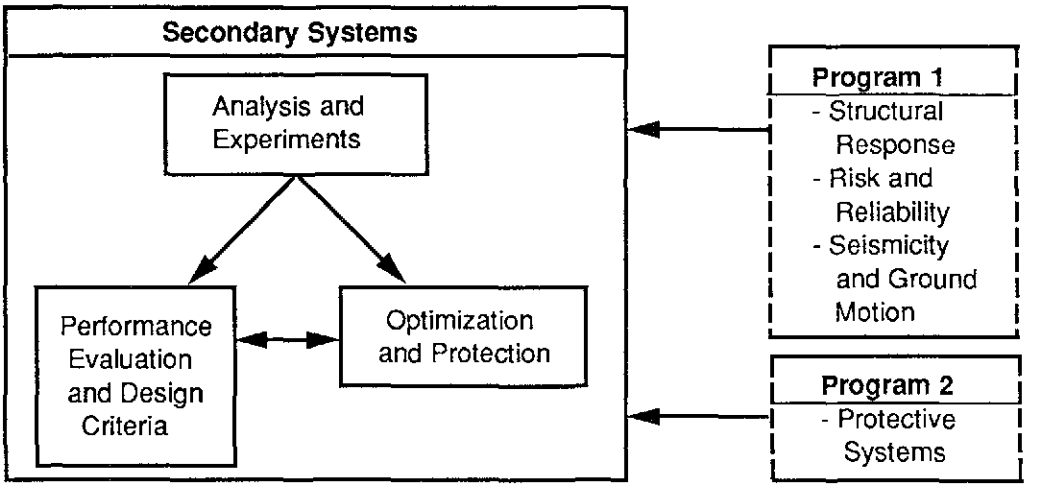

Response nonnormality has shown to significantly affect structural reliability based on first-passage failure or fatigue failure. In an earlier report (NCEER-88-0030), the authors have considered this nonnormality effect on the absolute acceleration of a primary structure. The study presented in this report focuses on the nonnormality of the relative displacement of a secondary system which is attached to a yielding primary structure. In particular, the probability of failure in the first-passage failure mode as well as in the fatigue mode of the secondary system is carefully examined.

ABSTRACT

Response nonnormality is investigated for a linear secondary system which is mounted on a yielding primary structure subjected to a normally distributed ground acceleration. The nonlinearity considered in the primary structure is bilinear hysteretic (BLH) yielding. The coefficient of excess (COE), which is a normalized fourth cumulant function, is used as a measure of the nonnormality in the current study. This work is a follow-up to an earlier study in which it was demonstrated that the response acceleration of the primary system can be significantly nonnormal in some situations.

Linear substitute methods are used for analytically evaluating the nonnormality of secondary response. The basic concept is to use a linear model with nonnormal excitation to replace the nonlinear primary element with normal excitation, with the goal of matching the trispectrum for the acceleration of these two systems. A two filters model (with a more narrowband fourth cumulant filter) gives good approximations for the COE values of secondary response in most cases including both cascade and noncascade analysis.

The probability of failure from either first-passage or fatigue is investigated for secondary response affected by nonnormality. It is shown that the nonnormality effect generally is more significant for first-passage failure than for fatigue failure based on the cases in this study, and both failure modes can be significantly affected by the nonnormality in some situations.

TABLE OF CONTENTS

TABLE OF CONTENTS

LIST OF ILLUSTRATIONS

LIST OF TABLES

SECTION I

INTRODUCTION

The term secondary systems is often used to describe various nonstructural elements, such as piping in industrial structures, computer systems in buildings, drilling and exploration equipment on offshore plateforms, communication and control devices on space vehicles, etc. Such subsystems often play critical roles in maintaining the operation or safety of the primary subsystem to which they are attached, particularly in the event of extreme loads. Hence, some secondary systems must be designed to survive being subjected to the vibratory effects of an earthquake induced ground motion which is transmitted to such a subsystem through its supporting primary structure.

The theory of the dynamic response of linear primary-secondary (P-S) systems is quite well developed [Newmark 1972, Scanlan and Sachs 1977, Sackman and Kelly 1979, Singh 1980, Der Kiureghian et al. 1983, Igusa and Der Kiureghian 1985, Asfura and Der Kiureghian 1986, Holung, Cai and Lin 1987, Suarez and Singh 1989]. Unfortunately, structural systems under dynamic loading often exhibit nonlinear behavior before serious damage occurs. The response of a nonlinear system, even under normal excitation, is not normal and this nonnormality can seriously alter the response behavior. However, few studies of nonnormality have been done in the past due to the analytical complexity and difficulty [Lin and Mahin 1985]. Some recent studies of fatigue damage accumulation [Hu 1982; Lutes et al. 1984; Winterstein 1985] and of first-passage failure [Grigoriu 1984] have shown that these two important quantities can be significantly affected by nonnormality of

the random process studied. This is not surprising since the normal models may significantly misrepresent the frequency of high response levels. Such nonnormality is particularly likely to occur in a situation involving significant nonlinearity, like the yielding effect in a hysteretic system.

A simple and natural way to include nonnormality in the analysis of a random variable is through consideration of moments higher than the second. In particular, the fourth moments are important for characterizing nonnormality (especially if the random variable is symmetric about its mean value so that the third moment gives no new information). In this study, the kurtosis or the coefficient of excess (COE) (i.e. kurtosis minus 3) will serve as the index to represent the degree of nonnormality of a random process.

This study investigates a simple nonlinear primary-secondary situation in which a very light secondary system is attached to a yielding single-degree-of-freedom (SDOF) bilinear hysteretic (BLH) primary structure. The nonnormality results only from the nonlinearity of the primary structure. The reasons for using such a simple model are that not only is it easy to analyze but also it may fairly accurately represent practical design situations. The use of a SDOF primary system may be justified by the fact that the first mode of the primary system is often of the most interest [US Nuclear Regulatory Guide 1975]. Since the secondary system is usually much less massive than the primary, it is commonly assumed that it does not affect the response of the primary structure. This implies that they can be analyzed as two independent or decoupled sub-systems. This is called cascade analysis and it has been widely used in many applications. Cascade analysis is very desirable, when it is justified, since it greatly simplifies the analytical work and also gives

better intuitive understanding of the system. Both cascade analysis and primary-secondary interaction will be considered in this study. The excitation of the primary system will be taken to be a normal white ground acceleration.

In order to analytically investigate the nonnormal response of the linear secondary system it is necessary to know the four-dimensional fourth cumulant function for its nonnormal base excitation, which is the primary absolute acceleration. Another form of this same information is the trispectrum, which is the triple Fourier transform of the fourth cumulant function. The COE of the nonnormal primary absolute acceleration was investigated in an earlier phase of this study [Chen and Lutes 1988] and those results will be extended here to include the trispectrum. Finally, the response of the secondary system to the nonnormal primary acceleration will be studied.

A linear substitute method will be proposed for analytically approximating the COE values of the secondary response. The basic approach will be to use a linear model with nonnormal excitation to replace the BLH primary element with normal excitation. The goal will be the matching of the trispectrum for primary acceleration of the substitute linear model to that of the BLH primary system. The choice of the linear filter will be based on the fitting of the power spectral density, and the nonnormal delta correlated excitation will be chosen to achieve matching of the COE of primary acceleration. The trispectrum, which is the Fourier transform of the fourth cumulant function, will also be used as a tool in investigating the acceptability of the linear substitute models. The philosophy in developing the analytical models is to be as simple as possible while providing a good estimate, and also providing intuitive insights regarding the P-S system. The method will

be shown to be appropriate for both cascade and noncascade analysis. Noncascade situations will be investigated with the mass of the secondary system equal to 0.1% and 1% of that of the primary system.

The effects of nonnormality on reliability will be investigated for both first-passage failure and fatigue failure of the secondary system. A nonnormality correction factor (NCF), which is equal to the ratio of the expected life for a Gaussian process to the expected life for the corresponding non-Gaussian process, will be used as the index of the influence of nonnormality. Results will be presented from simple approximations which depend only on the COE of the response. It will be shown that the reliability of the secondary system can sometimes be very significantly affected by yielding in the primary system. This is particularly true for reliability against first-passage failure.

SECTION II

BACKGROUND ON NONNORMALITY

II-1 Description of Random Processes:

A random process is a parametered family of random variables with the parameter (or parameters), belonging to an indexing set (or sets) [Lin, 1976]. In this study, the indexing parameter is time. Hence, a random process can be described as a family of random variables, $\{X(t) : t \in T\}$. Let the indexing set T be discrete, then the probability structure can be defined by the joint probability density function of n random variables as $p_{X_1 X_2 \cdots X_n}(x_1, x_2, \ldots x_n,)$ where $X_j = X(t_j)$. Alternatively, the probability structure also may be decribed by the joint characteristic function,

$$\Theta(u_1, t_1; \ldots; u_n, t_n) = E[\exp(iu_1 X_1 + \cdots + iu_n X_n)] \tag{2.1}$$

in which $E[\cdot]$ means expected value. Note that any lower order joint probability function or characteristic function can be obtained if a higher order one is known.

In many situations it is impractical and/or impossible to work with a complete description of a random process in terms of probability density functions or characteristic functions. One of the most common ways of giving a useful partial description of a process is in terms of moments. Let the order r moment function be written as

$$m_r(t_1, t_2, \ldots, t_r) = E[X_1 X_2 \cdots X_r] \tag{2.2}$$

This can be written as an integral using the order r probability density, or as a derivative of the characteristic function :

$$m_r(t_1,\ldots,t_r) = \frac{1}{i^r}\frac{\partial^r \Theta(u_1,t_1;\ldots;u_n,t_r)}{\partial u_1 \cdots \partial u_r}\bigg|_{u_1=\cdots=u_r=0} \tag{2.3}$$

An alternative way to present the information contained in the first n moment functions is in the form of the first n cumulants functions, where the rth cumulant is given by

$$k_r(t_1,\ldots,t_r) = \frac{1}{i^r}\frac{\partial^r \ln \Theta(u_1,t_1;\ldots;u_r,t_r)}{\partial u_1 \cdots \partial u_r}\bigg|_{u_1=\cdots=u_r=0} \tag{2.4}$$

The term $\ln \Theta(u_1,\ldots,u_r)$ is called the log-characteristic function.

Stratonovich [1963] noted that the cumulant functions involving distinct values of time related to correlations of the process at those particular times. Thus, cumulant functions are also called "correlation funtions". It may be noted that the lower order cumulant functions are simply related to the moment functions. For a zero mean process, in particular, $k_1 = 0, k_2 = m_2$ and $k_3 = m_3$. For r=4, however, the relation is not quite so simple, since

$$\begin{aligned} k_4(t_1,t_2,t_3,t_4) =& m_4(t_1,t_2,t_3,t_4) - m_2(t_1,t_2)m_2(t_3,t_4) \\ & - m_2(t_1,t_3)m_2(t_2,t_4) - m_2(t_1,t_4)m_2(t_2,t_3) \end{aligned} \tag{2.5}$$

II-1-1 Frequency Decomposition of a Stationary Process:

A random process is said to be stationary if its probability density functions

are invariant under a shift of the time scale. For a stationary process $m_2(t_1, t_2)$ and $k_2(t_1, t_2)$ are functions only of $t_2 - t_1$, and similarly $m_4(t_1, t_2, t_3, t_4)$ and $k_4(t_1, t_2, t_3, t_4)$ are functions of three time arguments, which can be chosen as $t_2 - t_1, t_3 - t_1$, and $t_4 - t_1$. Let

$$C_r(\tau_1, \tau_2, \ldots, \tau_{r-1}) = k_r(t_1, t_2, \ldots, t_r) \tag{2.6}$$

in which $\tau_j = t_{j+1} - t_1$. For the special cases of r=2 and r=4, these can be written as

$$R(\tau) = C_2(\tau) = k_2(t_1, t_2) \tag{2.7a}$$

and

$$Q(\tau_1, \tau_2, \tau_3) = C_4(\tau_1, \tau_2, \tau_3) = k_4(t_1, t_2, t_3, t_4) \tag{2.7b}$$

The Fourier transform of $R(\tau)$, and its inverse, are given by

$$S(\omega) = \frac{1}{2\pi} \int_{-\infty}^{\infty} R(\tau) \exp^{-i\omega\tau} \, d\tau \tag{2.8}$$

and

$$R(\tau) = \int_{-\infty}^{\infty} S(\omega) \exp^{i\omega\tau} \, d\omega \tag{2.9}$$

where $S(\omega)$ is called the power spectral density (or power spectrum) of the random process. It can be shown that $S(\omega)$ is a non-negative, even function of ω.

Analogous to eq. 2.9, a frequency decomposition of $Q(\tau_1, \tau_2, \tau_3)$ can be made in the following way

$$Q(\tau_1,\tau_2,\tau_3) = \int\int\int_{-\infty}^{\infty} D(\omega_1,\omega_2,\omega_3)\exp^{i(\omega_1\tau_1-\omega_2\tau_2+\omega_3\tau_3)}\,d\omega_1 d\omega_2 d\omega_3 \qquad (2.10)$$

where $D(\omega_1,\omega_2,\omega_3)$ is a three-dimensional Fourier transformation of $Q(\tau_1,\tau_2,\tau_3)$ and is called trispectral density:

$$D(\omega_1,\omega_2,\omega_3) = \frac{1}{(2\pi)^3}\int\int\int_{-\infty}^{\infty} Q(\tau_1,\tau_2,\tau_3)\exp^{-i(\omega_1\tau_1+\omega_2\tau_2+\omega_3\tau_3)}\,d\tau_1 d\tau_2 d\tau_3 \qquad (2.11)$$

II-1-2 Properties of Trispectral Density:

It is clear that exchanging any two arguments in $k_4(t_1,t_2,t_3,t_4)$ will not change the value of k_4. Thus, the symmetry of k_4 is simply that the cumulant is the same for each of the 24 permutations of the four arguments :

$$\begin{aligned} k_4(t_1,t_2,t_3,t_4) &= k_4(t_2,t_1,t_3,t_4) \\ &= k_4(t_3,t_2,t_1,t_4) \\ &= k_4(t_4,t_2,t_3,t_1) \\ &= \cdots \end{aligned} \qquad (2.12)$$

Rewriting eq. 2.12, the symmetry of a stationary fourth cumulant function, $Q(\tau_1,\tau_2,\tau_3)$, will be

$$
\begin{aligned}
Q(\tau_1,\tau_2,\tau_3) =& Q(-\tau_1,\tau_2-\tau_1,\tau_3-\tau_1)\\
=& Q(\tau_1-\tau_2,-\tau_2,\tau_3-\tau_2)\\
=& Q(\tau_1-\tau_3,\tau_2-\tau_3,-\tau_3)\\
=& Q(\tau_2,\tau_1,\tau_3)\\
=& \cdots
\end{aligned}
\tag{2.13}
$$

Therefore, there are also 24 symmetrical points in $Q(\tau_1,\tau_2,\tau_3)$.

On the frequency domain, the symmetry of $D(\omega_1,\omega_2,\omega_3)$ can be obtained similarly by taking the Fourier transformation of each term in eq. 2.13 which gives

$$
\begin{aligned}
D(\omega_1,\omega_2,\omega_3) =& D(-\omega_1-\omega_2-\omega_3,\omega_2,\omega_3)\\
=& D(\omega_1,-\omega_1-\omega_2-\omega_3,\omega_3)\\
=& D(\omega_1,\omega_2,-\omega_1-\omega_2-\omega_3)\\
=& D(\omega_2,\omega_1,\omega_3)\\
=& \cdots
\end{aligned}
\tag{2.14}
$$

In general, for the stationary mth cumulant function, which is a function of m-1 arguments, there are m! symmetrical points in D as well as in Q. In particular, D is the same when its three arguments are any choice of three values, in any order, from the set $\{\omega_1,\omega_2,\omega_3,-\omega_1-\omega_2-\omega_3\}$.

It can be seen from eq. 2.11 that the D function is usually complex even though Q is always real. Also it can be noted that $D(\omega_1,\omega_2,\omega_3)$ and $D(-\omega_1,-\omega_2,-\omega_3)$ are always a complex conjugate pair. That is,

$$D(-\omega_1, -\omega_2, -\omega_3) = D^*(\omega_1, \omega_2, \omega_3) \tag{2.15}$$

in which the star denotes complex conjugate. Similar relationships which can be found are

$$\begin{aligned} D(-\omega_1, -\omega_2, \omega_3) &= D^*(\omega_1, \omega_2, -\omega_3) \\ D(-\omega_1, \omega_2, -\omega_3) &= D^*(\omega_1, -\omega_2, \omega_3) \\ &\cdots \end{aligned} \tag{2.16}$$

Finally, it should be noted that there are certain planes within the frequency domain on which D is always real. In particular, $D(\omega_1, -\omega_1, \omega_3)$ is real for all (ω_1, ω_3) values since $D^*(\omega_1, -\omega_1, \omega_3) = D(\omega_1, -\omega_1, \omega_3)$, from the complex conjugate and symmetry properties given above. Of course, there are another five identical planes within other octants in this three dimensional space.

II-1-3 Degree of Nonnormality :

The physical significance of multiple correlations (i.e., correlations between several different random variables) decreases when the order increases. Hence the first few cumulant functions are most important in describing a random process. Many physical problems have small values of the higher order cumulant functions. In fact, for a normal process they are exactly zero for order greater than two. Thus, a simple and natural way to include nonnormality in the analysis of a random variable is through consideration of moments higher than the second. In particular, the fourth cumulant is important for characterizing nonnormality (especially if the

random variable is symmetric about its mean value so that the third cumulant gives no new information). However, in practice, it is not always easy to see the degree of nonnormality of a process directly from the fourth order cumulant function because of the multidimensional nature of that function.

In this study, the coefficient of excess (COE), a special case of normalized fourth cumulant function, will serve as the index to represent the degree of nonnormality of a random process. The COE is a normalized one-dimensional form of $k_4(t_1, t_2, t_3, t_4)$ corresponding to $t_1 = t_2 = t_3 = t_4$, which is same as $Q(0,0,0)$:

$$\begin{aligned} COE &= \frac{Q(0,0,0)}{\sigma^4} = \frac{k_4(t,t,t,t)}{\sigma^4} \\ &= Kurtosis - 3 \end{aligned} \tag{2.17}$$

where σ is the root-mean-square value.

For a normal distribution, the COE is equal to zero (i.e. kurtosis=3). When the COE is greater than zero, it means that more probability mass is in the tails of the distribution than for a corresponding normal distribution. If the COE is less than zero, it shows that there is less probability in the tails, giving what may be called an amplitude-limited type distribution. Note, though, that the COE only relates to each individual X_j random variable, whereas the more general fourth cumulant relates to the joint distribution of up to four such random variables.

II-2 Response of SDOF Linear System with Nonnormal Excitation:

The second order differential equation governing the motion of a typical mass-

spring-dashpot system will be

$$m\ddot{x} + c\dot{x} + kx = f = mp \tag{2.18}$$

in which m, c and k are mass, damping and stiffness of the system respectively, and p is the negative of the base acceleration. Eq. 2.18 can be rewritten as the so-called standard form

$$\ddot{x} + 2\beta_0\omega_0\dot{x} + \omega_0^2 x = p \tag{2.19}$$

where $\omega_0^2 = k/m$, is the undamped natural frequency, and $\beta_0 = c/2\omega_0 m$, is the ratio of the actual damping to the critical damping. It is assumed that p is a zero-mean random process so that the response is also random with zero-mean. Other terms are taken to be deterministic.

We shall assume that the random excitation begins at t=0, so that the response of the system can be expressed as a Duhamel integral as

$$x(t) = \int_0^\infty p(\tau)h(t-\tau)d\tau \tag{2.20}$$

or in the frequency domain as

$$x(t) = \int_{-\infty}^{\infty} \bar{p}(\omega)H(\omega)\exp(i\omega t)d\omega \tag{2.21}$$

where

$$\tilde{p}(\omega) = \frac{1}{2\pi} \int_0^\infty p(t) \exp(-i\omega t) dt$$

The function $h(t)$ is called the impulse response function of the system, and can be written as

$$h(t) = \begin{cases} \frac{1}{\omega_d} \exp(-\beta_0 \omega_0 t) \sin(\omega_d t) & \text{if } t \geq 0 \\ 0 & \text{if } t < 0 \end{cases} \tag{2.22}$$

in which $\omega_d = \omega_0 \sqrt{1 - \beta_0^2}$, the damped natural frequency of the system. The corresponding frequency response function is the Fourier transformation of the impulse response function:

$$H(\omega) = \int_{-\infty}^{\infty} h(t) \exp(-i\omega t) dt = \frac{1}{(\omega_0^2 - \omega^2) + i2\beta_0 \omega_0 \omega} \tag{2.23}$$

The cumulant function of the response can be expressed in terms of the cumulant of the excitation and the impulse response function as

$$\begin{aligned} k_x(t_1, t_2, \cdots, t_n) = \int_0^{t_n} \cdots \int_0^{t_1} & k_p(\tau_1, \tau_2, \cdots, \tau_n) \\ & h(t_1 - \tau_1) h(t_2 - \tau_2) \cdots h(t_n - \tau_n) d\tau_1 d\tau_2 \cdots d\tau_n \end{aligned} \tag{2.24}$$

where k_x and k_p are order n cumulant functions of response and excitation, respectively; and use has been made of the fact that $h(t - \tau) = 0$ for $t < \tau$. Equation 2.24 shows how knowledge of cumulant functions of excitation can be used to obtain corresponding cumulant functions of response by linear operations.

II-2-1 Stationary Processes:

For a stationary excitation, since the probability distributions are invariant under a shift of the time scale, the nth order cumulant function of response will be a function of only n-1 time arguments. Using $\tau_j = t_{j+1} - t_1$ gives

$$C_x(\tau_1, \tau_2, \cdots, \tau_{n-1}) = \int_0^\infty \cdots \int_0^\infty C_p(\nu_1, \nu_2, \cdots, \nu_{n-1}) \\ h(\nu)h(\nu - \tau_1 - \nu_1) \cdots h(\nu + \tau_{n-1} - \nu_{n-1}) d\nu d\nu_1 \cdots d\nu_{n-1} \tag{2.25}$$

Similarly in the frequency domain, the n-1 dimensional spectral density of response has the following relationship with the n-1 dimensional spectral density of excitation:

$$D_x(\omega_1, \omega_2, \cdots, \omega_{n-1}) = H(\omega_1)H(\omega_2) \cdots H(\omega_{n-1})H(-\sum_{j=1}^{n-1} \omega_j) \\ D_p(\omega_1, \omega_2, \cdots, \omega_{n-1}) \tag{2.26}$$

in which $D(\omega_1, \omega_2, \ldots, \omega_{n-1})$ is the n-1 dimensional generalization of the trispectral density $D(\omega_1, \omega_2, \omega_3)$ in eqs. 2.10 and 2.11. (Recall that the n-1 dimensional spectral density function is the Fourier transformation of the corresponding stationary nth order cumulant function.)

Note that if $p(t)$ is Gaussian, than $x(t)$ is also Gaussian. Then only the first two cumulants are non-zero and all other higher cumulants vanish. When n=2, the second cumulant function, $R_x(\tau)$ of response, can be expressed in terms of the cumulant of the excitation, $R_p(\tau)$ and the impulse function as

$$R_x(\tau) = \int_0^\infty \int_0^\infty R_p(\tau + \nu_1 - \nu_2) h(\nu_1) h(\nu_2) d\nu_1 d\nu_2 \tag{2.27}$$

The spectral density of response is given by

$$S_x(\omega) = S_p(\omega)\ H(\omega)|^2 \tag{2.28}$$

If $p(t)$ is not Gaussian, higher cumulants exist. The third cumulant won't give any new information if the probability distribution is symmetric. The fourth cumulant function of response, n=4, can be found as

$$Q_x(\tau_1, \tau_2, \tau_3) = \int\int\int\int_0^\infty Q_p(\tau_1 + \nu_1 - \nu_4, \tau_2 + \nu_2 - \nu_4, \tau_3 + \nu_3 - \nu_4) \\ h(\nu_1) h(\nu_2) h(\nu_3) h(\nu_4) d\nu_1 d\nu_2 d\nu_3 d\nu_4 \tag{2.29}$$

and

$$D_x(\omega_1, \omega_2, \omega_3) = H(\omega_1) H(\omega_2) H(\omega_3) H(-\omega_1 - \omega_2 - \omega_3) D_p(\omega_1, \omega_2, \omega_3) \tag{2.30}$$

II-2-2 Nonnormal Delta Correlated Excitation:

Let the excitation of eq. 2.18 be a non-Gaussian delta correlated (white noise) process for which

$$R_p(\tau) = 2\pi S_p \delta(\tau) \tag{2.31}$$

and

$$Q_p(\tau_1, \tau_2, \tau_3) = (2\pi)^3 D_p \delta(\tau_1)\delta(\tau_2)\delta(\tau_3) \tag{2.32}$$

where $\delta(\tau)$ is the Dirac delta function. Note that the constants S_p and D_p are the uniform power spectrum and uniform trispectrum of the excitation, respectively. Without loss of generality, let the mean of the excitation and the response be zero. The second cumulant or moment of response is

$$R_x(\tau) = 2\pi S_p \int_0^\infty h(\nu)h(\nu+\tau)d\nu \tag{2.33}$$

$$\begin{aligned} k_x(t,t) &= R_x(0) \\ &= 2\pi S_p \int_0^\infty h^2(\nu)d\nu \\ &= S_p \int_{-\infty}^\infty |H(\omega)|^2 d\omega \\ &= 2S_p \int_0^\infty |H(\omega)|^2 d\omega \end{aligned} \tag{2.34}$$

and the fourth cumulant of response is

$$Q_x(\tau_1, \tau_2, \tau_3) = (2\pi)^3 D_p \int_0^\infty h(\nu)h(\nu+\tau_1)h(\nu+\tau_2)h(\nu+\tau_3)d\nu \tag{2.35}$$

$$
\begin{aligned}
k_x(t,t,t,t) &= Q_x(0,0,0) \\
&= (2\pi)^3 D_p \int_0^\infty h^4(\nu) d\nu \\
&= \int\int\int_{-\infty}^{\infty} D_x(\omega_1,\omega_2,\omega_3) d\omega_1 d\omega_2 d\omega_3 \\
&= D_p \int\int\int_{-\infty}^{\infty} H(\omega_1)H(\omega_2)H(\omega_3)H(-\sum_{j=1}^{3}\omega_j) d\omega_1 d\omega_2 d\omega_3 \\
&= 2D_p \int_0^\infty \int_0^\infty \int_0^\infty H(\omega_1)H(\omega_2)H(\omega_3)H(-\sum_{j=1}^{3}\omega_j) d\omega_1 d\omega_2 d\omega_3 \\
&+ 6D_p \int_0^\infty \int_0^\infty \int_{-\infty}^{0} H(\omega_1)H(\omega_2)H(\omega_3)H(-\sum_{j=1}^{3}\omega_j) d\omega_1 d\omega_2 d\omega_3
\end{aligned}
\tag{2.36}
$$

The COE of response will be equation 2.36 divided by equation 2.34 squared.

If the linear system in the above equations is lightly damped, then eq. 2.23 shows that $H(\omega)$ has peaks with height of $O(\beta_0^{-1})$ near $\omega = \pm\omega_0$. From eq. 2.30, it can be observed that the trispectrum of this narrowband process then has a peak near $(\omega_0, -\omega_0, \omega_0)$ and this peak has a height of $O(\beta_0^{-4})$. As mentioned in Sec II-1-2, D is real on the plane $(\omega_1, -\omega_1, \omega_3)$ and on the other five "symmetric" planes in the trispectrum. Thus, $D(\omega_0, -\omega_0, \omega_0)$ is very large and real, as are the other five peaks with equal D values in other octants. These six high peaks dominate the D function so that all other points in this three dimensional space are relatively insignificant.

II-3 Response of SDOF Nonlinear System with Normal Excitation:

An earlier report [Chen and Lutes 1988] has described both simulation and analytical studies of the nonnormality of the primary absolute acceleration (which is the base excitation of the secondary system) for a bilinear hysteretic (BLH) primary system. The model used for the analytical investigation employed a nonlinear nonhysteretic substitute primary system. This model had been suggested previously [Lutes 1970], but it was substantially improved by adjusting the damping in the substitute system to give a better balance between the energy dissipation rate and power input. Also it was extended to predict the nonnormality of the absolute acceleration of the primary response. Obtaining response moments (RMS and COE) for the substitute primary structure generally required simple numerical integration, although closed-form solutions were also obtained for simplifications appropriate to either large or small values of the yield level. Figure 2.1 shows the results from that study which are most pertinent to the current investigation.

From the numerical results the following observations were made :

1. Nonnormality of the response of a secondary system should definitely be investigated, since the absolute acceleration of the primary structure is sometimes decidedly nonnormal.
2. The most nonnormal response acceleration found was in the direction of amplitude limiting (COE$\simeq$ -1.5). Nonnormality in the opposite sense (COE$\simeq$ 1.0) was also observed, though, for smaller values of the yield level.
3. The nonhysteretic substitute system gave quite good predictions of both the RMS and COE of the acceleration response.

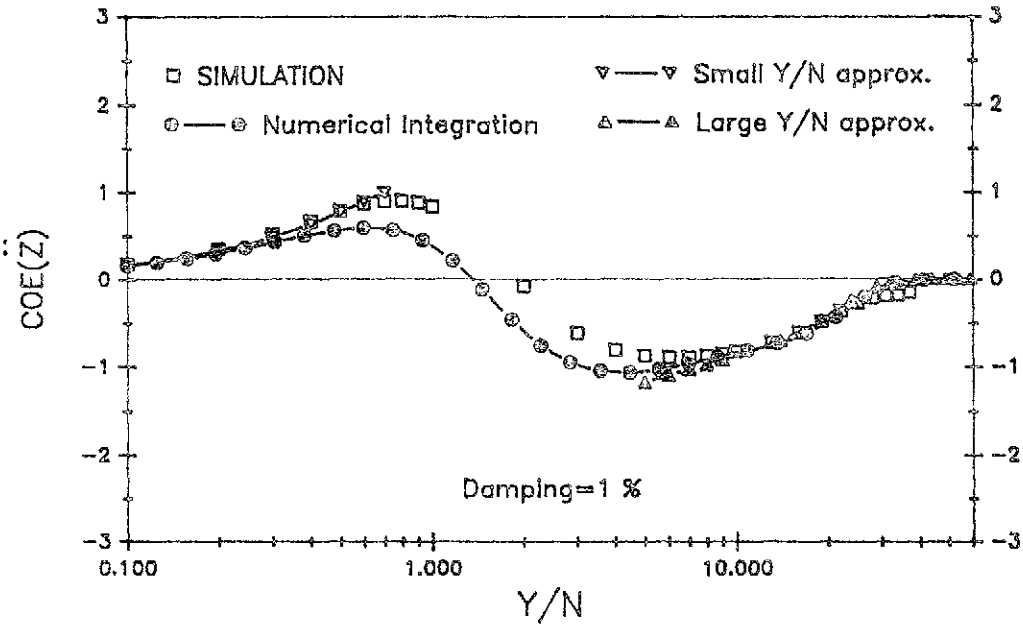

(a) α=0.5

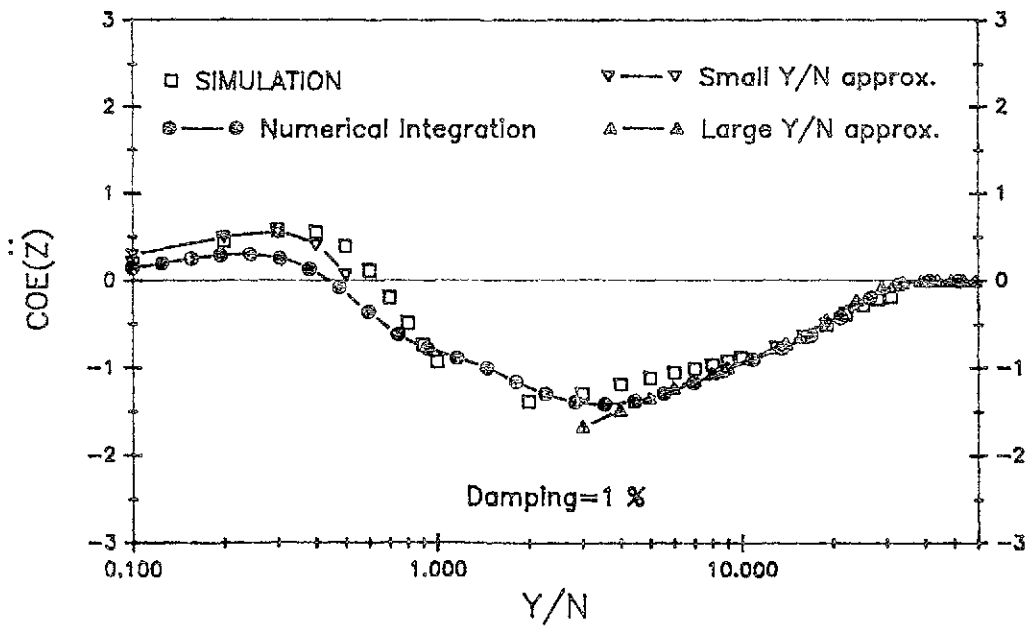

(b) α=1/21

Fig. 2.1 COE of primary absolute acceleration

II-4 Reliabilities:

Often when a dynamic system is subjected to random excitation, it is important to determine the probability that the system will not malfunction during a specific period of time. The reliability function R(T), which is the probability of nonfailure during the time interval $0 \leq t \leq T$, is therefore of central interest in many applications of random vibration theory. The two most common failure modes in civil engineering are (i) first-passage failure, and (ii) fatigue failure. The former mode may also be called first crossing failure, and it represents the situation in which failure occurs the very first time that some response quantity crosses a specified threshold. An example would be if fracture of a brittle structural member occurs the first time that the stress in the member reaches a critical level. In the fatigue failure mode, failure is due to an accumulation of many small increments of damage inflicted throughout the life of the system. In this study, general reliability estimates will be presented based on simple approximate theories. Results will be obtained using only RMS response and a normal distribution assumption, as well as by using nonnormal approximations, in which fourth order response cumulants are included. The emphasis will be on the effects of nonnormality, so other effects will be ignored. In particular, the approximations used for first-passage failure and fatigue damage will both neglect any effects due to the bandwidth of the power spectral density of the response process.

II-4-1 First-Passage Failure:

Let R(b,T) be the probability that the absolute value of the random process $\{X(t)\}$ remains below the level b at all times in the interval [0,T]. If the barrier

level b is sufficiently large then one can assume that $|X(t)|$ is sure to start below the barrier and upcrossings of b by $|X(t)|$ are independent events. This latter approximation is most accurate for a very broadband process. Bandwidth corrections could be obtained, but for simplicity they will be omitted here for both normal and nonnormal processes. Using the stated approximations for a process $\{X(t)\}$ which is symmetric about $X = 0$ gives the classic Poisson approximation :

$$R(b,T) \simeq \exp(-2\nu_b T) \tag{2.37}$$

One can then take $1 - R(b,T)$ as the cumulative distribution of the random variable representing the time until first passage. This gives first-passage time an exponential distribution and the mean time until first-passage is

$$E[T] = \frac{1}{2\nu_b} \tag{2.38}$$

The term ν_b is the stationary unconditional expected rate of upcrossing of the level b, and its value can be found from a classical result of S.O. Rice [1954] :

$$\nu_b = \int_0^\infty \dot{x} p_{X\dot{X}}(b,\dot{x}) d\dot{x} \tag{2.39}$$

If $\{X(t)\}$ is a zero mean normal process, then equation 2.39 can be simplified to :

$$\begin{aligned} \nu_b &= \frac{1}{2\pi}\frac{\sigma_{\dot{x}}}{\sigma_x}\exp(-\frac{b^2}{2\sigma_x^2}) \\ &= \nu_0 \exp(-\frac{b^2}{2\sigma_x^2}) \end{aligned} \tag{2.40}$$

in which $\sigma_{\dot{x}}$ and σ_x are the standard deviation of X and $\dot{X}$ and ν_0 is ν_b for $b = 0$.

If X(t) is not normal, then equation 2.39 cannot be integrated easily and the procedure of obtaining ν_b may become quite complicated. However, various alternative simplifying approximations can be made [Winterstein 1988]. One such approximation is of the form

$$\frac{\nu_x}{\nu_0} = \frac{p_X(x)}{p_X(0)} \tag{2.41}$$

This expression is precisely correct for the situation in which $X(t)$ and $\dot{X}(t)$ are independent. Note that they must be uncorrelated for a stationary process but they are usually not independent for a nonnormal process. Nonetheless, this approximation has been found to often give quite good results. There are several possible ways to approximate the ratio of probability densities in equation 2.41 based only on knowledge of a few moments of X. The Charlier and Edgeworth series [Crandall, 1980] are probably best known, but they have certain difficulties (including negative probability density values) which do not appear in an alternate approach introduced by Winterstein [1988]. Let U be a standardized normal distribution and $g(\cdot)$ be a function such that $X = g(U)$ has the desired nonnormal distribution. Then the probability density function of X can be written as

$$p_X(x) = \frac{1}{\sqrt{2\pi}} \exp[-\frac{1}{2}u^2(x)] \ \frac{du(x)}{dx} \tag{2.42}$$

and substituting this into the approximation of eq. 2.41 gives

$$\frac{\nu_x}{\nu_0} = \exp[-\frac{u^2(x)}{2}] \frac{du(x)}{dx} \tag{2.43}$$

Polynomials will be used to obtain appropriate $u(x)$ functions to use in these equations, but it is necessary to consider separately the two different nonnormal situations depending on the sign of COE(X).

When $COE(X) < 0$, then u versus x is concave upward and $u(x) \equiv g^{-1}(x)$ can be readily approximated by a monotonically increasing polynomial. A convenient form to use is an expansion in Hermite polynomials :

$$u(x) = g^{-1}(x) = x_0 - \sum_{n=3}^{N} h_n He_{n-1}(x_0) \tag{2.44}$$

in which x_0 for the symmetric X is simply x/σ_X. The Hermite polynomial of degree n, $He_n(x_0)$, is defined as a function which satisfies the relationship given by,

$$\frac{d^n}{dx_0^n} \exp(-x_0^2/2) = (-1)^n He_n(x_0) \exp(-x_0^2/2) \qquad n = 0, 1, 2, \ldots \tag{2.45}$$

and this yields lower order polynominals of : $He_0(x_0) = 1$, $He_1(x_0) = x_0$, $He_2(x_0) = x_0^2 - 1$, $He_3(x_0) = x_0^3 - 3x_0$, $He_4(x_0) = x_0^4 - 6x_0^2 + 3$, etc.. The coefficients h_n can be determined from

$$h_n = \frac{1}{n!} E[He_n(x_0)] \tag{2.46}$$

so that : $h_0 = 1$, $h_1 = E[X_0] = 0$, $h_2 = \frac{1}{2!}E[X_0^2 - 1] = 0$, $h_3 = \frac{1}{3!}E[X_0^3] = 0$, $h_4 = \frac{1}{4!}E[X_0^4 - 3] = \frac{1}{4!}COE[X_0]$, etc.. Note that h_n for the leading term of the summation in eq. 2.44 is negative so that the u versus x is concave upward.

When $COE(X) > 0$, then u versus x is convex upward so that a monotone transformation is obtained by taking $g(U)$ be in the form of a Hermite polynomial:

$$\begin{aligned} \frac{X - m_X}{\sigma_X} = X_0 = g(U) &= k\left[U + \sum_{n=3}^{N} \hat{h}_n He_{n-1}(U)\right] \\ &= k\left[U + \hat{h}_3(U^2 - 1) + \hat{h}_4(U^3 - 3U) + \cdots\right] \end{aligned} \tag{2.47}$$

in which k is a scaling factor ensuring that $X_0(t)$ has unit variance and its value can be obtained from the "second-order" approximation [Winterstein, 1987] :

$$k = \left[1 + \sum_{n=3}^{N} (n-1)!\hat{h}_n^2\right]^{-1/2} = (1 + 2\hat{h}_3^2 + 6\hat{h}_4^2)^{-1/2} \tag{2.48a}$$

The coefficient $\hat{h}_n$ can be expressed in terms of the corresponding Hermite moment h_n of eq. 2.46 as

$$\hat{h}_4 = \frac{\sqrt{1 + 36h_4} - 1}{18} = \frac{\sqrt{1 + 1.5(\chi_4 - 3)} - 1}{18} \tag{2.48b}$$

$$\hat{h}_3 = \frac{h_3}{1 + 6\hat{h}_4} = \frac{\lambda_3}{4 + 2\sqrt{1 + 1.5(\chi_4 - 3)}} \tag{2.48c}$$

By inverting eq. 2.47, $u(x)$ can be found as

$$u(x) = \left[\sqrt{\xi^2(x) + c} + \xi(x)\right]^{1/3} - \left[\sqrt{\xi^2(x) + c} - \xi(x)\right]^{1/3} - a \tag{2.49}$$

where

$$\xi(x) = 1.5b\left(a + \frac{x - m_X}{k\sigma_X}\right) - a^3$$

in terms of the constants $a = \frac{\hat{h}_3}{3\hat{h}_4}$, $b = \frac{1}{3\hat{h}_4}$, and $c = (b - 1 - a^2)^3$.

Let the nonnormality correction factor (NCF) of first-passage failure, Q, be defined as the ratio of the mean time to failure for a normal process to the mean time to failure for a corresponding nonnormal process. Employing eq. 2.38, the Q value can also be expressed in term of crossing rates as

$$\begin{aligned} Q &= \frac{\text{E(T) for normal process}}{\text{E(T) for nonnormal process}} \\ &= \frac{\nu_x}{\nu_u} \end{aligned} \tag{2.50a}$$

Note that the term ν_x/ν_u can be obtained from eq. 2.43 as simply

$$\frac{\nu_x}{\nu_u} = \frac{du(x)}{dx} \tag{2.50b}$$

Figure 2.2 illustrates the values of Q for several different COE values and for a range of x/σ_x values.

II-4-2 Fatigue Failure:

Estimates of stochastic fatigue life are based on knowledge of the S-N curve, or "fatigue curve" from constant amplitude periodic tests. Commonly, the S-N curve is approximated by a straight line on the log-log scale and the equation can be written as

$$N(S) = KS^{-m} \tag{2.51}$$

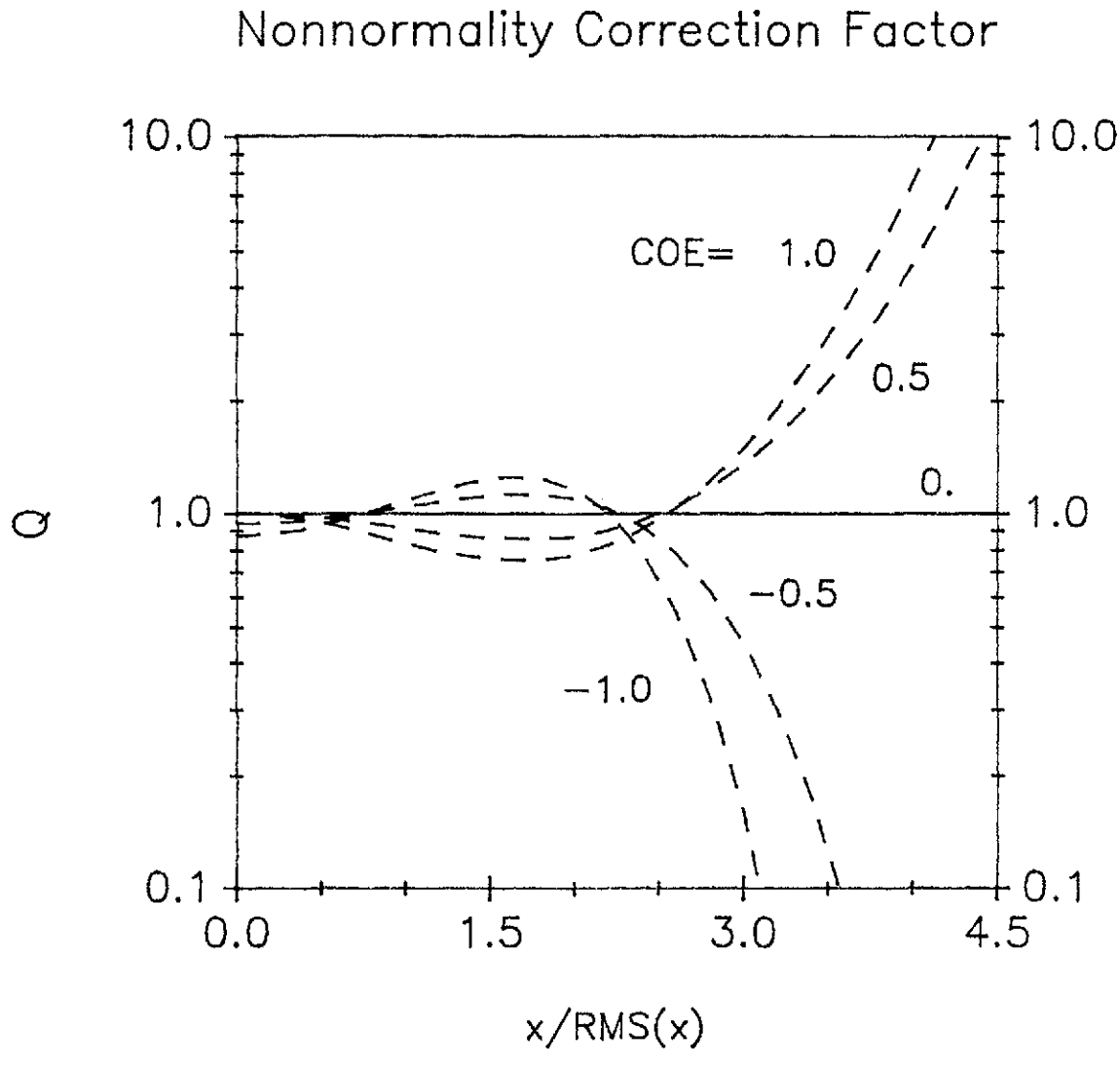

Fig. 2.2 NCF of first−passage failure

in which S represents the stress range (=twice the amplitude), ie., valley to peak excursion, of the cycle; K and m are constants which depend on the material; and $N(S)$ is the number of cycles at which failure occurs for constant range S.

The fatigue life, T, of a structure under stochastic excitation is a random variable and the primary problem is to estimate its mean value, $\mu_T \equiv E[T]$. The commonly used approximation can be written as

$$E[T] = \frac{1}{E[\Delta D]\nu} \tag{2.52}$$

in which ΔD is the damage per cycle and ν is the rate of occurrence of cycles. From the S-N curve the mean of ΔD is estimated as

$$E[\Delta D] = E[N(S)]^{-1} = \frac{1}{K}E[S^m] = \frac{1}{K}\int_0^\infty s^m p_S(s)ds \tag{2.53}$$

In order to evaluate the fatigue life from eq. 2.52, it is necessary to know the probability distribution of stress ranges and the rate of occurrence of cycles. This is not necessarily an easy task except in the special case in which the stress response is Gaussian and narrowband. The methods presented here are based on the narrowband condition, but the normality restriction has been relaxed.

If the process {X(t)} is Gaussian, then its amplitude (or envelope) will be a Rayleigh distribution. For a narrowband process the stress range S is clearly twice the amplitude, so it also has the Rayleigh probability distribution. In this case $E[\Delta D]$ can be evaluated from eq. 2.53 as

$$E[\Delta D] = \frac{1}{K}[2\sqrt{2}\sigma_X]^m \Gamma(1 + \frac{m}{2}) \tag{2.54}$$

in which $\Gamma(\cdot)$ denotes the gamma function. For this narrowband case one can take the rate of occurrence of cycles to be the zero crossing rate ν_0. Combining eq. 2.52 and 2.54, the fatigue life can be readily obtained, and this is the well-known Rayleigh method.

If the fatigue stress is a nonnormal process, then the Rayleigh method may not give a conservative result if the process has a higher probability of large extrema than does the Gaussian process. Lutes et al.[1984] characterized the effects of nonnormality on fatigue calculations by introducing a nonnormality correction factor (NCF) defined by:

$$L = \frac{\text{E(T) for normal process}}{\text{E(T) for nonnormal process}} \tag{2.55}$$

in which the normal and nonnormal processes have the same time of occurrence of extrema and zero-crossings and the same RMS values, but differ in probability distribution. When the S-N curve is as given in eq. 2.51, this gives

$$L = \frac{\text{E}(\text{S}^{\text{m}}) \text{ for nonnormal process}}{\text{E}(\text{S}^{\text{m}}) \text{ for normal process}} \tag{2.56}$$

Winterstein [1985] recently employed the Hermite series to predict nonnormal effects on fatigue damage. As in section II-4-1, let $g(U)$ be a monotonic function of a standard normal process. Then if the normal process $U(t)$ has a peak at level Y, the nonnormal process $X(t) = g[U(t)]$ has a corresponding peak at $g(Y)$. Thus,

if $U(t)$ is sufficiently narrowband and g is an odd function, then $E[S^m]$ in eq. 2.56 can be expressed as

$$E[S^m] = (2)^m E[\{g(Y)\}^m] \tag{2.57}$$

Note that Y has a Rayleigh distribution since $U(t)$ is narrowband. For the $COE(X) > 0$, substituting eq. 2.47 into eqs. 2.56 and 2.57, gives the first-order estimate of the nonnormality correction factor (NCF) as

$$L = 1 + m(m-1)h_4 \tag{2.58}$$

Nonnormality with the COE < 0 generally results in a reduced rate of fatigue damage (for which the NCF is less than unity) compared to a normal process. However, the above calculation technique does not work so well in this situation. Recall that the monotone Hermite polynomial for COE<0 (eq. 2.44) is for $u(x) = g^{-1}(x)$, whereas, eq. 2.57 requires moments of $g(Y)$. The truncated Hermite expansion can be inverted (similar to eq. 2.49) to give an expression for $g(u)$, but evaluation of the expectation in eq. 2.57 is still a problem. No acceptable analytical approximation of this calculation has been found so a less elegant type of approximation (not using Hermite expansions) will be used [Lutes and Hu, 1986]. Let $A = g(Y)$ denote the amplitude or peak value of the narrowband nonnormal process $X(t) = g[U(t)]$, where Y is the Rayleigh amplitude of the normal $U(t)$ process. Rather than using a general series expansion let

$$A = g(Y) = c_1 Y + c_2 G(Y) \tag{2.59}$$

in which $G(Y)$ is a specified nonlinear function, and c_1 and c_2 are two constants. Choosing an appropriate $G(Y)$ function and appropriate constants c_1 and c_2, allows a variety of situations to be approximated. The COE value of the narrowband process, X can be obtained from the moment funtions of A by using the approximations that

$$E[X^2] = \frac{1}{2}E[A^2]$$

and

$$E[X^4] = \frac{3}{8}E[A^4]$$

If m is chosen as an integer then the $E[A^m]$ moments can be obtained from a binomial expansion of eq. 2.59. In order to model a fairly wide range of situations let $G(Y) = Y^{1/5}$. This gives $COE(X)$ between -1.42 (for $c_1 = 0$) and 0 (for $c_2 = 0$). Note that different c_1 and c_2 values will produce different RMS values of X as well as different COE values. Equation 2.56 gives the NCF on the condition that the normal and nonnormal process have the same RMS values. Rather than explicitly solving for c_1 and c_2 to give this RMS condition, one can normalize eq. 2.56 by the appropriate RMS values, giving

$$L = \frac{(\mathrm{E}[\mathrm{A}^m]/\sigma_x^m)}{(\mathrm{E}[\mathrm{Y}^m]/\sigma_u^m)} \tag{2.60}$$

One can then vary the ratio c_2/c_1 and plot L versus $COE(X)$.

Figure 2.3 shows comparisons of the results of eqs. 2.58 and 2.60 (depending

on COE) with simulation results from Hu [1982]. It can be observed that the two nonlinear transfomation methods give reasonable approximations of the NCF.

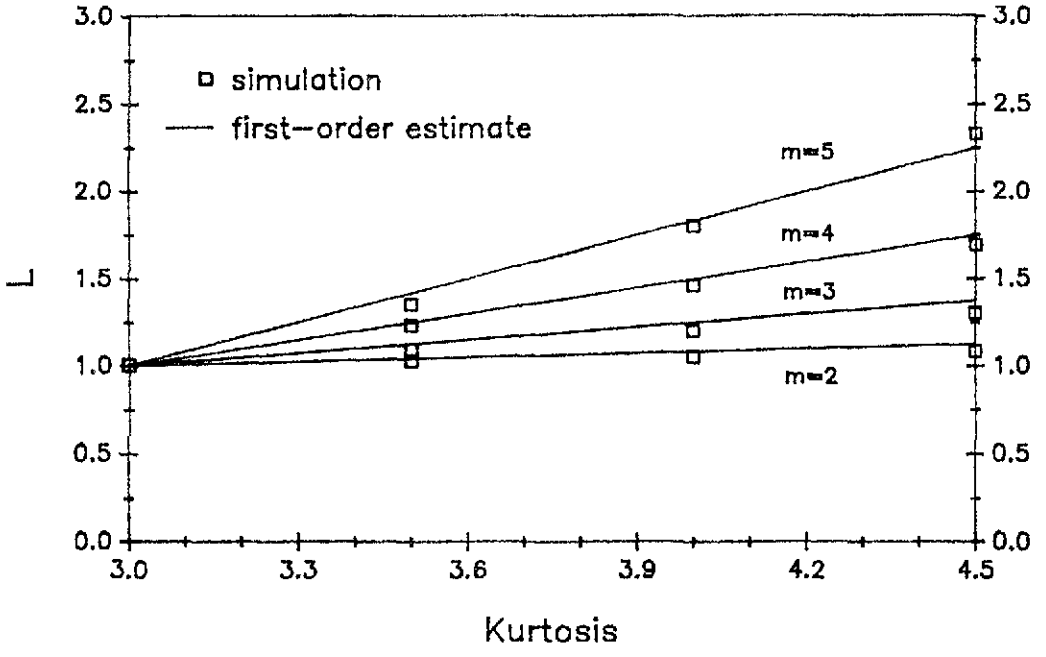

(a) Positive COE values

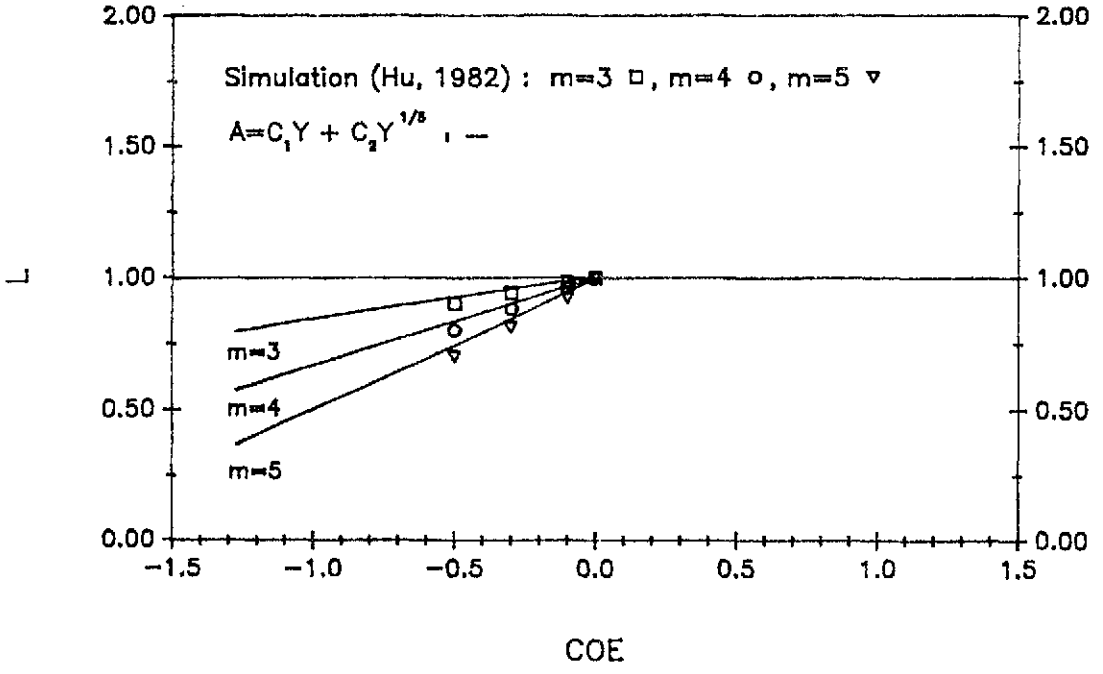

(b) Negative COE values

Fig. 2.3 NCF of fatigue failure

SECTION III

SYSTEM CONSIDERED AND COMPUTER SIMULATION

III-1 Description of P-S System:

The P-S system is modeled as a BLH primary system and a linear secondary system mounted in series (see figure 3.1). The equation of motion can be written as :

$$m_p(\ddot{x} + \ddot{y}) + c_p\dot{x} - k_p\phi(x) = c_s\dot{u} + k_s u$$

or

$$(\ddot{x} + \ddot{y}) + 2\beta_p\omega_p\dot{x} + \omega_p^2\phi(x) = 2\beta_s\omega_s\eta\dot{u} + \omega_s^2\eta u \tag{3.1}$$

and

$$m_s(\ddot{u} + \ddot{x} - \ddot{y}) + c_s\dot{u} - k_s u = 0$$

or

$$(\ddot{u} + \ddot{x} + \ddot{y}) + 2\beta_s\omega_s\dot{u} + \omega_s^2 u = 0 \tag{3.2}$$

where:

x denotes the displacement of the primary mass relative to the base,

u denotes the displacement of the secondary mass relative to the primary mass,

$\ddot{y}$ is the ground acceleration excitation,

m_p is the primary mass, m_s is the secondary mass,

$\omega_p = \sqrt{\frac{k_p}{m_p}}$, primary unyielded, undamped natural circular frequency,

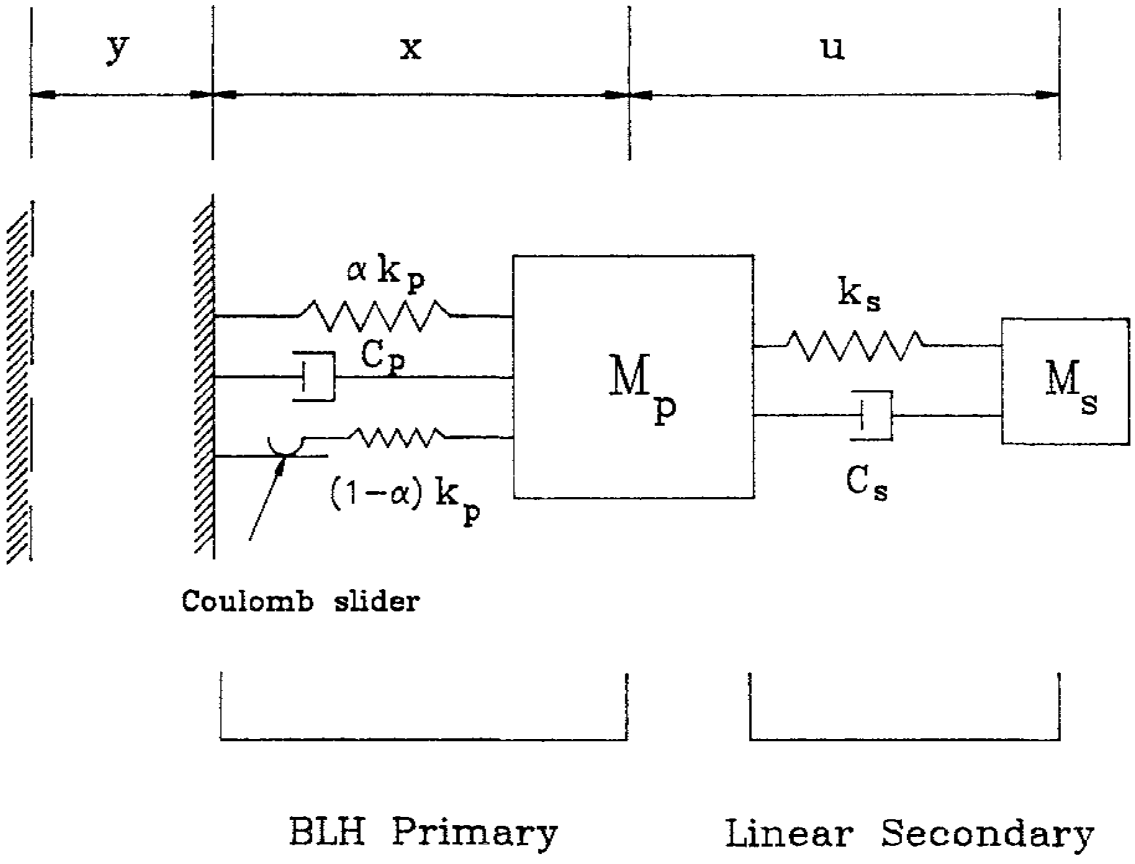

Fig. 3.1 Primary–Secondary System

$\omega_s = \sqrt{\frac{k_s}{m_s}}$, secondary undamped natural circular frequency,

$\beta_p = \frac{c_p}{2\omega_p m_p}$, primary small amplitude fraction of critical damping,

$\beta_s = \frac{c_s}{2\omega_s m_s}$, secondary fraction of critical damping,

$\eta = \frac{m_s}{m_p}$, mass ratio, and

$\phi(x)$ is the bilinear hysteretic restoring force as shown in fig. 3.2.

Note that $\phi(x)$ is chosen to have a unit slope for small amplitudes and a second slope of α. In general, $\phi(x)$ depends on previous values of $x(t)$ but with the limitation that if $x(t)$ is periodic, then $\phi(x)$ is also periodic. Note that the right-hand side of eq. 3.1 is the coupling term in the P-S system. This term will be eliminated if cascade analysis is used.

The SDF BLH system has probably been more widely studied than any other class of nonlinear hysteretic oscillator [Caughey 1960; Iwan and Lutes 1968; Lutes 1970, Chen and Lutes 1988]. Two particular values of the slope ratio were chosen to illustrate important situations. These are α=1/2, a moderately nonlinear system, and α=1/21, a nearly elastoplastic system.

No exact solutions for the statistics of the response of such a hysteretic system to random excitation have yet been obtained by an analytical technique. Thus, a computer simulation program has been used to obtain empirical data for BLH primary and linear secondary systems.

III-2 Excitation:

For the present investigation, the excitation $\ddot{y}(t)$ represents a ground acceleration. It is taken to be a mean-zero stationary, white, random process with a

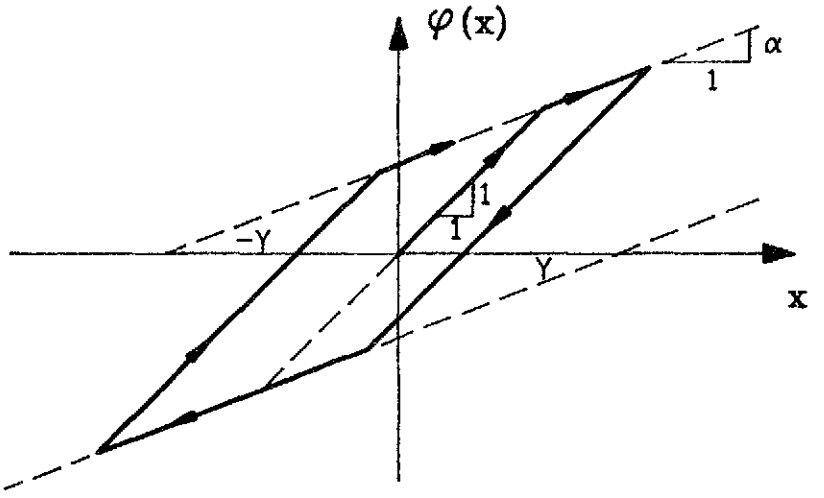

Fig. 3.2 Restoring force of a BLH system

normal probability distribution, and a uniform power spectral density equal to S_0 (per radian) for all frequency. That is, the auto-correlation function is given by

$$E[\ddot{y}(t_1)\ddot{y}(t_2)] = 2\pi S_0 \delta(t_1 - t_2) \tag{3.3}$$

in which $\delta(t)$ is the Dirac delta function.

Various methods exist for simulating stochastic processes [Shinozuka 1977]. In this study, the white noise excitation was simulated using a pulse method [Brinkmann 1980]. The acceleration at the base of the structure was taken to be a sequence of uniformly spaced Dirac delta functions, with each acceleration pulse giving an instantaneous change in the relative velocity $\dot{x}$. The pulse magnitude, in this study, is a standard normal random number, obtained from subroutine RNNOA in the IMSL-Library [1987], scaled by a constant R, which is given by

$$R = \sqrt{2\pi S_0 \Delta t} \tag{3.4}$$

where Δt is the time interval between two adjacent pulses. The interval Δt was chosen to give $\omega_p \Delta t$ =0.1 radian, giving approximately 63 pulses per cycle of the unyielded system.

It is convenient to characterize the excitation level by a measure with dimension length, so that the ratios of yield levels to excitation level (Y/N) and root-mean-square response level to excitation level can be plotted as dimensionless quantities. Such a length measure of the excitation level is

$$N = \frac{(2S_0\omega_p)^{\frac{1}{2}}}{\omega_p^2} \tag{3.5}$$

For a SDOF linear system as an example, the standard deviation (or RMS value) of displacement response may be expressed in the normalized form as

$$\frac{\sigma_x}{N} = \sqrt{\frac{\pi}{4\beta_0}}$$

or

$$\frac{\sigma_x}{Y} = \sqrt{\frac{\pi}{4\beta_0}}(\frac{N}{Y})$$

Similarly, the normalized velocity of responses can be written as

$$\frac{\sigma_{\dot{x}}}{\omega_0 N} = \sqrt{\frac{\pi}{4\beta_0}}$$

in which ω_0 and β_0 are the natural frequency and damping ratio of this system.

III-3 Integration Scheme and Statistical Accuracy:

The equation of motion for this P-S systems can be written in a matrix form as

$$\begin{bmatrix} m_p & 0 \\ 0 & m_s \end{bmatrix} \begin{Bmatrix} \ddot{x} \\ \ddot{u} \end{Bmatrix} + \begin{bmatrix} c_p & 0 \\ 0 & c_s \end{bmatrix} \begin{Bmatrix} \dot{x} \\ \dot{u} \end{Bmatrix} + \begin{bmatrix} (k_1 + k_2) & 0 \\ 0 & k_s \end{bmatrix} \begin{Bmatrix} \phi(x) \\ u \end{Bmatrix} = \vec{\ddot{f}} \qquad (3.6)$$

where

$$\vec{\ddot{f}} = \begin{Bmatrix} -m_p\ddot{y} + c_s\dot{u} + k_s u \\ -m_s(\ddot{x} + \ddot{y}) \end{Bmatrix}$$

The excitation $\ddot{y}$ is the stationary, white noise, Gaussian acceleration. Because of the nonlinearity of the restoring force $\phi(x)$, no exact solution to equation 3.6

has been obtained. However an exact stepwise calculation is possible due to the piecewise linear characteristic of the resistance deformation relationship. The computational effort of this approach is greatly reduced by using cascade analysis, for which equation 3.6 will describe two uncoupled systems. Note that the nonlinear function, $\phi(x)$, can always be described by one of three linear functions with the choice of the proper function depending on the position and velocity of the primary mass, m_p.

For noncascade analysis, equation 3.6 must be solved as simultaneous equations, which can be rewritten as four first order differential equations using the four state variables: x, $\dot{x}$, u and $\dot{u}$. Any of several numerical integration schemes can be used to solve the first order differential equations. In this study, a sixth-order Runge-Kutta-Verner method was used from subroutine IVPRK in the IMSL-Library [1987].

In this simulation, both time averages and ensemble averages have been used in order to obtain better statistical accuracy. Each sample of simulated response was long enough to contain approximately 2000 cycles of response of the unyielded system ($\omega_p t$=4000 π). The first 100 cycles of each sample were omitted from calculations, though, on the basis of possible nonstationarity due to initial conditions. Statistical accuracy was improved by using an ensemble of 100 such samples for each process investigated. The reproducibility of the results was verified by comparing numbers obtained from different ensembles and from ensembles of different lengths. The scatter of simulation statistics was investigated empirically [Chen 1990], and it was concluded that the ensemble size of 100 and length of 2000 cycles gave an acceptable sample.

The simulation results have also been verified for two limiting situations. First, by decoupling the two subsystems the results for the displacement x of the BLH primary system were found to agree very well with analog computer results in an early study [Lutes 1970]. Second, by letting the primary system be linear ($\alpha = 1$), the exact solutions of both primary and secondary response could be found. These results did coincide with the simulation results. Therefore, the overall accuracy and consistency of this simulation has been studied and considered acceptable.

SECTION IV

TRISPECTRAL ANALYSIS

IV-1 Introduction:

An earlier report [Chen and Lutes 1988] has presented a method which can provide satisfactory estimates of the coefficient of excess of the primary system response, without using computer simulation. This method uses a nonlinear nonhysteretic substitute primary system. However, knowledge of the coefficient of excess of the primary acceleration is not enough to allow evaluation of the coefficient of excess for the response of the linear secondary system. This is similar to the problem of evaluating the RMS value (or variance) of the secondary response, which requires, not only the variance but the autocorrelation function or the power spectral density of the primary system acceleration. From eqs. 2.29 and 2.30, it can be seen that in order to obtain the coefficient of excess of the secondary system, one must know not only the coefficient of excess of the primary acceleration but the whole fourth cumulant function of primary acceleration, $Q(\tau_1, \tau_2, \tau_3)$, or the trispectrum, $D(\omega_1, \omega_2, \omega_3)$. Thus, in order to evaluate the COE value of the secondary response, both the power spectral density and the trispectral density of the primary acceleration should be investigated. The trispectrum of the primary acceleration has not been studied previously and will present a challenging task in the current study.

Since the primary is nonlinear, no analytical form of the trispectrum of primary response can be obtained. However, the trispectrum of primary absolute acceleration can be evaluated numerically from simulated data, and this will provide

an empirical $D_{\ddot{z}}$ function for the nonnormal base excitation of the secondary system. The empirical $D_{\ddot{z}}$ function will also be used for comparisons with the $D_{\ddot{z}}$ from analytical models in the following chapter. It turns out that finding a simulated $D_{\ddot{z}}(\omega_1, \omega_2, \omega_3)$ function is not a trivial problem. A direct method of finding $D(\omega_1, \omega_2, \omega_3)$ for a given time history consists of first numerically evaluating necessary moments and cumulants, then implementing eq. 2.11 by a numerical triple Fourier integral of the fourth order cumulant. This is theoretically feasible but involves very considerable computation. Another approach is through the "Periodogram", which was first introduced by Schuster [1898]. The basic idea of Periodogram analysis is to estimate the kth order (k $\geq$ 2) spectral function by using a finite Fourier transform of a single time series. This has been practically applied up to the third order spectrum, which is called the bispectrum [Brillinger and Rosenblatt 1967a,b; Hasselman et al. 1963; Subba Rao and Gabr 1984]. In this study, the method is extended to investigate the fourth order spectrum, which is called the trispectrum. Prior to considering periodogram analysis, though, it is useful to investigate some general characteristics of trispectral functions.

IV-2 Methods for Comparing Trispectral Functions:

Finding an adequate approximation of the $D(\omega_1, \omega_2, \omega_3)$ function is considerably more difficult than the more common frequency domain problem of approximating the power spectral function, $S(\omega)$. In the latter situation one can plot $S(\omega)$ versus ω and use this plot in making judgements regarding the adequacy of an approximation. This is made easier by the facts that $S(\omega)$ is real, and it is an even function so that only $\omega \geq 0$ need be considered. The $D(\omega_1, \omega_2, \omega_3)$, however, not

only is defined on a three dimensional space but also is generally complex. Thus, fitting D amounts to fitting two functions (the real and imaginary parts), each being a function of three arguments. The symmetry of $D(\omega_1, \omega_2, \omega_3)$ (see Section II-1-2) helps somewhat, but it also is rather complicated inasmuch as it is basically a four-dimensional symmetry in a three dimensional space. Thus, it is very difficult to conceive of any simple plotting scheme that would reveal all aspects of the $D(\omega_1, \omega_2, \omega_3)$ function for all points within a domain having a given finite range for each frequency argument. Because of these difficulties, the approximations presented here are compared with simulation data only in certain limited regions of the three-dimensional space of ω values. The following paragraph explains why one particular region is considered more important than most other regions.

Recall from Section II-2-2 the nature of $D_x(\omega_1, \omega_2, \omega_3)$ when x is the response of a lightly damped linear oscillator having a delta correlated excitation. Then $H(\omega)$ has peaks with height of $O(\beta_0^{-1})$ near $\omega = \pm\omega_0$. This, in turn, gives $D_x(\omega_1, \omega_2, \omega_3)$ as having peaks of $O(\beta_0^{-4})$ near $(\omega_0, -\omega_0, \omega_0)$ and each of the other five points "symmetric" to this point. Furthermore, these six high peaks dominate the D_x function, so that all other points are relatively insignificant. In the present situation, the primary system is nonlinear so the behavior of $D_{\ddot{z}}(\omega_1, \omega_2, \omega_3)$ will surely not be this simple, but some similarity may still be expected. Thus, it is anticipated that $D_{\ddot{z}}(\omega_1, \omega_2, \omega_3)$ may be dominated by major peaks near points like $(\omega_r, -\omega_r, \omega_r)$, where ω_r denotes a type of "resonant" frequency of the bilinear hysteretic primary system. The value of ω_r is unknown, but the existence of such peaks can be investigated by studying $D_{\ddot{z}}$ in the vicinity of the line $(\omega, -\omega, \omega)$. This line through one octant of the three-dimensional ω space must include the point $(\omega_r, -\omega_r, \omega_r)$ if

it exists, and the existence of a high peak of $D_{\tilde{z}}$ along this line will at least partially confirm the assumed similarity between the present problem and the one involving a linear primary system. Note, also, that D is a real function at every point on the $(\omega_1, -\omega_1, \omega_3)$ plane, simplifying the study of D in this vicinity.

IV-3 Periodogram Analysis:

IV-3-1 Polyspectra:

In order to implement the Fourier transfrom in a digital computer, the discrete Fourier transform (DFT) has to be used. Cooley and Tukey [1965] developed an efficient DFT algorithm, called the Fast Fourier transform (FFT), which tremendously increased the computational speed. Therefore, the FFT has become a universal standard algorithm for the DFT and also enhanced the feasibility of using periodogram analysis.

Suppose that an order k stationary process $\{X_n | n = 1, \ldots, N\}$ is known on the set $\{\Delta t, \ldots, j\Delta t, \ldots, N\Delta t\}$ in which Δt is the sample interval and $T = N\Delta t$ is the total length of the time sample. The finite Fourier transform of the process $\{X_n\}$ is defined by

$$d_x(r\Delta\omega) = \sum_{n=1}^{N} (X_n - \bar{X}) \exp(-i\frac{2\pi nr}{N}) \tag{4.1}$$

in which $\bar{X}$ denotes the sample mean and $\Delta\omega = 2\pi/T$ is the frequency increment. Note that $d_x((r+N)\Delta\omega) = d_x(r\Delta\omega)$ so that d_x is a periodic function. Similarly the inverse Fourier transform of $d_x(\omega)$:

$$X_n = \bar{X} - \frac{1}{N}\sum_{r_m=1}^{N} d_x(r\Delta\omega)\exp(i\frac{2\pi nr}{N})$$

gives $X_{n+N} = X_n$. Thus, we will consider $\{X_n\}$ to have this periodicity in all calculations involving the Fourier transform. This simplifies certain calculations. For example, we can write the second cumulant as

$$C_2(\tau_n) = k_2(t_j, t_j + \tau_n) = \sum_{j=1}^{N}(X_j - \bar{X})(X_{j+n} - \bar{X}) \tag{4.2}$$

in which $\tau_n = n\Delta t$. Even though the $j - n$ subscript on the final term goes outside the original range of $1, \ldots, N$, the term is unambiguously defined by the periodicity property. Note from eq. 4.2 that C_2 also has the periodicity property

$$C_2(\tau_{n+N}) = C_2(\tau_n)$$

this periodicity also extends to higher order cumulants such as $C_k(\tau_1, \ldots, \tau_{k-1})$ which is periodic in each of its $k - 1$ time arguments.

The kth-order polyspectrum (or kth-order cumulant spectrum) is defined by an order (k-1) Fourier transform of the kth-order cumulant function. This is the same idea as in Sec. II-1-1, but the discrete form can be written as

$$f_k(\omega_1, \ldots, \omega_k) = \\ (\frac{\Delta t}{2\pi})^{k-1}\sum_{n_1=1}^{N}\cdots\sum_{n_{k-1}=1}^{N} C_k(\tau_1, \ldots, \tau_{k-1})\exp\Big[-i\sum_{j=1}^{k-1}\omega_j n_j \Delta t\Big] \tag{4.3}$$

where $\tau_j = n_j\Delta t$, $1 \le n_j \le N$ and $\omega_j = r_j\Delta\omega$.

A sufficient condition to assure that the above Fourier transform exists is,

$$\sum_{n_1} \cdots \sum_{n_{k-1}} |C_k(\tau_1, \ldots, \tau_{k-1})| < \infty$$

In general, $f_k(\omega_1, \ldots, \omega_k)$ is complex-valued and bounded. The final argument of f_k in eq. 4.3 is determined from the condition that the sum of the k variables satisfy

$$\sum_{j=1}^{k} \omega_j = 0$$

Points in the general k dimensional frequency space which satisfy this condition are said to belong to the principal manifold, which is actually of dimension $k-1$. The function f_k is only defined on this manifold. Since the second-order cumulant $C_2(\tau)$ is just the covariance function, it follows that the second-order polyspectrum is exactly the same as the conventional power spectrum, i.e. $f_2(\omega, -\omega) \equiv S(\omega)$. The third-order polyspectrum, $f_3(\omega_1, \omega_2, -\omega_1 - \omega_2)$ has been called the bispectrum, and the fourth-order spectrum, $f_4(\omega_1, \omega_2, \omega_3, -\omega_1 - \omega_2 - \omega_3)$ has been called the trispectrum. Since all polyspectra of higher than second order vanish if $\{X_n\}$ is Gaussian, the power spectrum is the only necessary information for a Gaussian process. On the other hand, the bispectrum, trispectrum and all higher-order polyspectra can be regarded as measures of the departure of the process from Gaussianity. In this study, the bispectrum vanishes due to the symmetric distribution of $\{X_n\}$, so that the trispectrum becomes the most important representation of the non-Gaussian process.

IV-3-2 The Estimation of Polyspectra:

The basic idea of the periodogram analysis involves using the finite Fourier transform of eq. 4.1 on a sampled time series. The relevant products of these finite Fourier transforms are then "smoothed" by averaging over neighboring sets of frequencies to produce estimates of the required polyspectrum.

Let $I_N(\omega_1, \ldots, \omega_k)$ be called the kth-order periodogram, or briefly periodogram, and be defined as

$$I_N(\omega_1, \ldots, \omega_k) = \frac{(\Delta t)^{k-1}}{N(2\pi)^{k-1}} \prod_{j=1}^{k} d_x(\omega_j) \tag{4.4}$$

It can be shown that the expected value of a kth-order periodogram is an asymptotically unbiased estimate of the kth-order polyspectrum (cumulant spectrum) as

$$\lim_{N \to \infty} E\Big[I_N(\omega_1, \ldots, \omega_k)\Big] = f_k(\omega_1, \ldots, \omega_k) \tag{4.5}$$

provided that the $\omega_1, \ldots, \omega_k$ do not lie in any proper submanifold of the principal manifold, with the submanifolds defined as

$$\sum_{j \in J} \omega_j = 0$$

in which J is a nonvacuous proper subset of $1, \ldots, k$. The expected value in eq. 4.5 typically diverges as $N \to \infty$ if the ω's do lie in a proper submanifold [Brillinger and Rosenblatt 1967a, 1967b].

It can, however, be proved that the periodogram is not a consistent estimate in the sense of mean square convergence. That is, the variance of $I_N(\omega_1, \ldots, \omega_k)$ does not tend to 0 when N $\rightarrow \infty$. To construct a consistent estimate one must "smooth" the function $I_N(\omega_1, \ldots, \omega_k)$ by using a weight function which becomes increasingly more concentrated as the sample size N goes to ∞ [Priestley 1988]. There are many possible choices for a specific form of the weight function (or window). Two of the commonly used forms are those of Hanning and Bartlett, but a simpler form is used here.

To estimate $f_k(\omega_1, \ldots, \omega_k)$ at any point that is not in a submanifold, one can simply "smooth" or average the periodogram in the neighborhood of the point. For an estimate at a point in a submanifold, one must average the periodogram for ω's in a neighborhood of the point, but not actually in the submanifold [Brillinger and Rosenblatt 1967a, 1967b].

The estimation of bispectra has been investigated quite extensively [Hasselman et al. 1963; Subba Rao and Gabr 1984; Choi et al. 1985], but is not within the scope of this study. It appears that very little has been done on the estimation of trispectra. The principal manifold for the trispectrum is $\omega_1 + \omega_2 + \omega_3 + \omega_4 = 0$, and the possible submanifolds of interest have any $\omega_i + \omega_j = 0$, for $i, j \in \{1, 2, 3, 4\}$. Unfortunately, a region of particular interest is along the line $(\omega, -\omega, \omega, -\omega)$ and all points on this line do lie in these submanifolds. This somewhat complicates the estimation of trispectra in the periodogram analysis. In order to obtain information about the trispectrum on submanifolds, as mentioned early, one needs to take the average of values fairly near the submanifold. This can be accomplished with any simple weighted average over some range of the k-th order periodogram. However,

the crucial issue is how large a range to use for the average? To investigate this problem, a rectangular window (an "on-off"average) has been employed for simplification. The periodogram, $\bar{I}_N$, smoothed by the rectangular window with width equal to $(2n+1)\Delta\omega$, can be defined as

$$\bar{I}_N(\omega_1,\ldots,\omega_4) = \frac{1}{M}\sum_{b_1=-n\Delta\omega}^{n\Delta\omega}\cdots\sum_{b_4=-n\Delta\omega}^{n\Delta\omega} I_N(\omega_1+b_1,\ldots,\omega_4+b_4) \\ W(\omega_1+b_1,\ldots,\omega_4+b_4) \tag{4.6}$$

in which $W(\eta_1,\eta_2,\eta_3,\eta_4) = 1$ if the four frequencies do lie in the manifold $\eta_1+\eta_2+\eta_3-\eta_4 = 0$ but off the submanifolds, $\eta_i+\eta_j \neq 0$ for $i \neq j$ and $W(\eta_1,\eta_2,\eta_3,\eta_4) = 0$ otherwise. The normalization term M in eq. 4.6 is the total number of I_N within the range of four dimensional smoothing,

$$M = \sum_{b_1=-n\Delta\omega}^{n\Delta\omega}\cdots\sum_{b_4=-n\Delta\omega}^{n\Delta\omega} W(\omega_1+b_1,\ldots,\omega_4+b_4)$$

When a proper average width $(2n+1)\Delta\omega$ is chosen, eq. 4.6 will give a consistent estimate of $D(\omega_1,\omega_2,\omega_3)$ on the submanifolds.

A simple first-order linear system with damping has been employed for obtaining an appropriate value for n in eq. 4.6. The equation of motion for the linear system subjected to a delta correlated excitation can be written as

$$\dot{x}+bx = y(t) = \sum A_j\delta(t-j\Delta t) \tag{4.7}$$

in which the $A_j's$ are independent random variables. The impulse response function, $h(t)$, and the transfer function, $H(\omega)$, are given by

$$h(t) = \exp(-bt)$$

$$H(\omega) = \frac{1}{b + i\omega}$$

Therefore, both the response power spectral density, $S_x(\omega)$ and the trispectrum $D_x(\omega, \omega, -\omega)$ (on a submanifold) can be obtained analytically as

$$S_x(\omega) = \frac{E(A^2)}{2\pi\Delta t} \frac{1}{\omega^2 + b^2} \tag{4.8}$$

and

$$D_x(\omega, \omega, -\omega) = \frac{E(A^4) - 3E(A^2)^2}{(2\pi)^3 \Delta t} \left(\frac{1}{\omega^2 + b^2}\right)^2 \tag{4.9}$$

Note that Δt is the time increment of the process. The fourth moment, $E(A^4)$ and second moment, $E(A^2)$, of the excitation can be chosen so as to completely define the response trispectrum. The ratio of $D(\omega, \omega, -\omega)/S(\omega)^2$ can be used as an index of the normalized tripectrum which is somewhat similar to the COE value. It is clear from equations 4.8 and 4.9 that D/S^2 for this process $X(t)$ is a constant and is equal to the $COE(A)$ times $\frac{\Delta t}{2\pi}$. Thus, the extent to which $X(t)$ is non-Gaussian is directly related to the $COE(A)$, and if A is Gaussian then $X(t)$ is also Gaussian. For the numerical simulation the parameters have been chosen as $\Delta t = 0.1(\text{sec})$, and $b = 0.5(\text{sec}^{-1})$. The $COE(A)$ values have been chosen to be 0 (for a Gaussian process) and 22.2 for a non-Gaussian process which gives $D/S^2 = 0.353$. Figs. 4.1 and 4.2 illustrate the implementation of eq. 4.6 to find $D(\omega, \omega, -\omega)/S^2(\omega)$ values at three different frequencies. It can be seen that when n is between 14 and 17, the smoothed periodogram gives a quite good estimate for the trispectrum. It

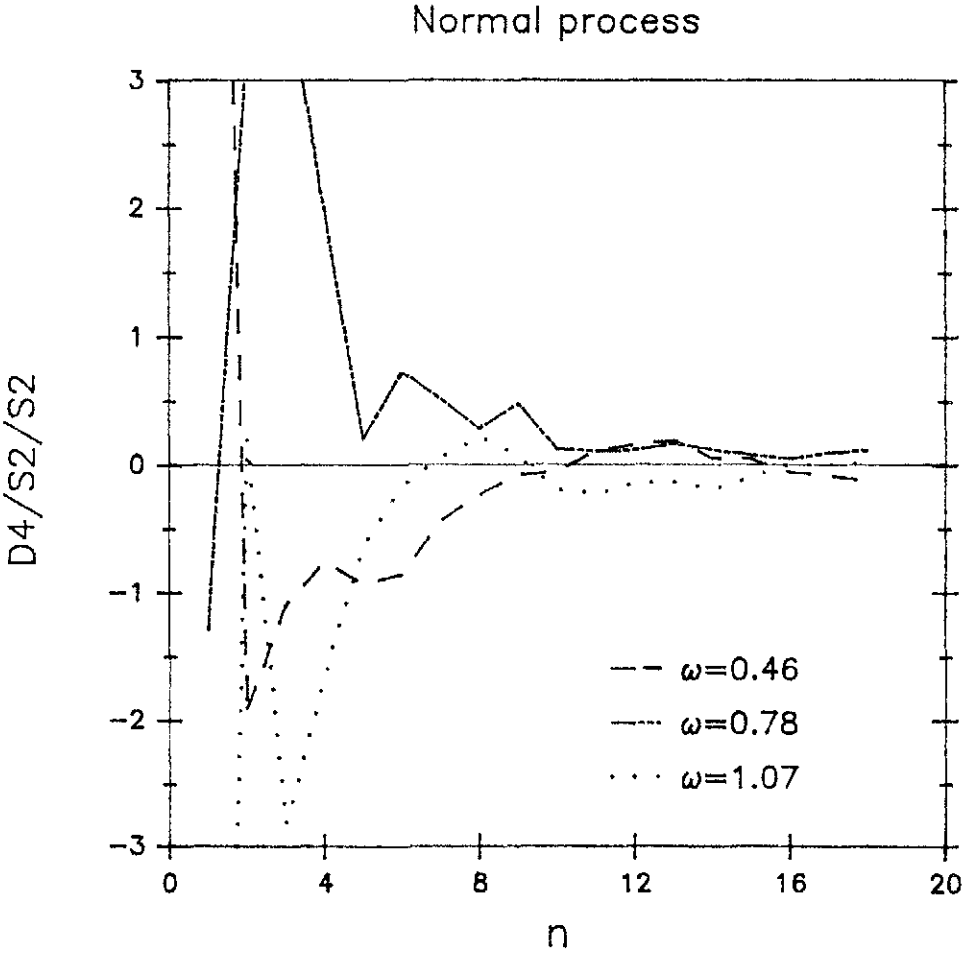

Fig. 4.1 Trispectrum of normal process

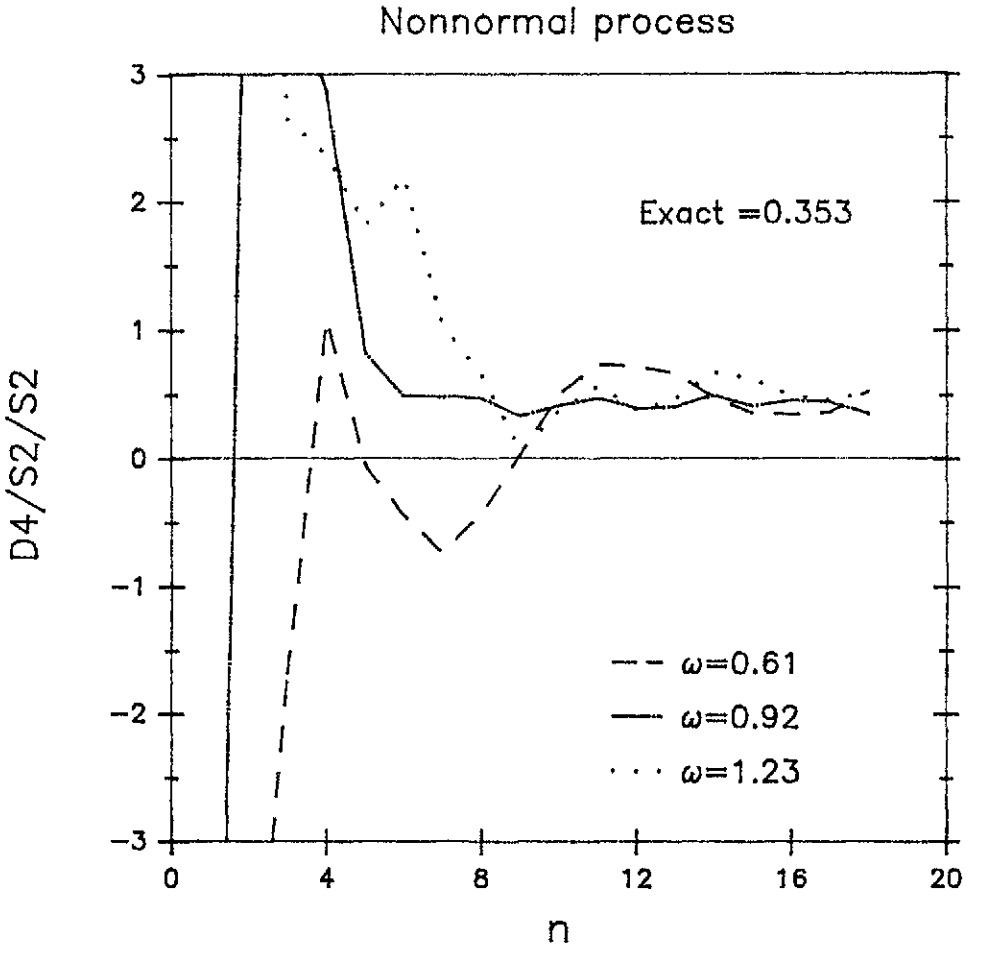

Fig. 4.2 Trispectrum of nonnormal process

should also be noted that when n is larger than 18, the estimate becomes chaotic, but these values have not been plotted in the figures. Overall, one can conclude that the estimation of the trispectrum on the submanifolds is feasible, however, it requires averaging over a fairly large range of frequencies. One disadvantage of this approach is that the frequency averaging causes the estimations of the trispectrum from the periodogram analysis to appear quite broadband, even if the process of interest is narrowband.

IV-3-3 Trispectrum of Primary Acceleration:

This section presents the results of using eq. 4.6 to estimate the trispectrum for the primary absolute acceleration of the nonlinear primary system for the case: $\alpha = 0.5$, $\beta_p = 1\%$, $Y/N = 1$. In order to obtain accurate simulated results, both ensemble averaging and block averaging have been used. The term block averaging refers to a procedure of generating a very long time history then dividing it into a number of blocks covering different time intervals. The finite Fourier transform of each block is then calculated and these transforms are averaged over the different blocks [Priestley 1981]. Thus, block averaging is essentially the same as ensemble averaging except that the time samples (blocks) in the former approach are related to each other, rather than being independent. In this study, a block contains 4096 (or 2^{12}) time increments. The normalized time increment, $\omega_p \Delta t$ has been chosen to be 0.1 radian giving approximately 63 excitation pulses per cycle of the unyielded system (the same as in the other simulations for the P-S system). The ensemble consists of four long time histories, each of which is divided into 10 blocks. The resulting block and ensemble averaging seems to give satisfactory simulation results

for trispectral analysis.

To avoid the difficulty of describing the full four dimensional behavior of $D(\omega_1, \omega_2, \omega_3)$, one possible approach is to restrict attention to some particular plane within the frequency space. In particular, it seems desirable to to study a plane containing a line like $(\omega, -\omega, \omega, -\omega)$, since it is anticipated that D may have major peaks on such lines. Obviously, there are infinitely many planes containing the line, $(\omega, -\omega, \omega, -\omega)$ in the $(\omega_1, \omega_2, \omega_3, -\omega_1 - \omega_2 - \omega_3)$ domain. One simple choice is the plane described by ω_1 and ω_3, and given by $(\omega_1, -\omega_1, \omega_3, -\omega_3)$. The line $(\omega, -\omega, \omega, -\omega)$ is clearly the diagonal of this plane.

A $D_{\hat{z}}$ contour map plotted for the $(\omega_1, -\omega_1, \omega_3, -\omega_3)$ plane is shown in figure 4.3 (recall that D has no imaginary part on this plane). The plot has been split into two parts, with figure 4.3a giving more detail on negative $D_{\hat{z}}$ values and figure 4.3b concentrating on positive $D_{\hat{z}}$. Note that the trispetrum has been "smoothed" over a fairly wide range (n=15), so that each number on the map does not represent the "real" trispectrum value but an averaged value. It can be seen that a very high positive peak occurs at normalized frequency (ω/ω_p) coordinate $(0.72, -0.72, 0.72, -0.72)$ and two negative troughs appear symmetrically to the line $(\omega, -\omega, \omega, -\omega)$ at coordinates of about $(1.0, -1.0, 0.8, -0.8)$ and $(0.8, -0.8, 1.0, -1.0)$. It should be noted that the frequency (0.72) giving a peak of this function is exactly the same as the frequency giving the maximum power spectral density of this yielding BLH system.

In order to investigate further the negative troughs, another plane which is orthogonal to the line $(\omega_1, -\omega_1, \omega_3, -\omega_3)$ and which contains these two troughs

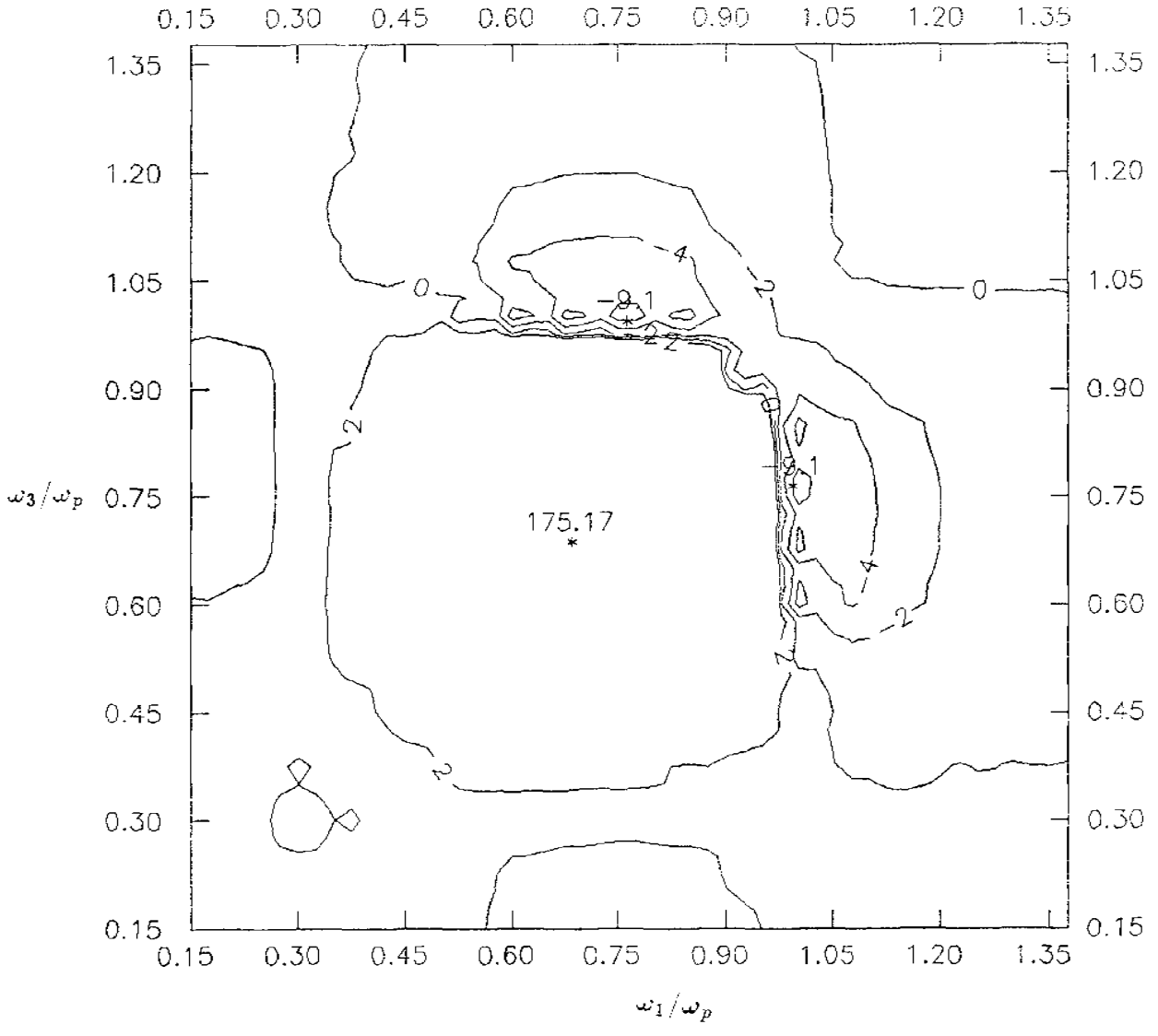

Fig. 4.3(a) Contour map, $D_{\Xi}(\omega_1, -\omega_1, \omega_3)$

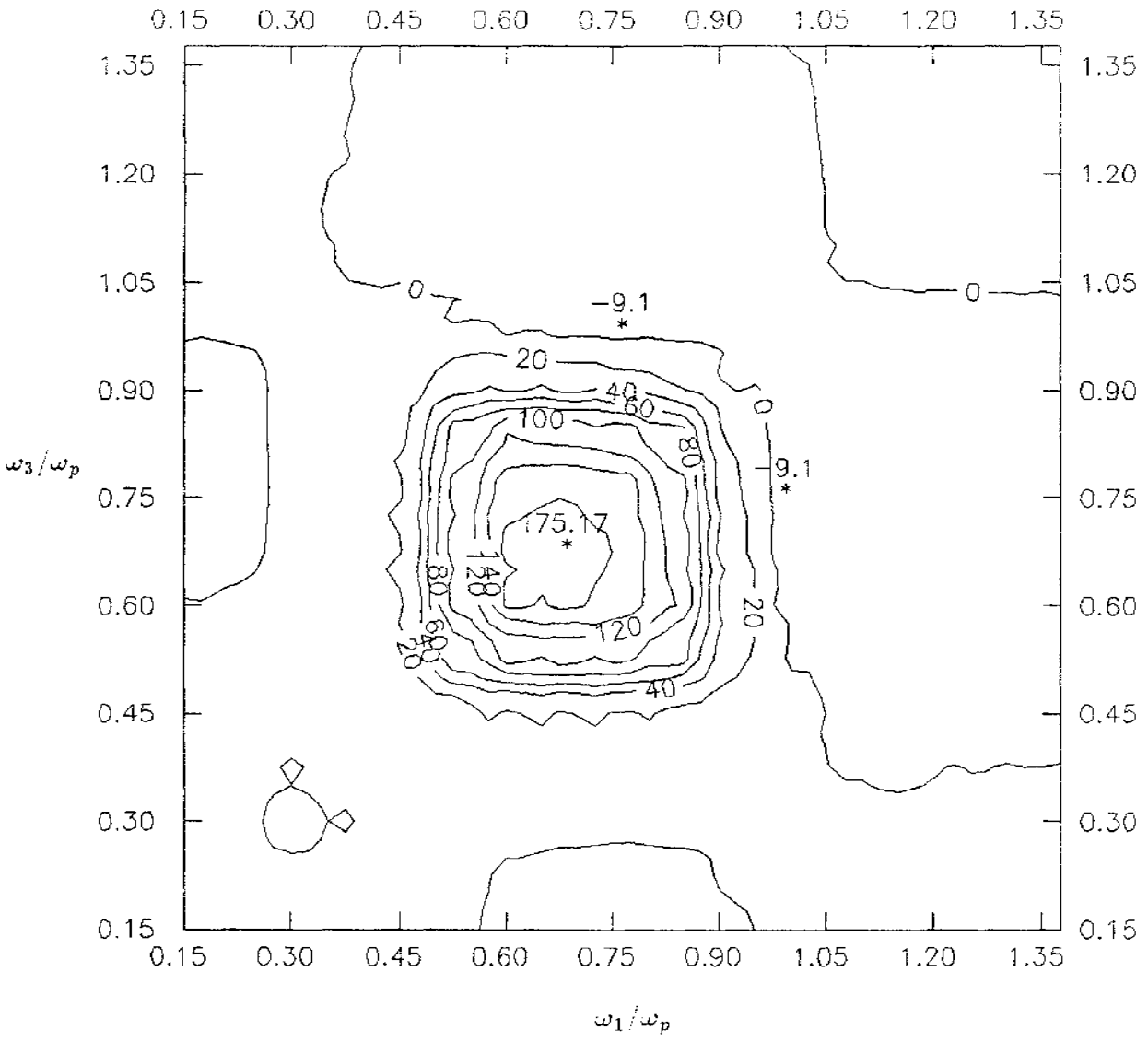

Fig. 4.3(b) Contour map, $D_{\Xi}(\omega_1, -\omega_1, \omega_3)$

has been investigated. This plane can be defined as $(\omega_1, \omega_2, 2a - \omega_1, -2a - \omega_2)$ where a is the distance from the origin to the plane and it has been chosen as $a = 0.85\omega_p$. A contour map of the real part of $D_{\bar{z}}$ for this plane has also been plotted in fig. 4.4, with major emphasis being placed on the negative $D_{\bar{z}}$ values. It is interesting to note that the negative part is basically shaped like a ring (or donut). The center of the ring seems to be located at about $(0.9, -0.9, 0.9, -0.9)$ which is a little higher than the positive peak on $(\omega, -\omega, \omega, -\omega)$. Figs. 4.3 and 4.4, provide some valuable qualitative as well as quantitative information. Fig. 4.3 can also be used to compare these simulation results with the "smoothed" D function from substitute linear models in the following chapter. This will allow assessment of the acceptability of schemes for "matching" the trispectrum for a BLH system with that for a substitute linear system.

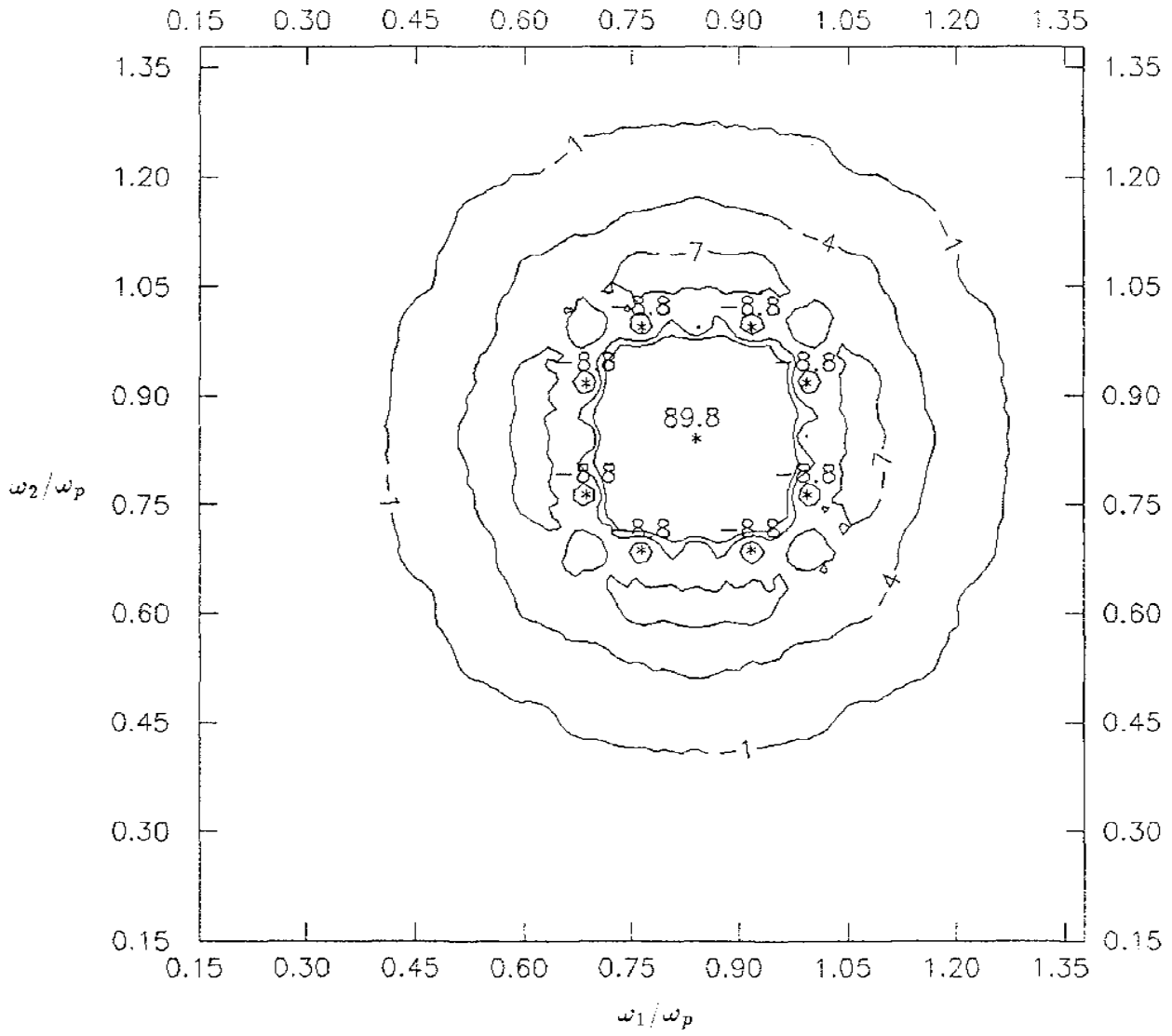

Fig. 4.4 Contour map, $D_{\Sigma}(\omega_1, \omega_2, 2a - \omega_1)$, $a = 0.85\omega_p$

SECTION V

RESPONSE OF LINEAR SECONDARY SYSTEM

V-1 Concept of an approximate model:

A central interest of this study is to develop an analytical model, which can approximate the trispectrum, $D(\omega_1, \omega_2, \omega_3)$ for the absolute acceleration of the nonlinear primary system, as simulated in the preceding chapter. This will give a description of the nonnormal base excitation of the linear secondary system, so that the COE value of the secondary response can then be evaluated analytically. Note that in order to evaluate the COE value of the secondary response, the analytical model also must adequately approximate the power spectral density of the primary acceleration. However, the estimation of a power spectral density is much simpler than the approximation of a trispectrum.

The basic approach used here consists of simultaneously replacing the nonlinear primary system with a substitute linear primary and replacing the Gaussian excitation of the original primary with a non-Gaussian excitation. Obviously, the non-Gaussian excitation is required in the substitute system, since a Gaussian excitation of a linear primary would give a Gaussian primary response (and a Gaussian secondary response). A major advantage of using a linear substitute system is that it allows the use of linear methods (such as state space moment equations) to find the secondary response. The major question is whether it is possible to find a substitute primary system and a substitute excitation such that the $D(\omega_1, \omega_2, \omega_3)$ function for the primary response acceleration is adequately approximated. It should be noted that the substitute excitation and the original excitation are both delta-correlated,

so that they differ only in probability distribution.

The term "equivalent linearization technique" as generally used in analysis of nonlinear vibrations refers to a somewhat different method from the "linear substitute method" used here. The former term is often used to refer to some version of the Krylov and Bogoliubov method [1943], in which the parameters of the equivalent linear system are obtained by minimizing some measure of the difference between the original and the linearized system. The RMS value of the response of the "equivalent linear system" can then be found and the power spectral density can also be approximated [Caughey 1959, Spanos and Iwan 1978]. In this study, the linear substitute system also has a substitute excitation. This makes it infeasible to evaluate parameters by a strict minimization technique, so more intuitive and approximate methods are used. Also, the linearization has been extended for approximating the absolute acceleration in the mean square sense, whereas linearization has usually concentrated on displacement and velocity response.

In some situations a much simpler concept is used in lieu of matching the $D_{\ddot{z}}(\omega_1, \omega_2, \omega_3)$ function at any particular point. Recall that the COE is a normalized fourth order cumulant for the special case when all time arguments are the same, $k_4(t,t,t,t)$, and is the triple integral of the $D(\omega_1, \omega_2, \omega_3)$ function over the entire frequency space. Thus, a good approximation of $D_{\ddot{z}}(\omega_1, \omega_2, \omega_3)$ would necessarily give a good approximation of the COE of $\ddot{z}$ (although the inverse is not necessarily true). In some situations one can determine some parameters in an approximation of $D_{\ddot{z}}(\omega_1, \omega_2, \omega_3)$ on the basis of matching the approximate COE to a simulated value. Matching of the COE value is a reasonable condition to impose on any good

approximation for $D(\omega_1, \omega_2, \omega_3)$, and COE matching is generally much simpler than D matching, even along a prescribed line in the ω space. The idea involved here is exactly equivalent to noting that matching a target variance value is a reasonable condition for any good approximation of a target $S(\omega)$ function.

V-2 Simulation Results for COE of Secondary Response:

Before proceeding to the linear substitute method for the P-S system, it is appropriate to summarize the results from simulation and seek to understand the physical phenomenon of secondary response.

V-2-1 Cascade Analysis :

The simulation results for the coefficient of excess of secondary response, $COE(u)$, versus the frequency ratio (ω_s/ω_p) can be found in figs. 5.1 to 5.6 for the BLH systems with $\alpha = 0.5$ and $1/21$ and with the excitation level varied to give the Y/N and σ_x/Y values shown. The other curves on these figures represent analytical approximations which will be explained later.

It can be seen from the figures that the $COE(u)$ is nearly 0 (Gaussian) at a low frequency ratio, goes to an asymptotic value when the frequency ratio becomes large (usually about 5 or 6), and generally has a peak (local extremum) at some intermediate frequency. At low ω_s/ω_p values, the secondary response (u) is proportional to the absolute displacement of primary response $(x + y)$. The low frequency $COE(u)$ values show that $x + y$ is essentially normal. At first this may seem surprising, but it can be explained by considering the magnitudes of the

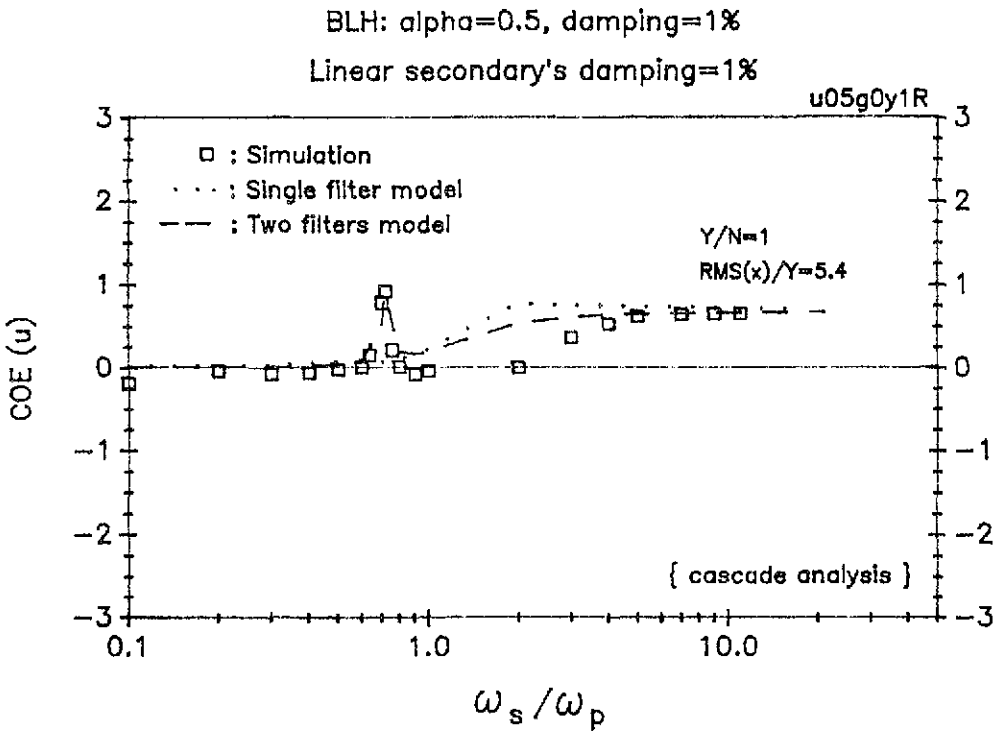

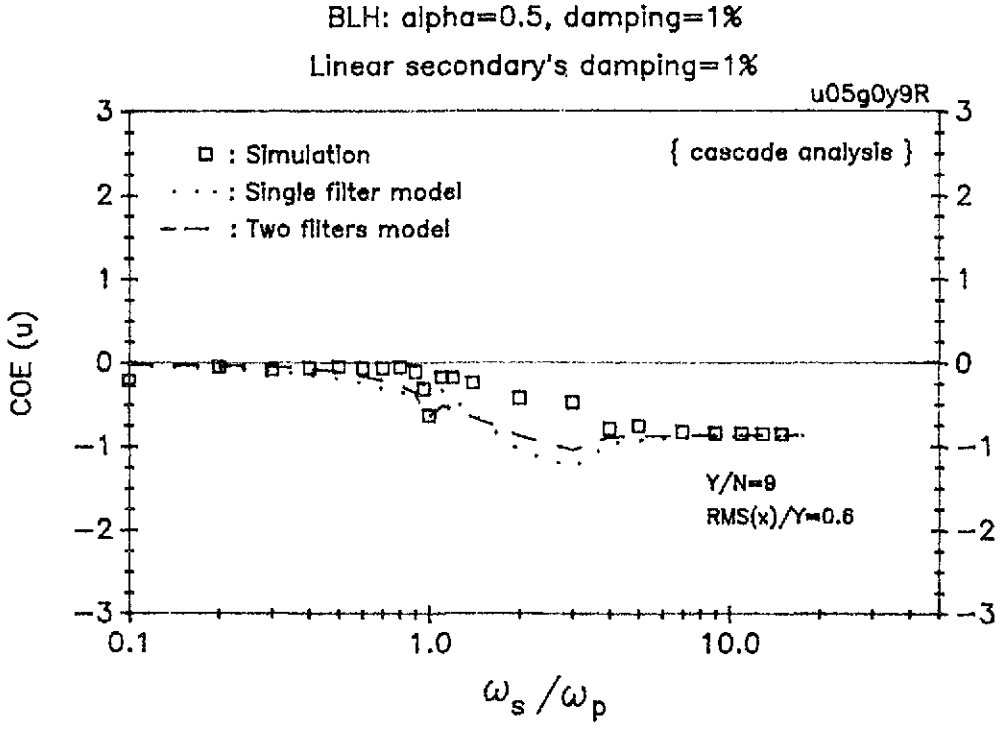

Fig. 5.1 COE for secondary response, α=0.5

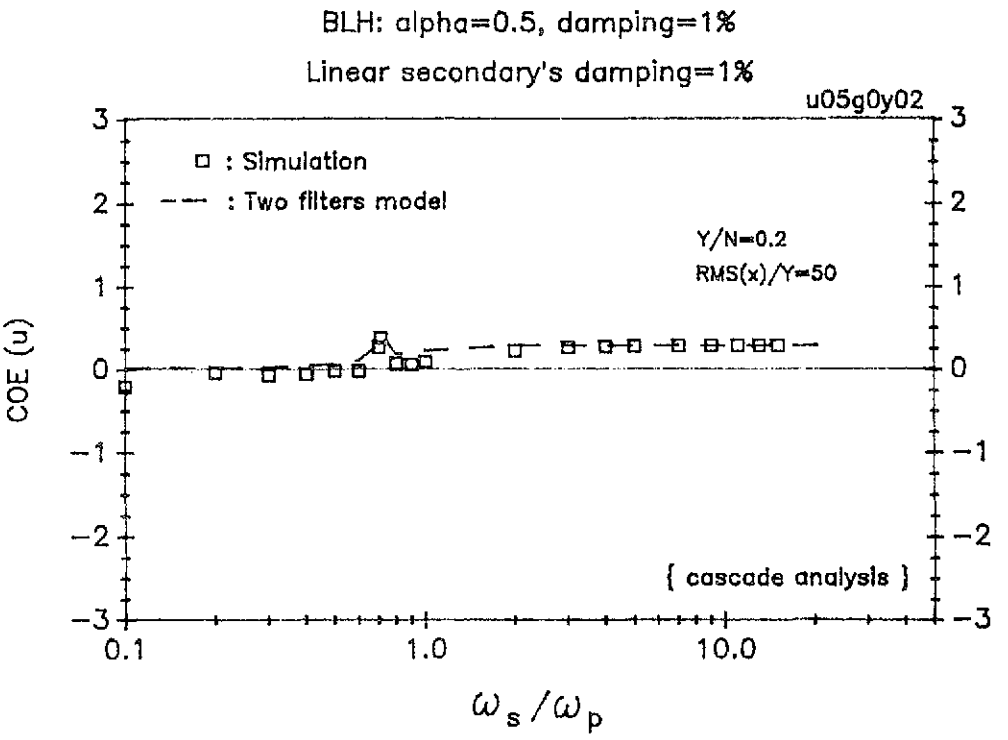

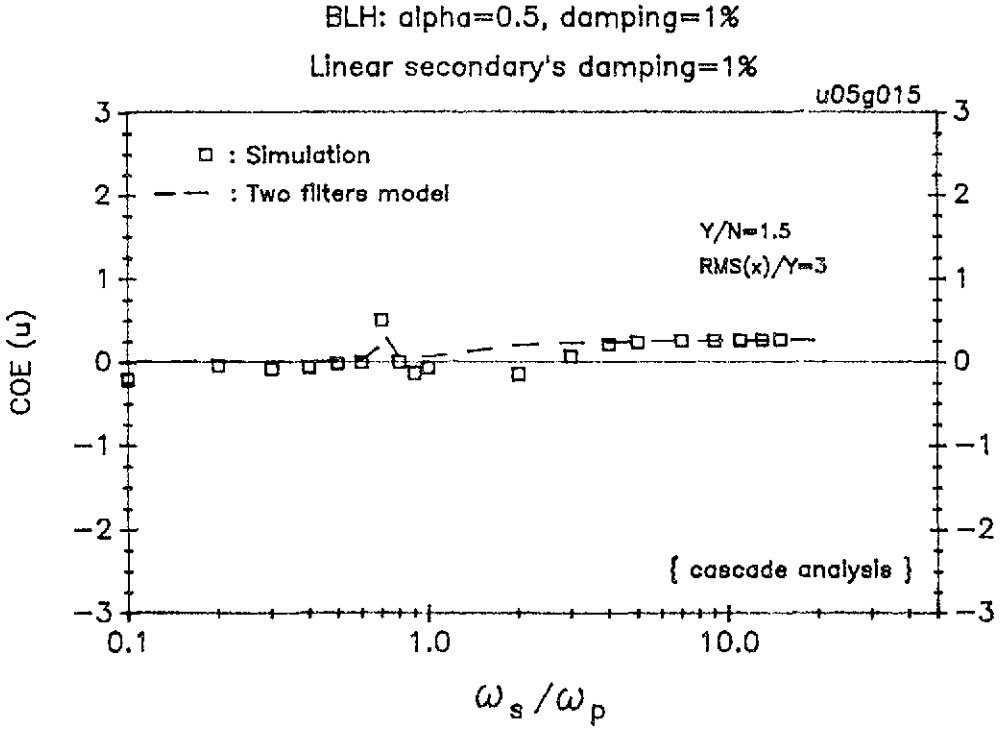

Fig. 5.2 COE for secondary response, α=0.5

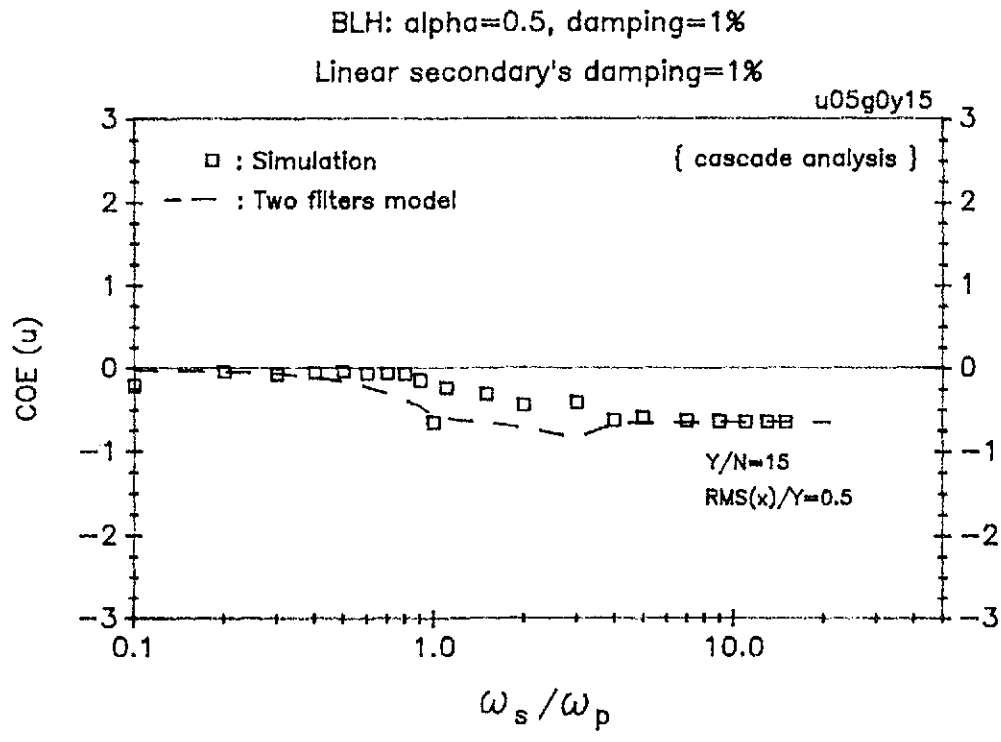

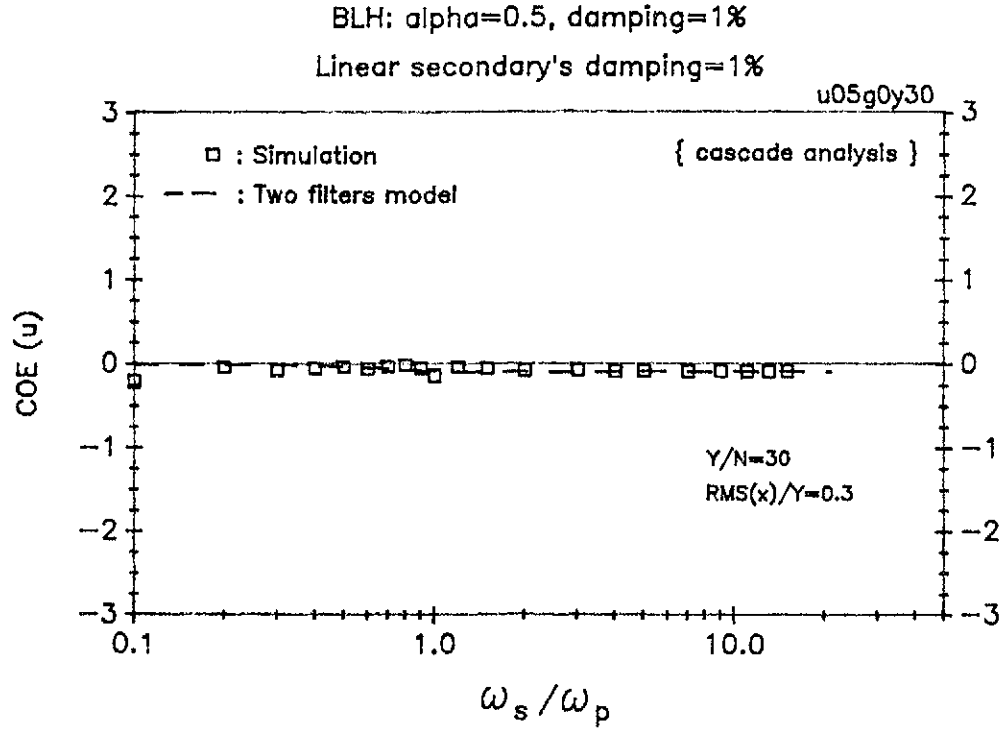

Fig. 5.3 COE for secondary response, α=0.5

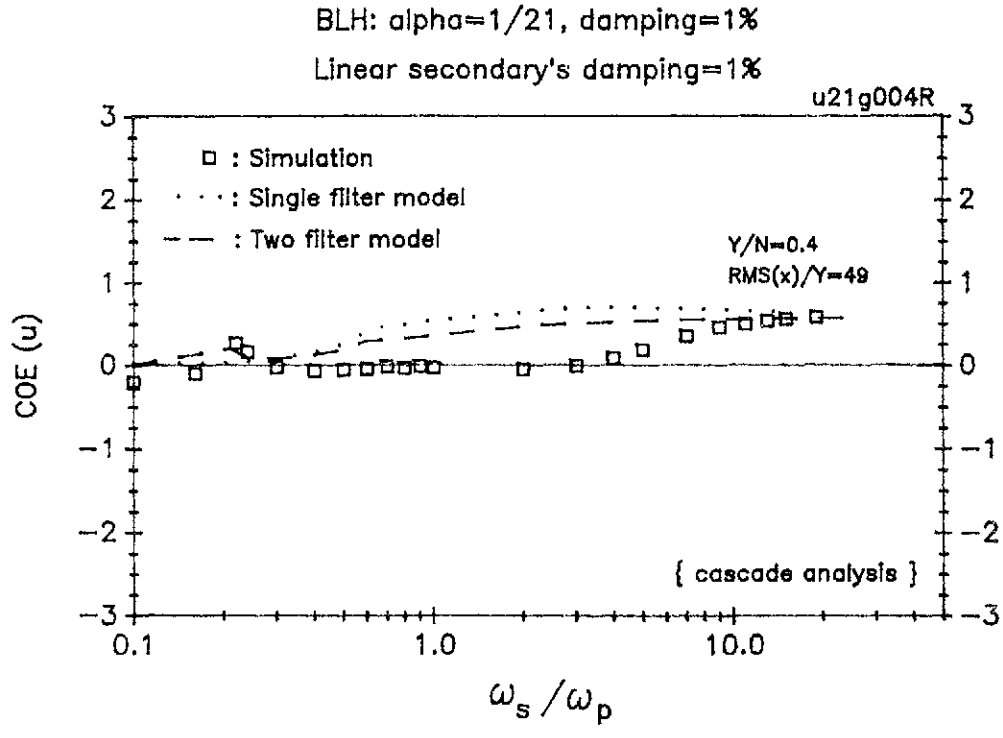

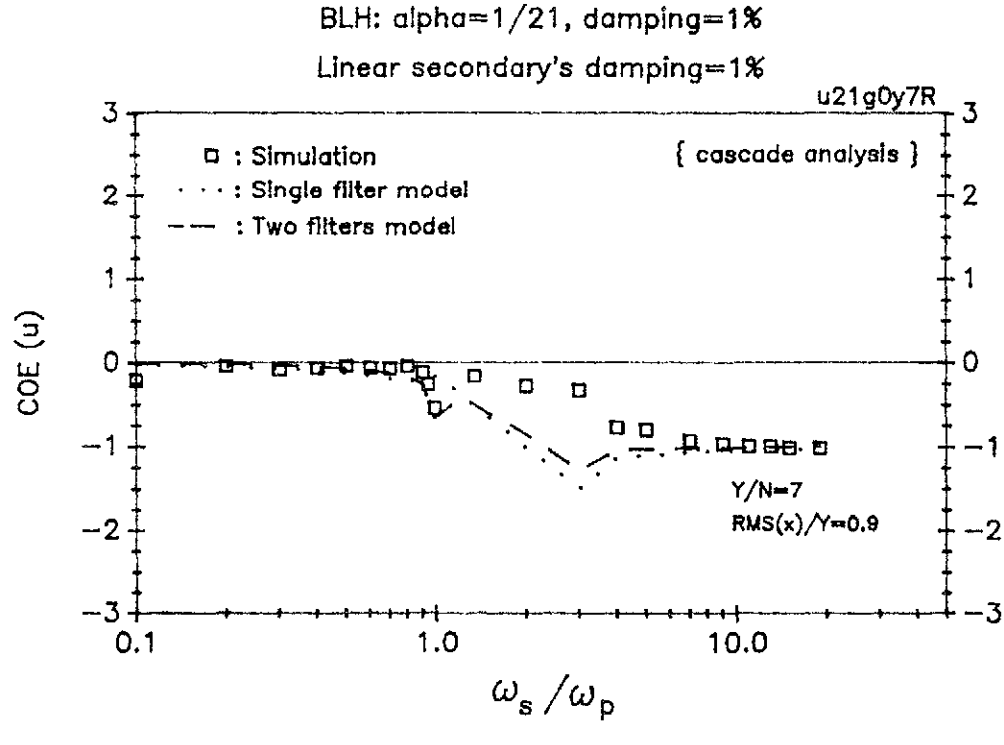

Fig. 5.4 COE for secondary response, α=1/21

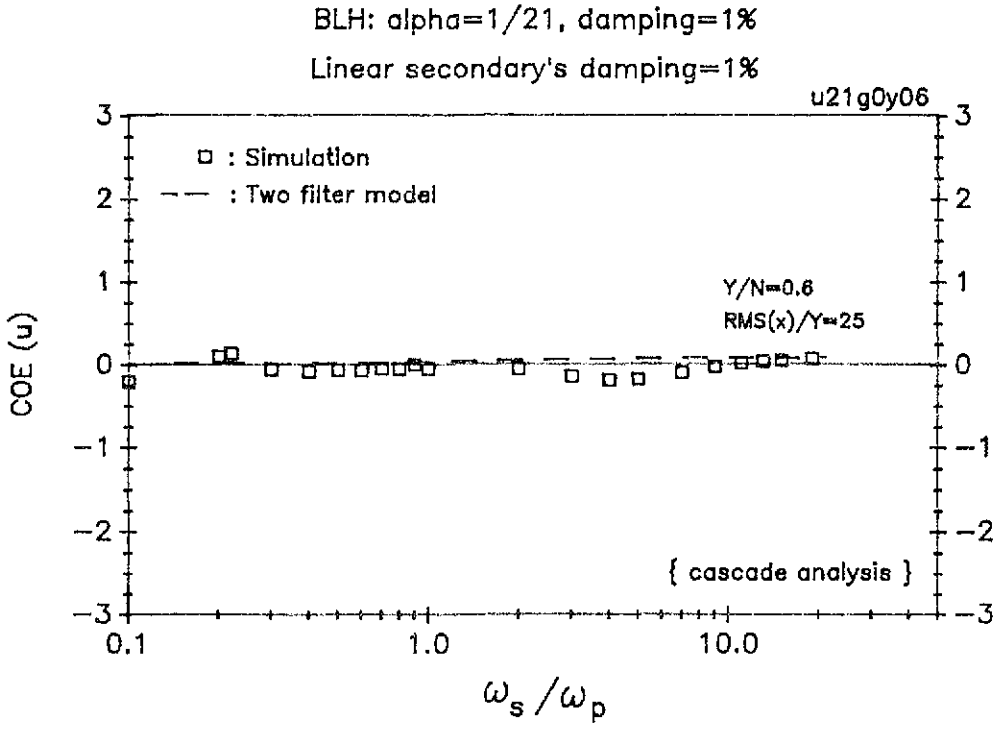

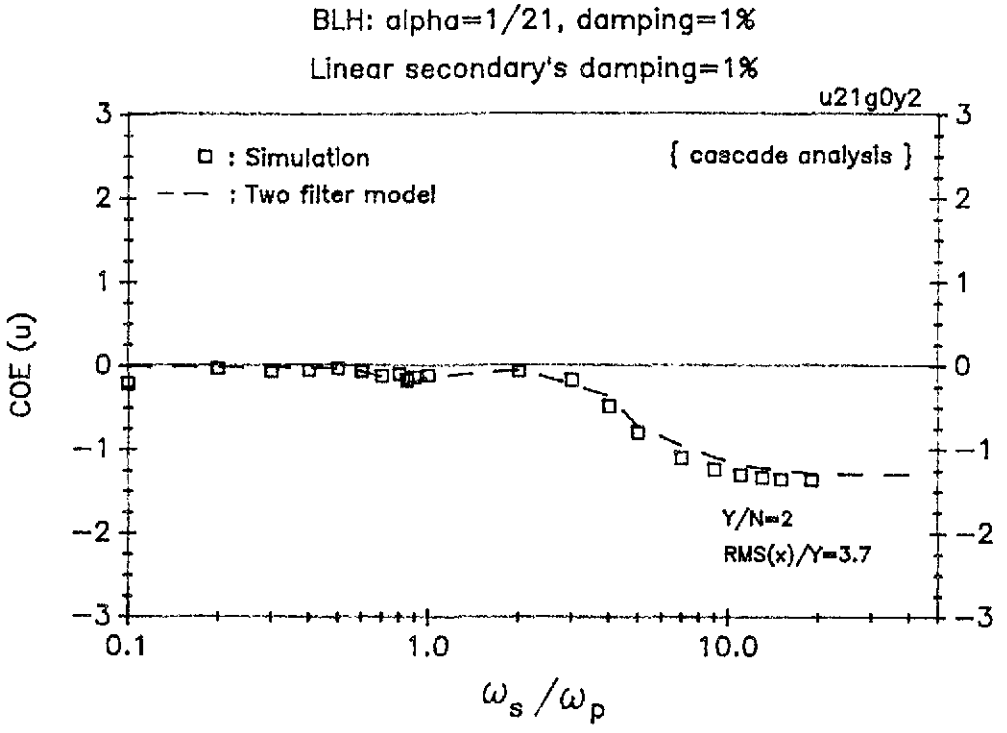

Fig. 5.5 COE for secondary response, α=1/21

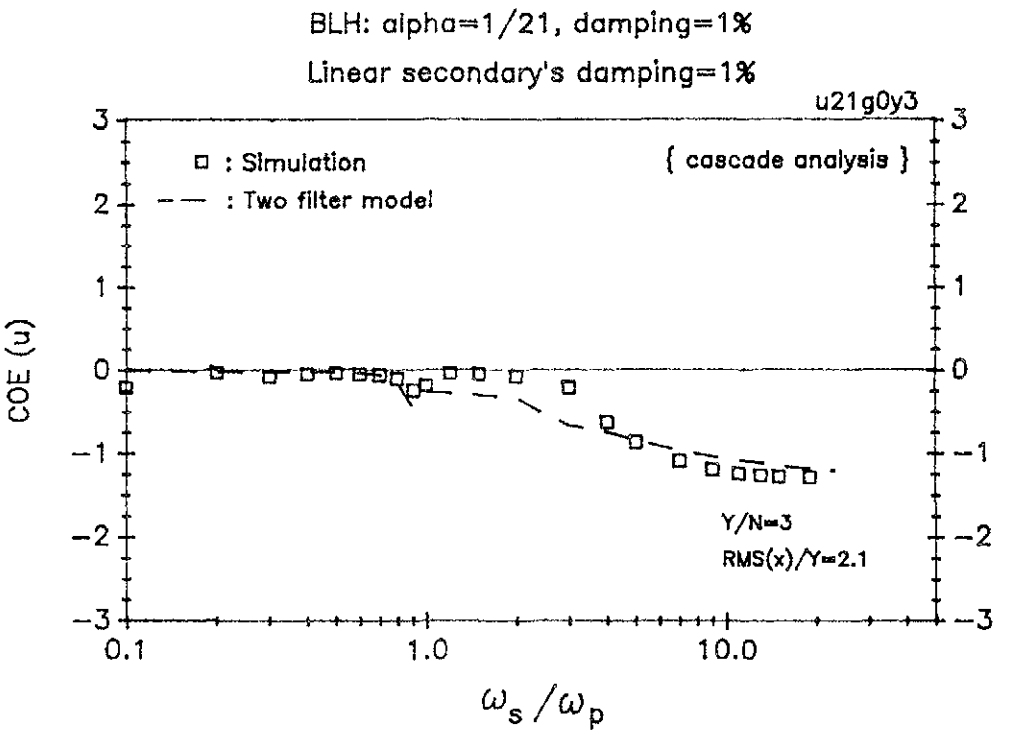

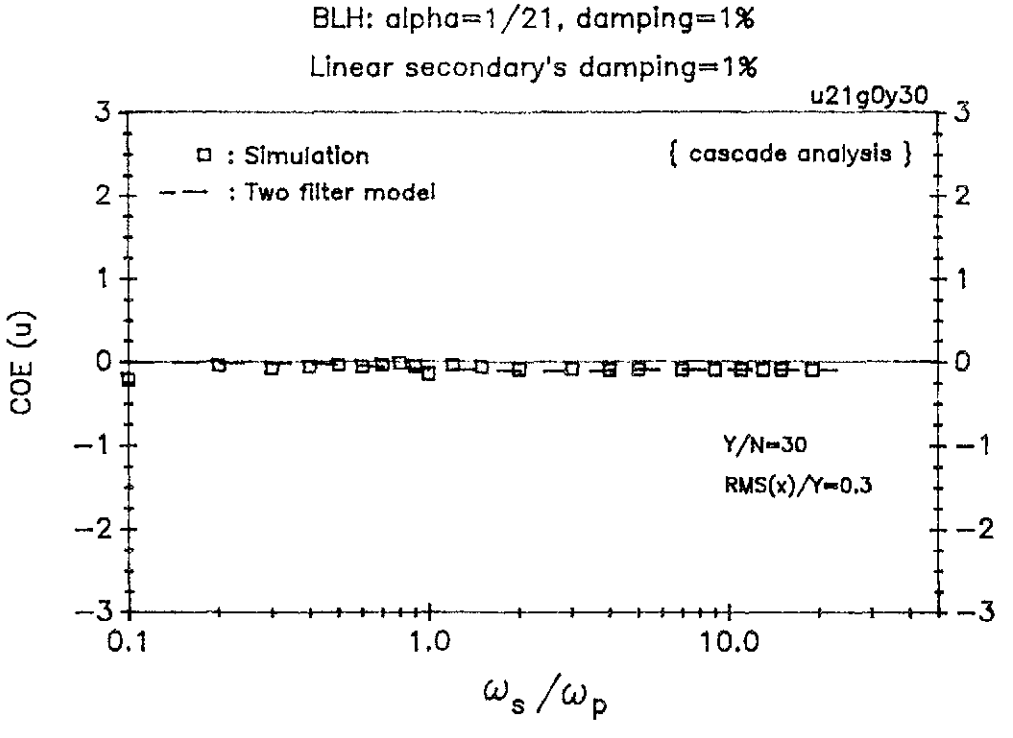

Fig. 5.6 COE for secondary response, α=1/21

component terms. In particular, consider the variances. Since the variance of the normal delta correlated excitation, y, is infinity compared to a finite variance of the nonnormal displacement, x, the sum should be dominated by y, so should be nearly normal. When the secondary becomes very stiff, u becomes proportional to the primary absolute acceleration ($\ddot{x} + \ddot{y}$ or $\ddot{z}$), and the $COE(\ddot{z})$ is usually nonnormal because of the nonlinearity in the primary system. The COE of primary absolute acceleration has been mentioned in Section II, and the values there agree with the asymptotic values in figs. 5.1 to 5.6. It is presumed that the local peak of $COE(u)$ at an intermediate frequency is due to an effective "tuning" between the secondary system and a "resonant" frequency of the nonlinear primary system. This resonant frequency, which will be denoted by ω_r, is smaller than ω_p, particularly for small Y/N values. Note that the tuning peak value of $COE(u)$ has the same sign as the $COE(u)$ for $\omega_s >> \omega_p$.

The simulation values in figure 5.7 illustrate the $COE(u)$ values at tuning for $\alpha = 0.5$ and $\alpha = 1/21$. The tuning $COE(u)$ values are plotted versus σ_x/Y for the response of the primary system. In general, each tuning value occurs for a different frequency ratio, and these ω_s/ω_p values are given in parentheses adjacent to data points on the figures. It may be noted that $COE(u)$ varies from negative values for small σ_x/Y to positive values for large σ_x/Y. This is similar to the trends previously found for $COE(\ddot{z})$ (Chen and Lutes 1988) as shown in figure 2.1, but the magnitudes of the COE are different. The $COE(u)$ changes sign at $\sigma_x/Y \simeq 2$ for $\alpha = 0.5$, and $\sigma_x/Y \simeq 25$ for $\alpha = 1/21$. The most significant nonnormality of secondary response at tuning can be up to $COE(u) = 1$, which occurs at σ_x/Y values of 5 to 15 for $\alpha = 0.5$, and down to $COE(u) = -1$ at σ_x/Y about 0.5

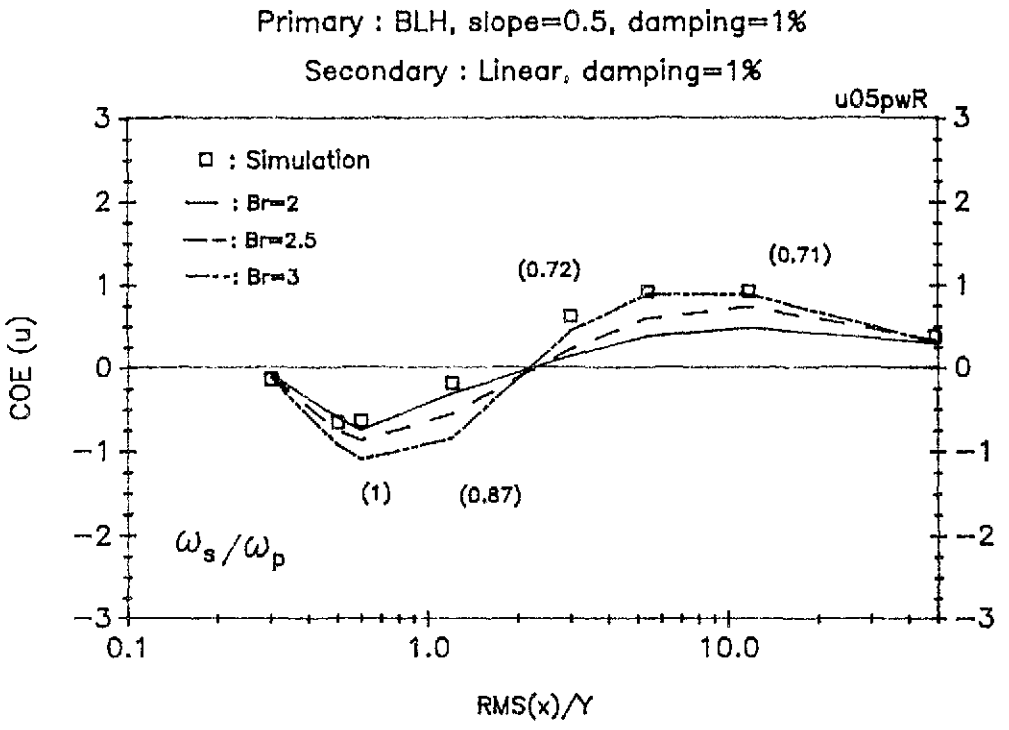

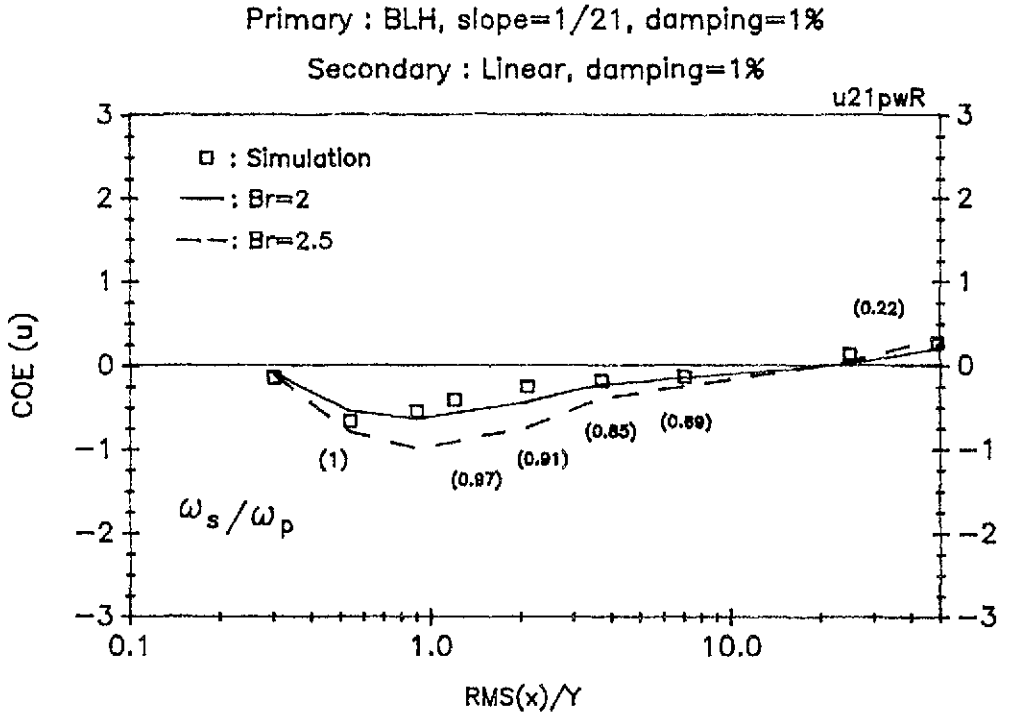

Fig. 5.7 COE at tuning for secondary response

for both α values. The tuning frequencies, ω_s/ω_p, are usually smaller than unity since the resonant frequency of a yielding BLH system is less than ω_p. Normally, ω_s/ω_p decreases as the excitation level is increased and varies from 1 to 0.71 for $\alpha = 0.5$ and 1 to 0.22 for $\alpha = 1/21$. The other information in figure 5.7 relates to an analytical model which will be discussed later.

It is interesting to note that the $COE(u)$ values for $\alpha = 1/21$ are generally smaller than for $\alpha = 0.5$, indicating that an increase of the second slope, α, has increased the nonnormality of secondary response in this case. This is consistent with the earlier result that the nonnormality of primary absolute acceleration (input to the secondary system) is more significant for the $\alpha = 0.5$ case [Chen and Lutes 1988].

v-2-2 Noncascade Analysis :

The basic assumption of the P-S system is that the mass ratio m_s/m_p is relatively small such that the interaction between primary and secondary can usually be neglected. For RMS values, it has been shown that ignoring the interaction effects would be acceptable so long as the frequencies of the two systems are not close, but a significant error on the conservative side may occur when tuning exists [Crandall and Mark 1963, Kelly and Sackman 1978]. For COE values, however, the effects of interaction on the nonnormality of the secondary system is of interest and is investigated in this Section.

For the noncascade study of P-S systems, the Rugge-Kutta method has been employed for solving the coupled BLH primary and linear secondary in the

simulation, as has been mentioned in Section III. The first case that has been studied is for a mass ratio of $\eta = 1\%$. The $COE(u)$ values, along with analytical results which will be discussed later, are shown in fig. 5.8 for both $\alpha = 0.5$ and $1/21$. It can be seen that the effects of interaction are significant at tuning, for which the change in the COE value can be 50% for the 1% mass ratio. However, the influences of the secondary system are relatively small at other frequencies. Note that in the asymptotic frequency range there is almost no effect due to the existence of the secondary system. Therefore, the study of interaction effects on nonnormality can be focused on the tuning situation only. Since a 1% mass ratio is usually an upper bound for P-S systems and cascade analysis ($\eta = 0$) is the lower bound, another intermediate mass ratio of 0.1% has also been investigated. For different excitation levels, the tuning peak values of the COE of secondary response have been studied from both simulation and the analytical approach. Figures 5.9 and 5.10 illustrate the results from simulation and from an analytical model using $\eta = 0$, 0.1%, and 1% for different excitation levels.

V-3 Single Linear Filter Model:

Figure 5.11 illustrates the principle of using a linear substitute method for the analysis of a P-S system. The basic idea is to use a linear filter having a nonnormal excitation to replace the BLH primary element having a normal excitation; with the hope that both the second and the fourth order cumulants of the primary absolute acceleration for the substitute system will match those of the original system.

The choice of the linear substitute element has been primarily based on matching the power spectral density (or its area which is the mean square value)

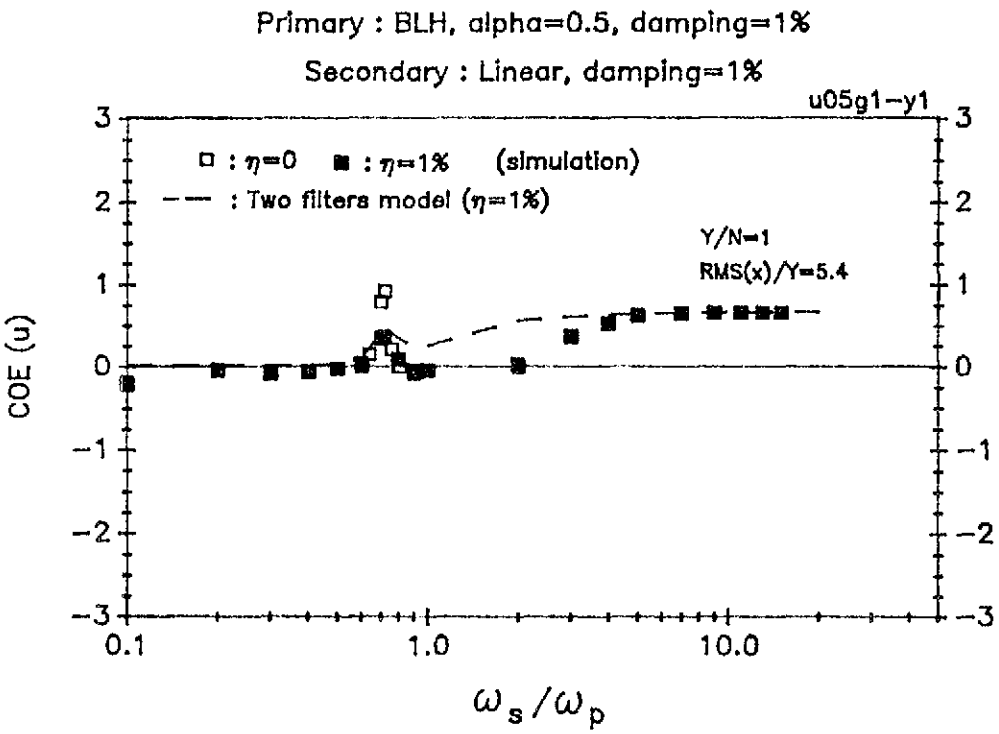

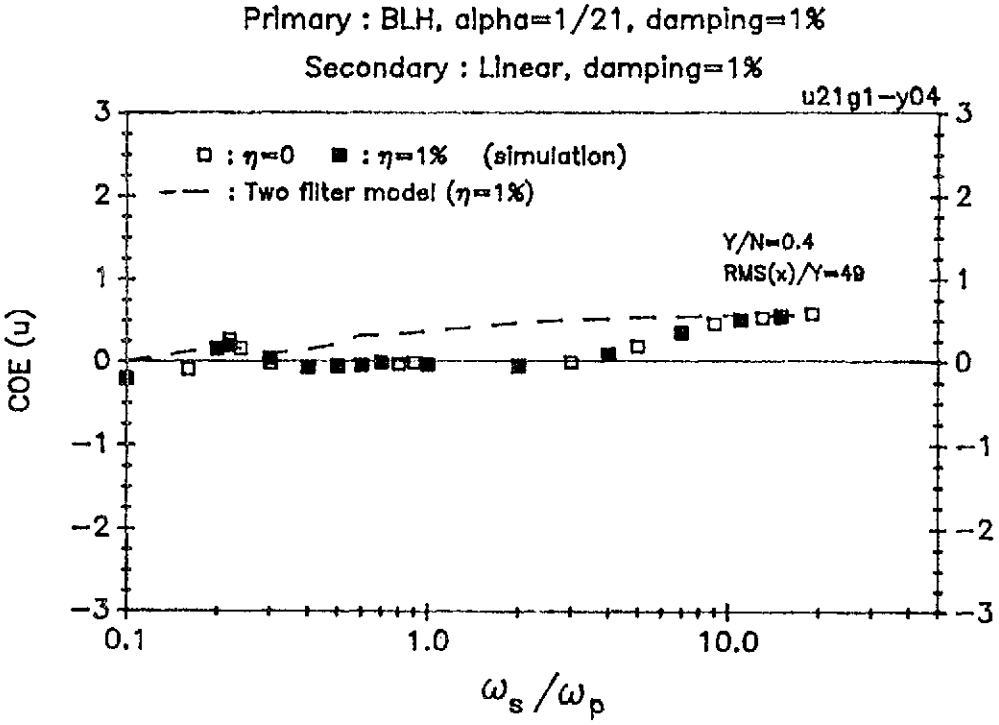

Fig. 5.8 COE of secondary response for noncascade analysis

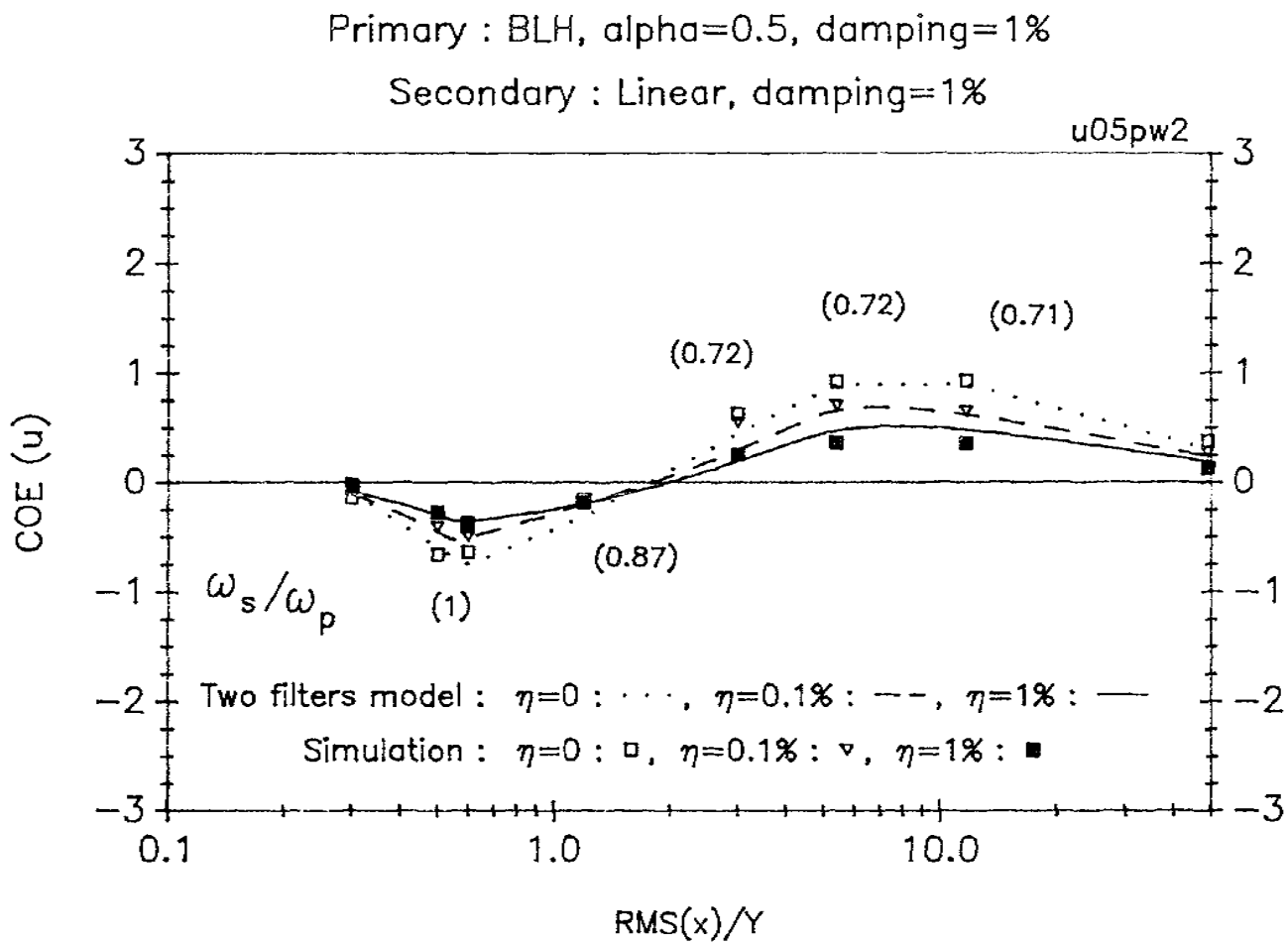

Fig. 5.9 Noncascade COE at tuning, α=0.5

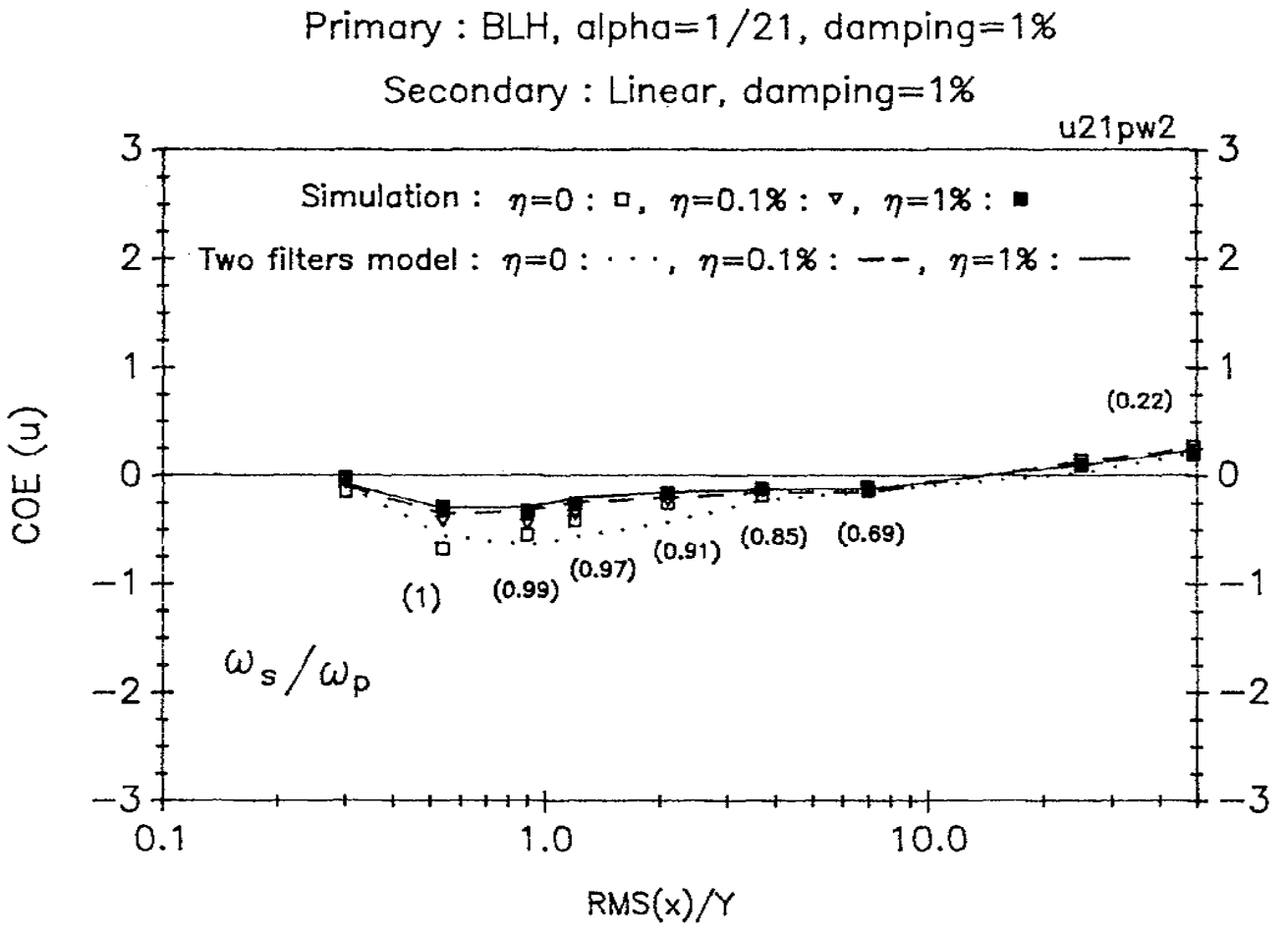

Fig. 5.10 Noncascade COE at tuning, α=1/21

• Simulation:

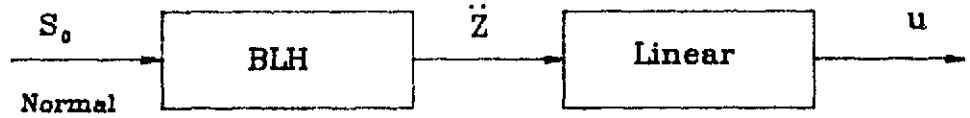

• Single Linear Filter:

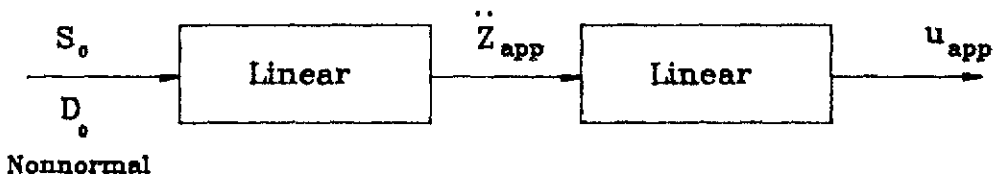

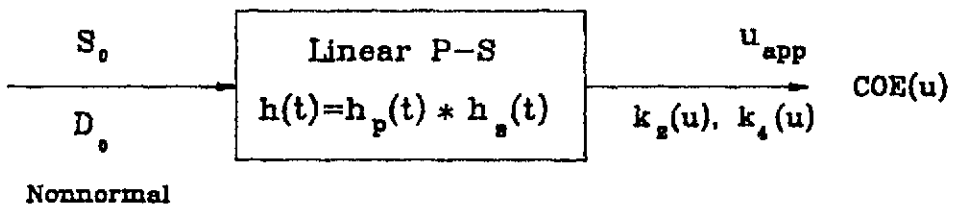

Fig. 5.11 Linear substitute method of P–S analysis

of the primary absolute acceleration. A third order linear substitute system has been used in some previous studies [Hseih 1979, Lutes and Jan 1983] for predicting the power spectral density for the response displacement of a BLH system. This model was considered for approximating the power spectral density of response acceleration, along with a second order linear substitute system with parameters chosen to achieve approximate matching of the RMS values of velocity and absolute acceleration of responses (Appendix A). It was found [Chen 1990] that the response of the second order linear system better approximates that of the BLH system, especially when α is small (like 1/21). Therefore, the second order linear system will be employed in the current study as the linear substitute system.

A delta correlated excitation with parameter value D_0 (see eq. 2.32) was chosen in this study. The value of D_0 was chosen such that the model matched the COE of the primary response acceleration. Let $k_n(\cdot)$ denote the stationary nth cumulant function. Since $COE(\ddot{z})$ or $k_4(\ddot{z})$ is known, the constant D_0 can be obtained from the equation:

$$k_4(\ddot{z}) = (2\pi)^3 D_0 \int_0^\infty h_p^4(t)dt \tag{5.1}$$

in which $h_p(t)$ is the impulse response function for the primary acceleration. The h_p for the second order linear substitute system can be found in Appendix A.

After the nonlinear primary of the P-S system has been replaced by a linear substitute system, the fourth and second response cumulants of the secondary response ($k_4(u)$ and $k_2(u)$) can be calculated by applying any linear method to the fourth order system representing the composite of the linear secondary and the

linearized primary systems. In this study the cumulant functions for the fourth order linear system subjected to delta correlated excitation were found from state space moment equations [Chen 1990]. Figures 5.1 and 5.4 show representative COE values of the secondary response from this single linear filter substitute method for comparison with the results of cascade computer simulation. It can be observed that the linear model works well for the two limiting ranges of $\omega_s << \omega_p$ and $\omega_s >> \omega_p$.

When $\omega_s << \omega_p$, the displacement response of the secondary system is proportional to the absolute displacement of the primary response, which is nearly Gaussian in general. Thus, $COE(u)$ approaches zero for $\omega_s << \omega_p$, and this is true for either a linear or nonlinear primary. At the other extreme of $\omega_s >> \omega_p$, the displacement of the secondary response is proportional to the absolute acceleration of the primary response. Recall, though, that the linear substitute primary has been chosen to match $COE(\ddot{z})$ to that of the nonlinear primary. Thus, the substitute system must match $COE(u)$ for $\omega_s >> \omega_p$. For intermediate values of ω_s/ω_p, though, the single linear filter model in figs. 5.1 and 5.4 completely misses the tuning peak of $COE(u)$ which appears in the simulation data.

If the linear substitute model had adequately matched the general D function (or Q function) of the BLH primary acceleration, then it would also have have matched the nonnormality of the secondary response of the original system. In fact, though, the $COE(u)$ for the simulated secondary response was not matched by the response of this particular linear model. Thus, the D function for the primary acceleration must not have been adequately matched even though $k_4(\ddot{z})$ was matched. A case of $\alpha = 0.5$, $\beta_p = 1\%$ and $Y/N = 1$ has been studied in order to experimentally investigate the matching of the primary acceleration D functions

between the linear model and the BLH system. Fig. 5.12 illustrates the "smoothed" $D_{\ddot{z}}$ function from this single linear filter model for comparison with the $D_{\ddot{z}}$ function from the BLH system (periodogram analysis) as shown in fig. 4.3. From the contour maps, it can be observed that the BLH $D_{\ddot{z}}$ function is not accurately matched by the linear system especially, near the peak, even though the total volume under the $D_{\ddot{z}}$ (i.e., the $COE(\ddot{z})$ value) has been matched.

The failure of the single linear filter model to predict a tuning peak of $COE(u)$ can perhaps best be seen by considering the response of the secondary system to an "equivalent" delta correlated excitation. The idea of an equivalent delta correlated excitation is to seek to accurately model $S_u(\omega)$ and $D_u(\omega_1, \omega_2, \omega_3)$ only in the neighborhood of the major peaks of these two functions. If almost all the significant contributions to $k_2(u)$ and $k_4(u)$ come from these neighborhoods, then this technique will give accurate estimates of the cumulants. In general one can expect the approximation to be acceptable when the secondary system is lightly damped, since $S_u(\omega)$ will then be very large for $\omega \simeq \pm\omega_s$ and $D_u(\omega_1, \omega_2, \omega_3)$ will be very large near $(\omega_s, \omega_s, -\omega_s)$ and its five symmetric points (see Section II-2-2). The constant values for $S_{\ddot{z}}$ and $D_{\ddot{z}}$ for this delta correlated excitation of the secondary should then be $S_{\ddot{z}}(\omega_s)$ and $D_{\ddot{z}}(\omega_s, \omega_s, -\omega_s)$ in order to properly model S_u and D_u in the neighborhoods of these points. It should be noted that this delta correlated excitation approach may not work well if $S_{\ddot{z}}(\omega_s)$ and $D_{\ddot{z}}(\omega_s, \omega_s, -\omega_s)$ are much smaller than $S_{\ddot{z}}$ and $D_{\ddot{z}}$ at some other points in the frequency space. For example, if $S_{\ddot{z}}(\omega_r) >> S_{\ddot{z}}(\omega_s)$ then $S_u(\omega)$ can be expected to have major peaks both near $\omega = \pm\omega_r$ and near $\omega = \pm\omega_s$, and the delta correlated excitation approach would ignore the contribution of the former of these peaks.

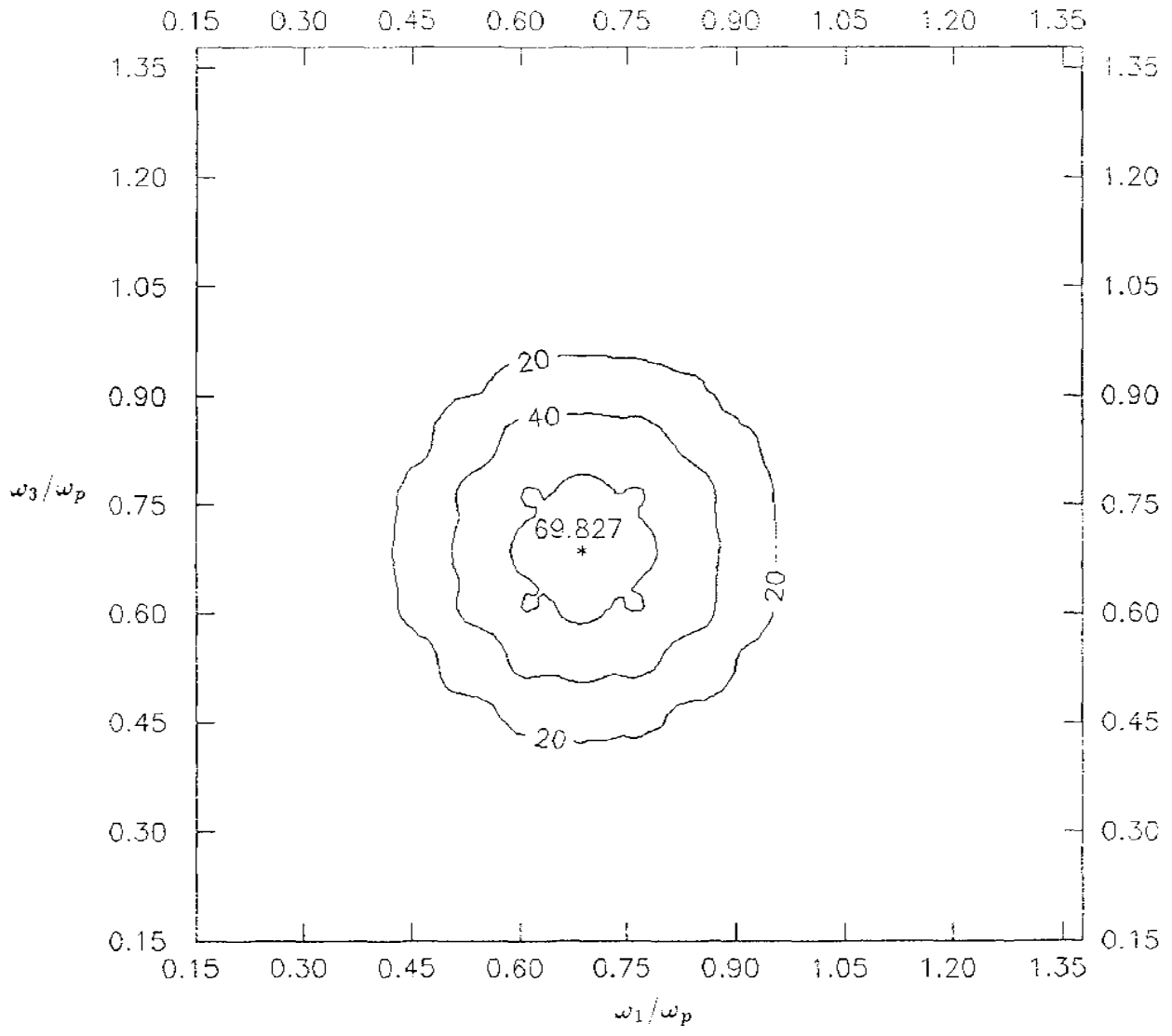

Fig. 5.12 Trispectrum of single filter model, $D_{\ddot{z}}(\omega_1, -\omega_1, \omega_3)$

One expects $S_{\ddot{z}}(\omega)$ and $D_{\ddot{z}}(\omega_1,\omega_2,\omega_3)$ to achieve their largest values near points ω_r and $(\omega_r,\omega_r,-\omega_r)$, respectively. So long as $S_{\ddot{z}}(\omega_s)$ and $D_{\ddot{z}}(\omega_s,\omega_s,-\omega_s)$ are not much much smaller than $S_{\ddot{z}}(\omega_r)$ and $D_{\ddot{z}}(\omega_r,\omega_r,-\omega_r)$, the equivalent delta correlated excitation approximation gives

$$S_u(\omega) \simeq S_{\ddot{z}}(\omega_s)|H_s(\omega)|^2 \tag{5.2a}$$

and

$$D_u(\omega_1,\omega_2,\omega_3) \simeq D_{\ddot{z}}(\omega_s,\omega_s,-\omega_s)H_s(\omega_1)H_s(\omega_2)H_s(\omega_3)H_s(-\sum_{j=1}^{3}\omega_j) \tag{5.2b}$$

For the single linear filter model for the primary these can be rewritten as

$$S_u(\omega) \simeq S_0|H_p(\omega_s)|^2|H_s(\omega)|^2 \tag{5.3a}$$

and

$$D_u(\omega_1,\omega_2,\omega_3) \simeq D_0|H_p(\omega_s)|^4 H_s(\omega_1)H_s(\omega_2)H_s(\omega_3)H_s(-\sum_{j=1}^{3}\omega_j) \tag{5.3b}$$

Integrating eq. 5.3a with respect to ω, and eq. 5.3b with respect to ω_1,ω_2 and ω_3 then gives the approximations for $k_2(u)$ and $k_4(u)$. Dividing the latter of these by the former squared gives the approximation of $COE(u)$. Note, though, that the characteristic H_p of the linear primary enters eqs. 5.3a and 5.3b only as the constant value $H_p(\omega_s)$ and it completely cancels out of the $COE(u)$ approximation. Thus, using the equivalent delta correlated excitation of the secondary system causes

$COE(u)$ to be completely independent of the characteristics of the single linear filter substitute primary system. In particular, $COE(u)$ is independent of ω_r and this precludes the possibility of obtaining a $COE(u)$ peak at tuning ($\omega_s \simeq \omega_r$).

It should be noted that $\omega_s << \omega_p$ and $\omega_s >> \omega_p$ are situations in which the equivalent delta correlated excitation approximation may not be justified, since they may give $S_z(\omega_s) << S_z(\omega_r)$ and $D_z(\omega_s, \omega_s, -\omega_s) << D_z(\omega_r, \omega_r, -\omega_r)$. As noted above, the single linear filter model does work well in these extreme cases. For $\omega_s \simeq \omega_r$, though, the equivalent delta correlated result should be reasonably accurate, and the absence of a tuning peak in $COE(u)$ appears to confirm this conclusion.

The tuning peaks of $COE(u)$ for the simulation data in figures 5.1 to 5.6 show that D_z must be more sharply peaked in the vicinity of $(\omega_r, \omega_r, -\omega_r)$ than was predicted by the single linear filter model. This is confirmed by the contour map comparison of D_z in figures 4.3 and 5.12 (even though the smoothing in these latter plots hides much of the details). The following section presents an alternate model chosen to give this more peaked D_z by using a more narrowband filter for the fourth cumulant.

V-4 Two Filters Model:

The fact that P-S frequency tuning causes a peak (local extremum) of the COE value of the secondary response provides evidence that the fourth cumulant of the primary response is more narrowbanded than is the second cumulant. In order to approximate this tuning peak, another model, called the two filters model, is

proposed as shown in figure 5.13. The only change from the single filter model is in the addition of a separate filter, $H_{p4}(\omega)$ for finding the fourth cumulant of $\tilde{z}$ in the analytical model. The parameters of this fourth cumulant filter are chosen on the basis of matching the peak COE value of the secondary response at tuning for cascade analysis.

V-4-1 Cascade Analysis:

The maximum values of $S(\omega)$ and $D(\omega, -\omega, \omega)$ appear to occur at essentially the same frequency, in general. Thus, the linear fourth cumulant filter will be taken to have the same resonant frequency as the second cumulant filter (as investigated in the previous section). This leaves the damping ratio (or bandwidth) as the only parameter to be determined for the fourth cumulant filter, and this can be chosen to match the height of the peak in $COE(u)$ at P-S tuning. A convenient way to present the results of this parameter choice will be as a bandwidth ratio, B_r, which is defined as the ratio of the damping of the second cumulant filter to the damping of the fourth cumulant filter. A preliminary study of the bandwidth ratio based on matching the tuning peak $COE(u)$ values showed that B_r should generally be in the range of 2 to 3. Figure 5.7 illustrates the estimates of $COE(u)$ at tuning by using several B_r values in the two filters model (The frequency ratios, ω_s/ω_p corresponding to these peak COE values are given in parentheses). Compared to the simulation data in the figure, it can be seen that the $COE(u)$ predictions obtained by using a single bandwidth ratio such as $B_r = 2.5$ may be acceptable for many purposes, but sometimes have significant errors. To obtain better estimates, one can use a larger B_r value (like 3) for $\alpha = 0.5$ when $\sigma_x/Y > 2$ and a smaller B_r

Two Filters Model :

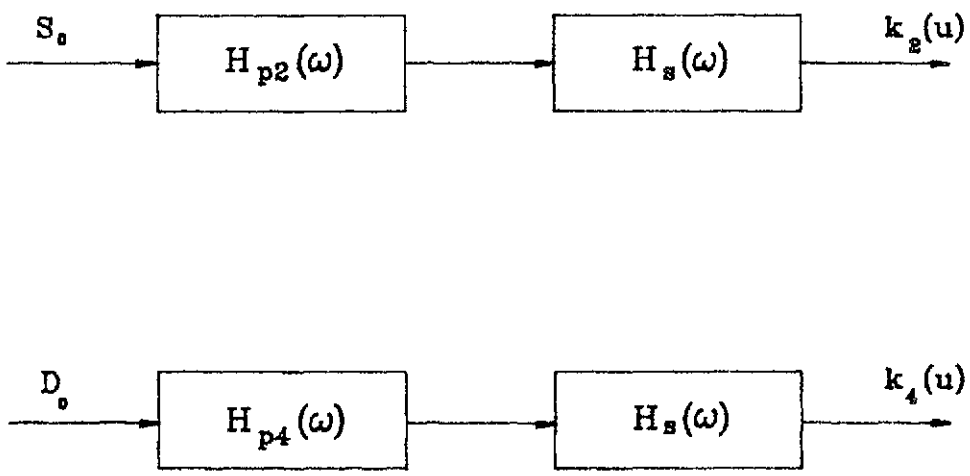

Fig. 5.13 Two linear filters model

value (like 2) for all the other situations shown.

Using the B_r as 2 and 3 (according to the preceding observations), $COE(u)$ values have been obtained for several different Y/N values for 1% damping and $\alpha = 0.5$ and $1/21$. These results from the two filters model are shown in figures 5.1 to 5.6 for comparison with those from simulation and with those from the single filter model (in figures 5.1 and 5.4 only). One can see that the $COE(u)$ at tuning has been significantly improved by using the two filters model with a narrower fourth cumulant filter.

It should be noted that theoretically B_r should go to unity in the two limiting cases: $Y \to \infty$ or 0, since the nonlinear primary tends to a linear system (a single linear filter primary) in these situations. However, the $COE(u)$ values also approach zero in these two extreme situations. Using $B_r = 2$ or 3 even in these situations seems to give acceptable errors in $COE(u)$, since the absolute values are so small. Table 5.1 shows all the parameter values used in the two filters model for the situations studied here.

Even though the tuning peaks of $COE(u)$ have been quite accurately matched by using the two filters model, the error in the $COE(u)$ for an intermediate frequency range (say $\omega_s \simeq 2\omega_p$) still has not been significantly improved. In order to allow more detailed investigation of this remaining discrepancy, the smoothed $D_{\bar{z}}$ function for the two filters model has been evaluated for comparison with the simulation results for the BLH system. Fig. 5.14 shows the "smoothed" $D_{\bar{z}}$ function contour plots for the linear model for the case: $\alpha = 0.5$, $\beta_p = 1\%$ and $Y/N = 1$. When this plot is compared with figs. 4.3 and 5.12, it can be observed that the peak

(a). BLH : $\alpha = 0.5$, $\beta_p = 1\%$:

Y/N	ω/ω_p	damping of k_2	damping of k_4	$D_0\omega_p/S_0^2$
30.	1.0	1.0 %	0.5 %	-30.04
15.	1.0	1.53 %	0.76 %	-139.84
9.	0.87	2.87 %	1.44 %	-101.64
1.5	0.72	8.61 %	2.87 %	10.0
1.	0.72	7.8 %	2.6 %	35.74
0.2	0.71	2.15 %	0.72 %	41.69

(b). BLH : $\alpha = 1/21$, $\beta_p = 1\%$:

Y/N	ω/ω_p	damping of k_2	damping of k_4	$D_0\omega_p/S_0^2$
30.	1.0	1.0 %	0.5 %	-32.55
7.	0.99	4.75 %	2.4 %	-72.48
3.	0.91	17.25 %	8.6 %	-33.0
2.	0.85	50. %	25. %	-31.71
0.6	0.22	22.4 %	8.9 %	7.01
0.4	0.22	16.6 %	6.6 %	53.08

Table 5.1 Parameters in Two Filters Model

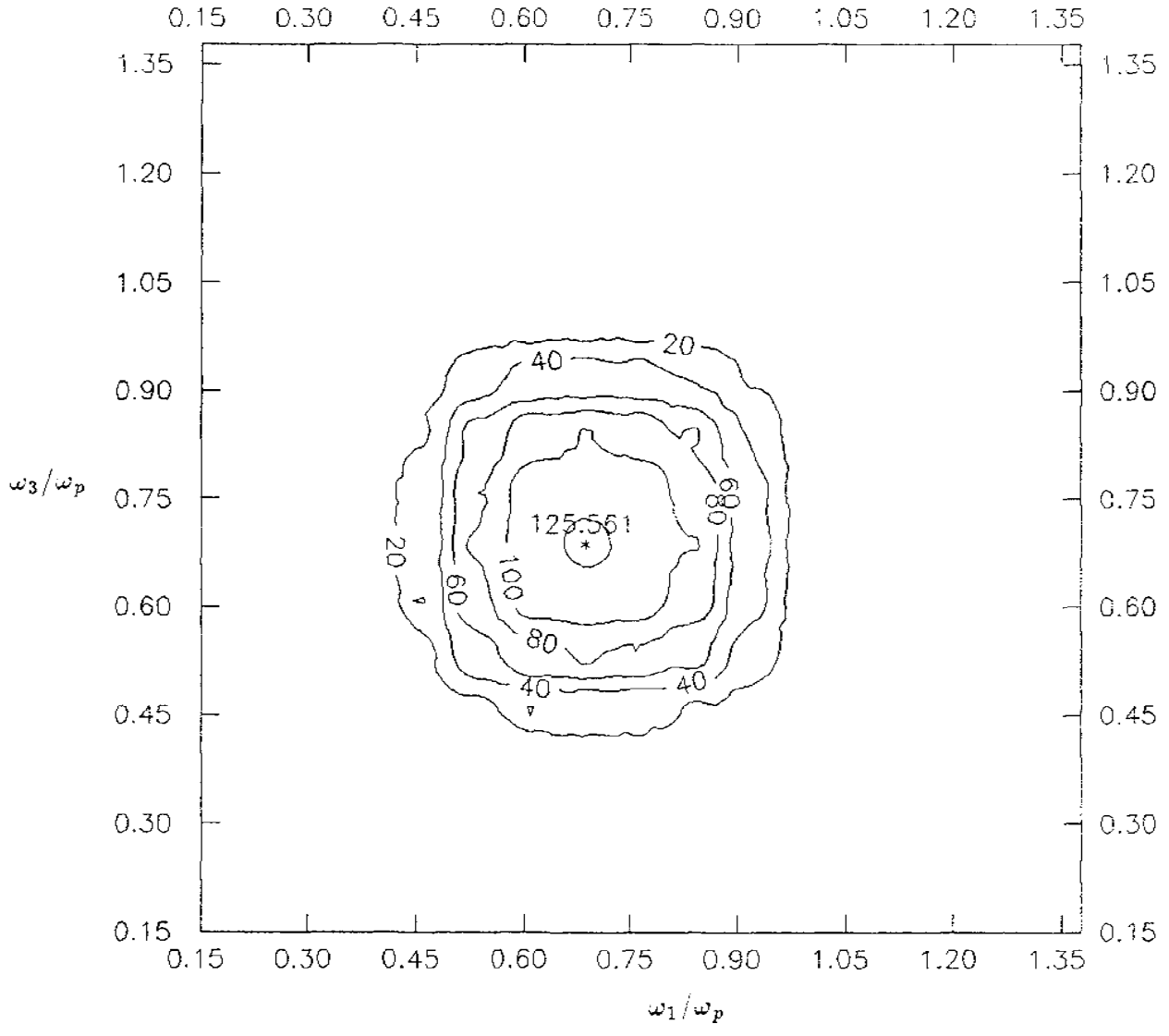

Fig. 5.14 Trispectrum of two filters model, $D_3(\omega_1, -\omega_1, \omega_3)$

in the contour map has been significantly improved by using the more narrowband fourth cumulant filter. However, figs. 4.3 and 4.4 also show negative D_z values on a "ring" area centered at $(\omega,\omega,-\omega)$ for a frequency ω higher than ω_r at the positive peak. These negative values do not appear in fig. 5.14. In fact, they could not possibly appear for any linear substitute primary since the trispectrum of the output of any linear model cannot be negative if the input constant D_0 is positive. This reveals an inherent shortcoming of any linear model for approximating the trispectrum of a BLH system. Namely, the BLH system sometimes has frequency regions giving a trispectrum of the "opposite" sign, and a linear model with delta correlated input never gives this behavior.

One can again consider the idea of an equivalent delta correlated excitation to seek to explain the discrepancy of the two filters model for intermediate frequencies above tuning. Consider $\alpha = 0.5$, $\beta_p = 1\%$ and $Y/N = 1$, since that is the situation for which the smoothed trispectrum from simulation has been presented (figs. 4.3 and 4.4). The negative values of $D_z(\omega,-\omega,\omega)$ for $\omega/\omega_p \simeq 1$ could be expected, based on the equivalent delta correlated excitation model, to give negative $COE(u)$ values for $\omega_s \simeq \omega_p$. Fig. 5.1 shows that this does, in fact occur. The results are not exactly in agreement with the delta correlated excitation predictions since the bandwidth of the secondary system is finite. Nonetheless, the negative D_z trispectrum values in the vicinity of $(\omega,-\omega,\omega)$ for $\omega \simeq \omega_p$ should be expected to reduce the $COE(u)$ values for ω_s anywhere in this vicinity. Since the linear model never gives these negative D_z values, it should overpredict the $COE(u)$ in this area.

Thus, one can conclude that the discrepancy of $COE(u)$ in the intermediate frequency range is inevitable when using the linear models. Fortunately, the linear

system estimate is always on the conservative side for positive $COE(u)$ values (which are of most interest), and the largest COE values usually occur either at tuning or in the asymptotic region. Thus, the discrepancy for intermediate frequencies may not be a problem for practical applications.

V-4-2 Noncascade Analysis:

The two filters model can be extended with little effort to provide a noncascade analytical approach, once the parameters of cascade analysis have been established. The model is illustrated in fig. 5.15 in which the parameters of the two linear substitute primary systems and of the nonnormal excitation can be obtained from the previous discussion. In particular $k_{p4} = k_{p2}$, with the value chosen according to eq. A.7, and $c_{p4} = c_{p2}/B_r$, with c_{p2} chosen according to eq. A.6. The influence of the secondary system can be studied by considering the mass ratio ($\eta = m_s/m_p$) in the state space equations, in which $\eta = 0$ was used for cascade analysis. From figs. 5.8, 5.9 and 5.10, it can be seen that these analytical predictions normally agree well with simulation results for different mass ratios.

Since the effects of interaction in P-S systems at tuning can be significant for the most nonnormal situations, the influence of the secondary system should be taken into account if the nonnormality of secondary response is significant. The two filters model seems to give a simple way to perform this analysis with reasonable accuracy.

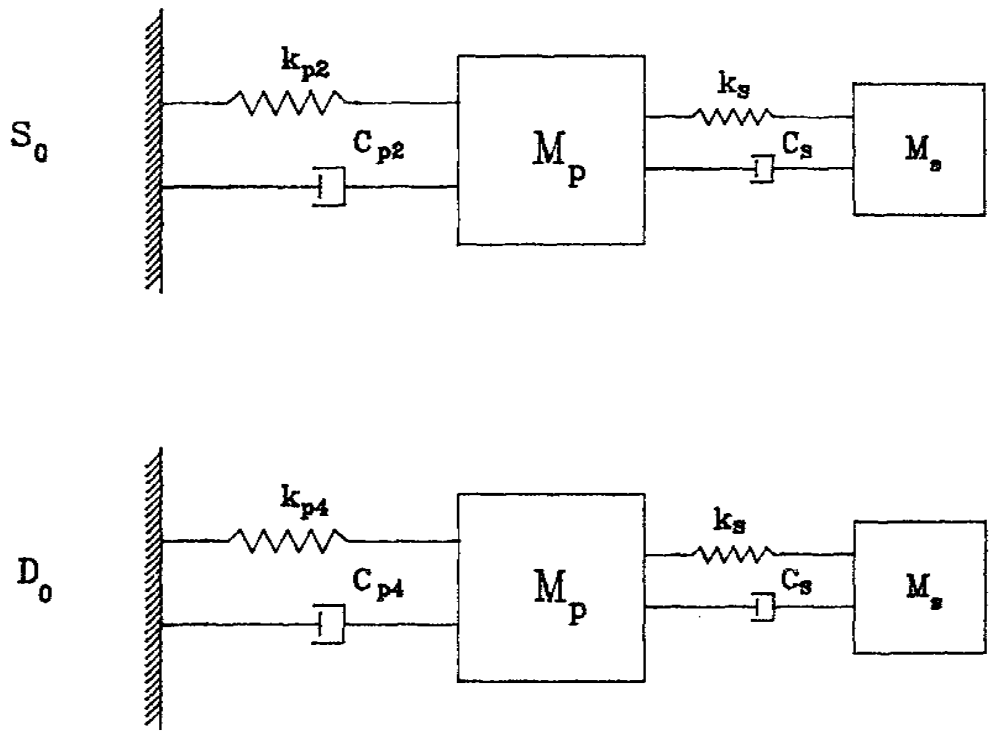

Fig. 5.15 Two filters model for noncasade analysis

V-5 Reliabilities Affected by Nonnormality:

Approximations were presented in Section II-4 which used COE information in order to obtain improved reliability estimates for both first-passage and fatigue reliability. Recall that the nonnormality correction factor (NCF) was defined as the ratio of the mean time to failure for normal process to the mean time to failure for a corresponding nonnormal process. This NCF was denoted by Q for first-passage and L for fatigue failure. Note that an NCF$>$ 1 denotes a situation in which neglecting nonnormality would be nonconservative, inasmuch as it would overpredict the life of the structure.

The magnitude of the Q and L values for the secondary system can be easily calculated by using the $COE(u)$ values presented earlier in this section along with the equations in Section II, or along with figs. 2.2 and 2.3. Results of this calculation are presented here for only a few of the situations studied, in order to demonstrate the extent to which yielding in the primary system can affect the reliability of the secondary system. Most of the results shown are for $\alpha = 0.5$, since the largest nonnormalities were observed in that situation.

As noted above, the most significant nonnormality of secondary response occurs when the secondary frequency (ω_s) is either tuned to a resonance of the primary system or is much larger than the frequency of the primary system. These two secondary frequency situations will be referred to as tuning and the asymptotic region, respectively. The numerical results for the nonnormality correction factors (NCF) are presented here only for these two critical situations. The NCF has also been evaluated for both cascade analysis ($m_s/m_p = 0$) and noncascade analysis

$(m_s/m_p = 0.1\%, 1\%)$.

The NCF for first-passage failure (Q) of secondary response can be evaluated from eq. 2.50 (or fig. 2.2). The two u/σ_u values which have been considered are 3 and 4. Note that u is the displacement of the secondary system and σ_u is the RMS value. For tuning, fig. 5.16 shows the Q values plotted versus the RMS ductility (σ_x/Y) of the nonlinear primary system. Each Q value shown corresponds to the local extreme value of $COE(u)$ achieved at P-S tuning. In general the value of ω_s/ω_p giving this tuning is different for each σ_x/Y value. These tuning values of ω_s/ω_p are given in parentheses adjacent to selected data points on the figures. Fig. 5.17 illustrates the NCF of the first-passage failure in the asymptotic region for which the secondary displacement response becomes proportional to the primary absolute acceleration. Only cascade analysis is shown in fig. 5.17 since the mass ratio has no practical significance in this asymptotic region.

As noted earlier, and illustrated in fig. 2.2, nonnormality has a much greater effect on first-passage when the barrier level is higher. This is supported by figs. 5.16 to 5.17 in which the Q values for $u/\sigma_u = 4$ diverge from unity much more than those for $u/\sigma_u = 3$. For $u/\sigma_u = 4$ it can be seen that the NCF can be much greater than unity, indicating that neglecting nonnormality may significantly underestimate the probability of first-passage failure. In particular, Q is approximately 6 at tuning for $\alpha = 0.5$ and σ_x/Y in the range of 2 to 10. Similarly large values occur in the asymptotic frequency region for this same system. Neglecting nonnormality in these situations would clearly be unacceptable.

When $COE(u) < 0$, the NCF is less than unity. Figs. 5.16 to 5.17 show that

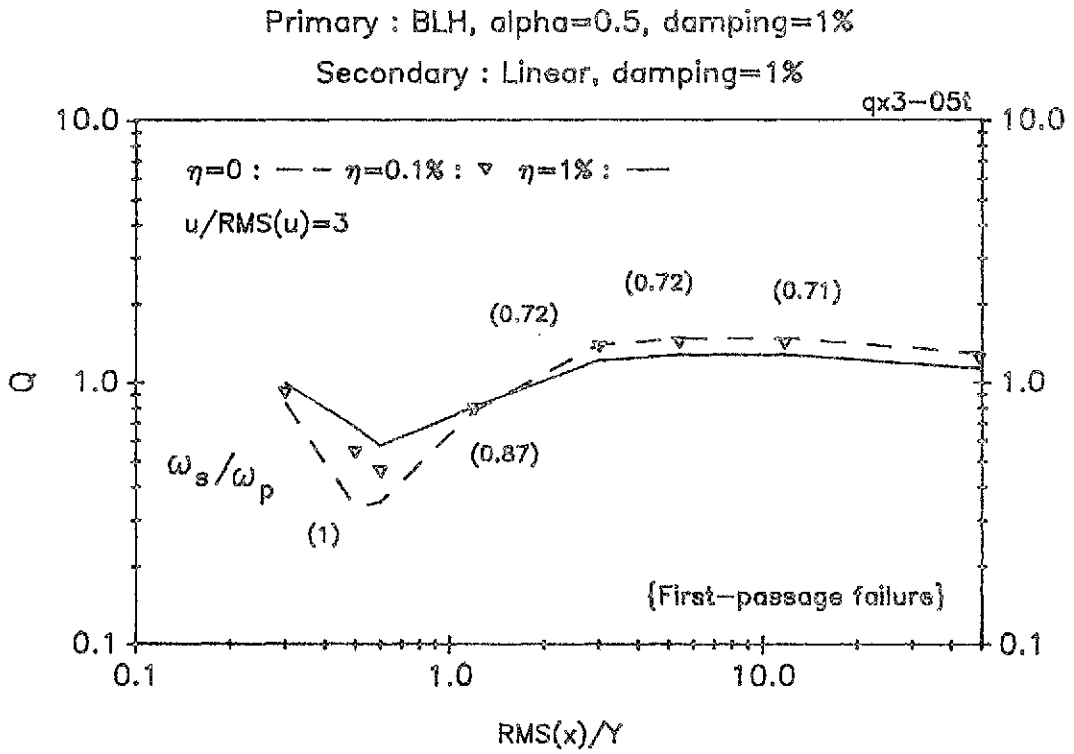

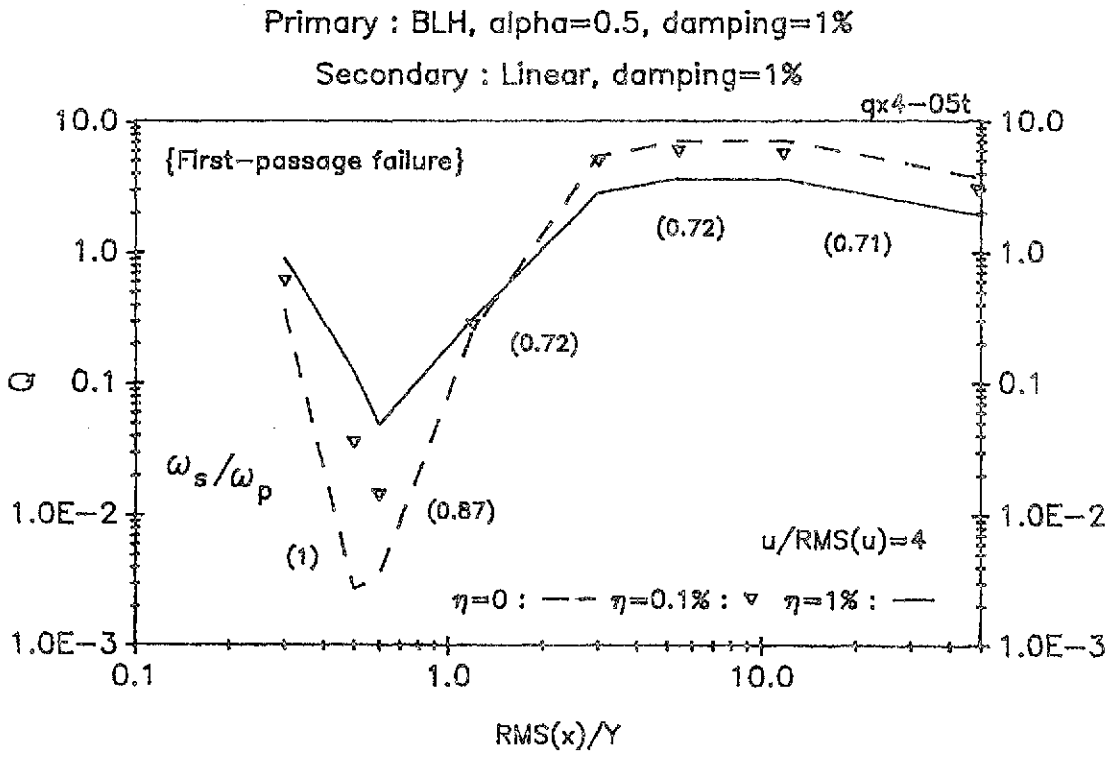

Fig. 5.16 NCF of first-passage failure at tuning for α=0.5

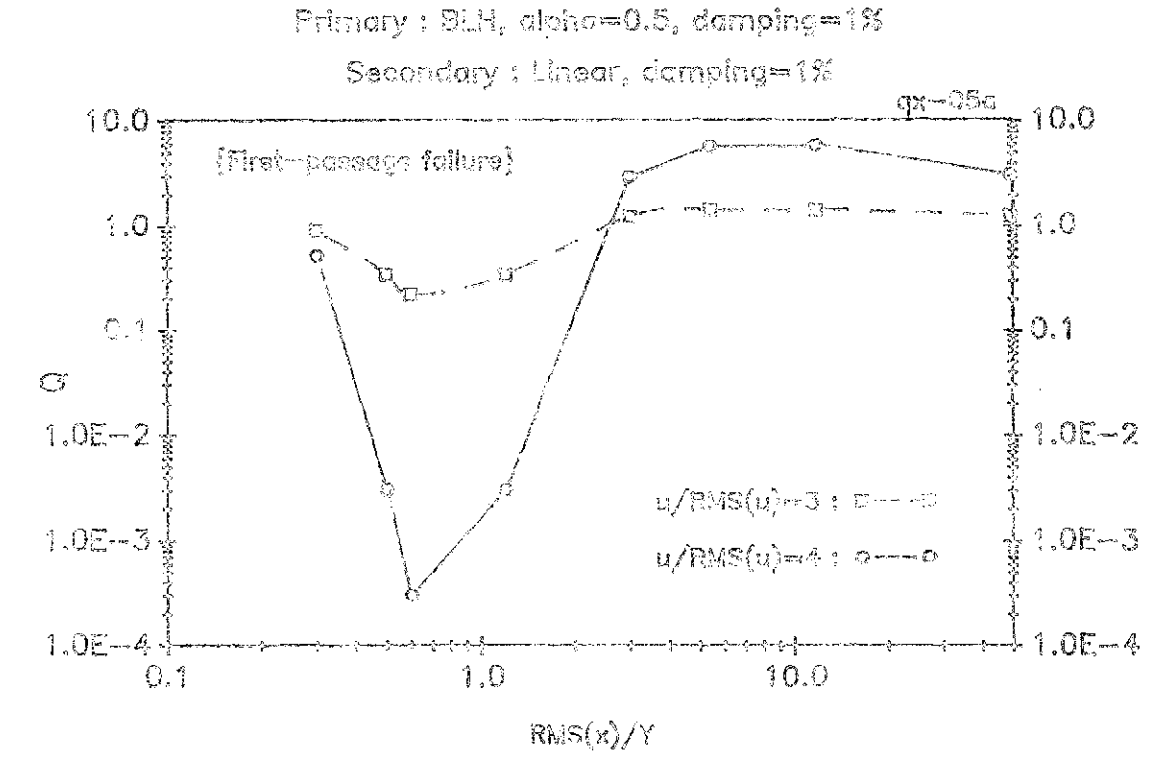

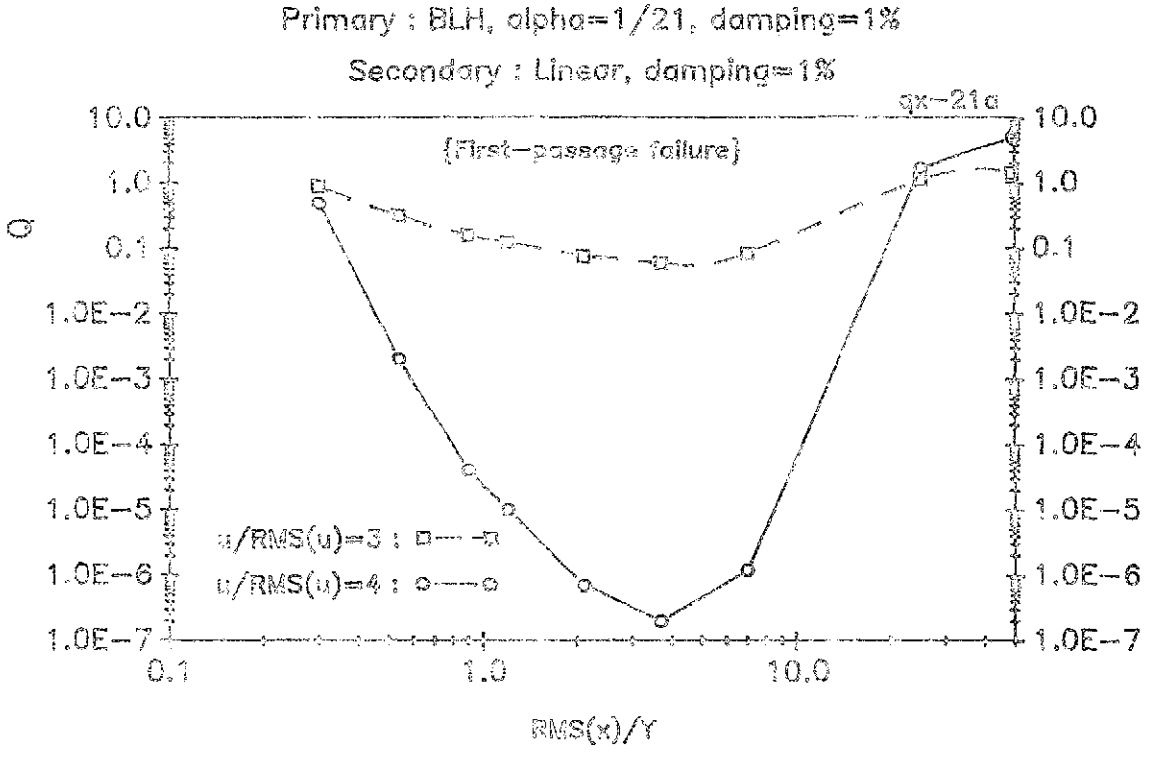

Fig. 5.17 NCF of first-passage failure at asymptotic region

these deviations are sometimes huge. For example, neglecting nonnormality for the asymptotic frequency region would underestimate the time to first passage by over 6 orders of magnitude for the system with $\alpha = 1/21$ and $\sigma_x/Y \simeq 4$. While this discrepancy is very large, it does not have as much practical significance as the Q>1 situations. For Q<1 neglecting nonnormality may sometimes cause large error, but it is a conservative procedure in that it overestimates the probability of failure.

From fig. 5.16 one notes that noncascade analysis brings the NCF values at the tuning frequency closer to unity. This, of course, is because the nonzero mass ratio reduces the nonnormality of the response of the tuned secondary, as shown in the previous section.

The NCF of fatigue failure (L) for the secondary response can be calculated from eq. 2.58 for positive COE values and eq. 2.60 for negative COE. The fatigue constant, m, have been chosen to have values of 3 and 5, in order to present results appropriate to usual welded structures. The results are presented in fig. 5.18 for tuning and in fig. 5.19 for the asymptotic region. The form of the plot is the same as in the preceding figures for Q. For $m = 3$, the L values are generally less than 1.25, indicating that it may be acceptable to neglect the nonnormality effects in this situation. However, when m becomes as large as 5, the NCF can be up to 1.75, so that the effects probably should not be ignored. It is also interesting to note that for the same degree of nonnormality, the NCF of fatigue failure (L) values seem much smaller than the NCF of first-passage failure (Q) values for the m and u/σ_u values considered. This is an indication that first-passage failure is more sensitive than fatigue failure to the probability distribution of the extreme values. Thus, consideration of nonnormality effects is more critical for first-passage failure than

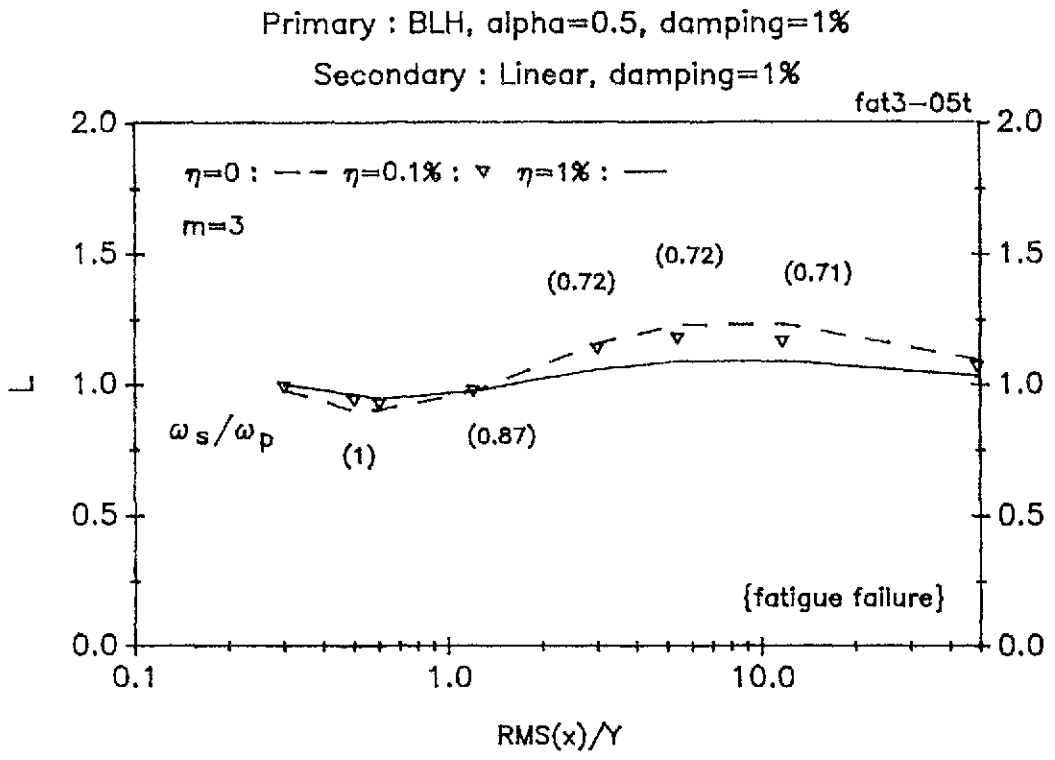

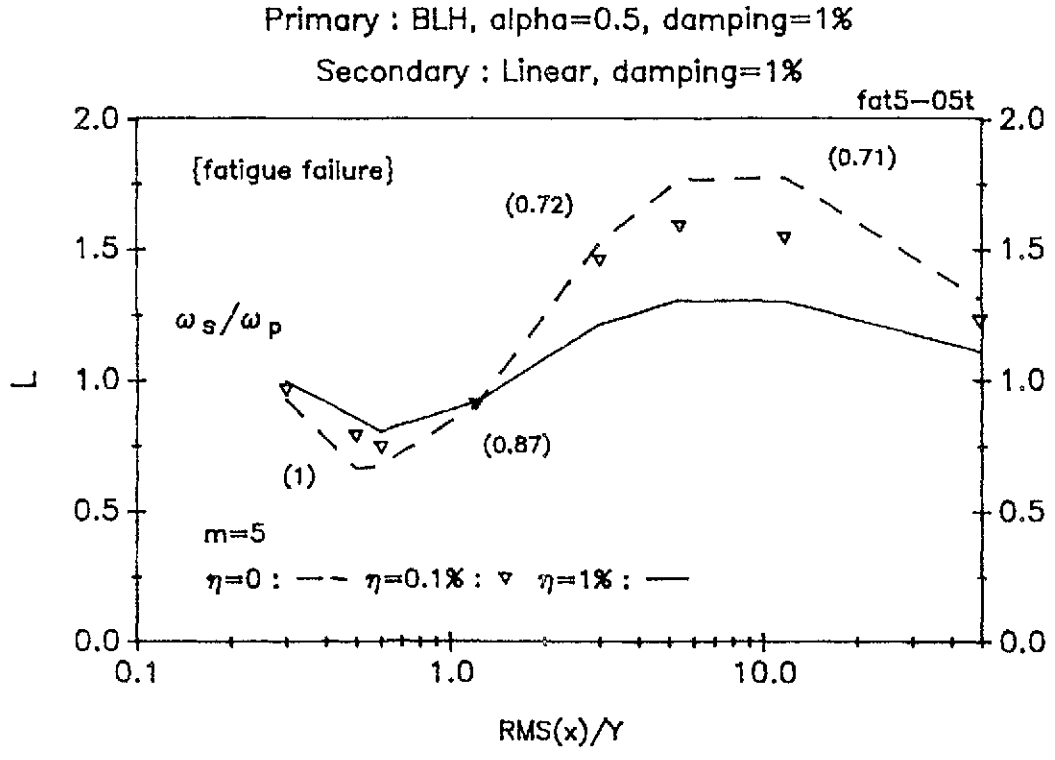

Fig. 5.18 NCF of fatigue failure at tuning for α=0.5

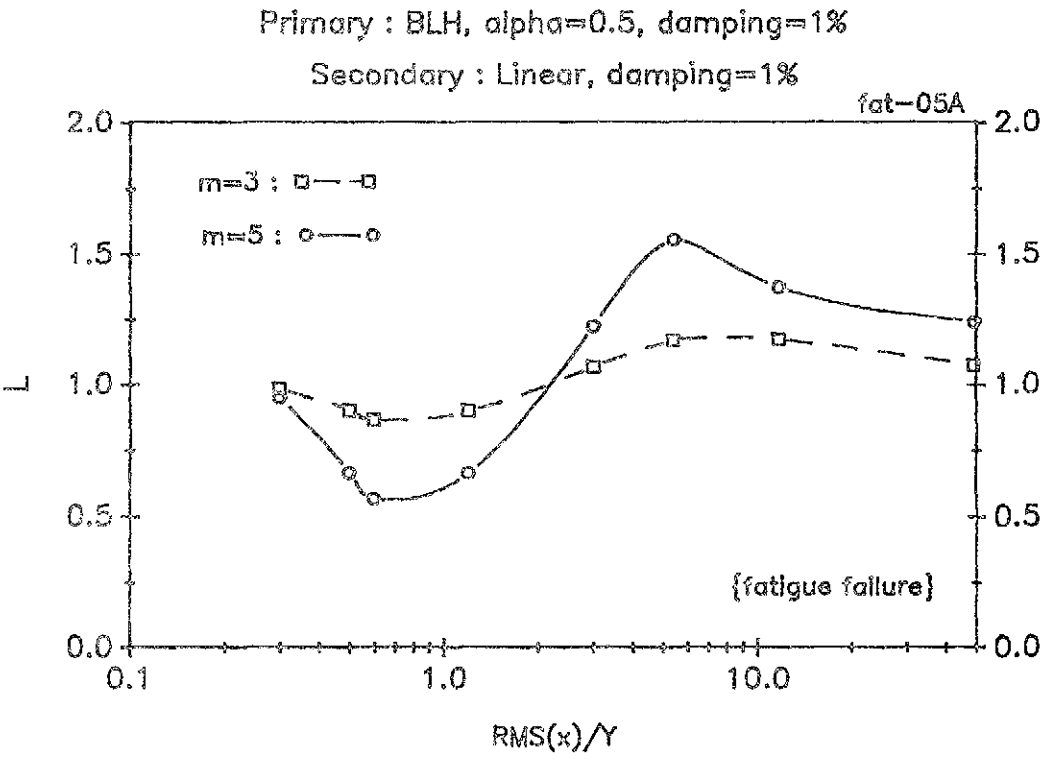

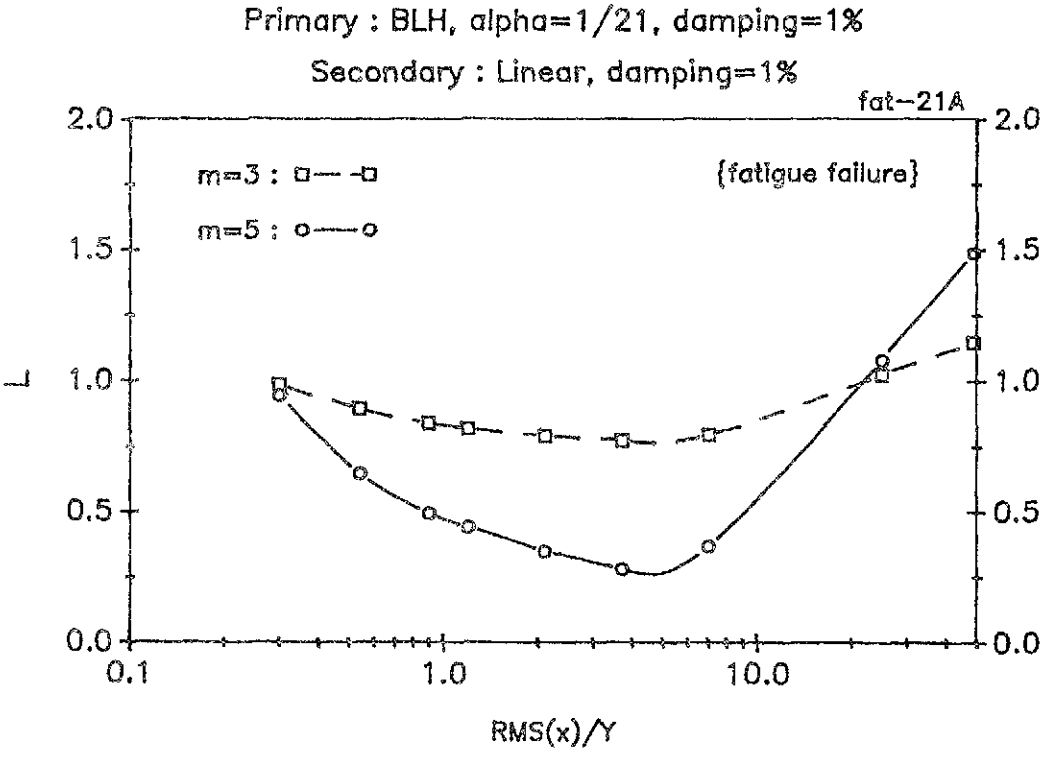

Fig. 5.19 NCF of fatigue failure at asymptotic region

for fatigue failure.

Overall, it can be seen that the NCF can be significant in some situations, indicating that reliability predictions for secondary response can be greatly in error if nonnormality is ignored. It also can be observed that if nonnormality is neglected, then the probability of failure of secondary response will generally be overestimated for small σ_x/Y values and underestimated when σ_x/Y becomes large. Fortunately the former situation will more commonly occur when the yielding takes place in the seismic response of a primary system. It may also be noted that for the same value of σ_x/Y, $\alpha = 0.5$ usually gives a larger nonnormality correction than $\alpha = 1/21$, and the difference is quite significant. In addition, it has been shown that the reliability effects of nonnormality are as large in the asymptotic region as at tuning. This is significant since secondary systems are commonly designed to operate in the asymptotic frequency region, and nonnormality effects have usually been neglected in the past.

SECTION VI

SUMMARY AND CONCLUSIONS

Some recent studies have shown that the reliability of a structure can be significantly affected by nonnormality of the stochastic structural response. This is not surprising since use of a normally distributed model may significantly misrepresent the frequency of the high response levels, which are likely to contribute to failure. Such nonnormality is particularly likely to occur in a situation involving significant nonlinearity, like the yielding effect in a hysteretic system. In this study, response nonnormality has been investigated in a system composed of a bilinear hysteretic (BLH) yielding primary structure and a linear secondary system subjected to a normally distributed ground acceleration. The secondary system is much less massive than the primary structure and it would usually represent some nonstructural elements. The behavior of secondary system is very important since they often play critical roles in maintaining the operation or safety of the primary structure in the event of extreme loads. This study has focused on nonnormality due to structural yielding in the primary system, and has considered the effects of nonnormality on the probability of failure of the secondary system.

The fourth cumulant function and the simplified, normalized form called the coefficient of excess (COE) have been used to characterize nonnormality in this study. An earlier report [Chen and Lutes 1988] considered this nonnormality for the absolute acceleration of the response of the primary system, which is the base excitation of the secondary system. This study focuses on the nonnormality of the relative displacement of the secondary system.

Numerical simulation has been used to obtain COE values for comparison with the results of various analytical methods. In order to obtain results with small statistical variation a combination of ensemble averaging and time averaging has been used. Each ensemble has contained 100 samples and each sample has contained approximately 2000 cycles of response of the primary structure

The trispectrum, which is the Fourier transform of the fourth cumulant function, has been investigated in a few situations in order to gain better understanding into the nonnormal behavior. Attention on the trispectrum has focused on the vicinity of a single line within the three dimensional frequency space, since that line has been shown to contain the dominant frequency components in at least some important situations. Furthermore, the trispectrum is real along this particular line whereas it is complex over most of the frequency space. Periodogram analysis has been used to obtain smoothed trispectra from discrete Fourier transforms of simulated time histories. This has required empirical determination of appropriate averaging schemes and development of plotting schemes to reveal the most important features of the complex and complicated trispectrum.

The analytical approaches used for calculating the nonnormal secondary response have been based on the concept of using a linear model with nonnormal excitation to replace the BLH primary element with normal excitation. The goal has been the matching of the trispectrum for primary accelerations of the substitute linear model to that of the BLH primary system. The choice of the linear filter has been based on the fitting of the power spectral density, and the nonnormal delta correlated excitation has been chosen to achieve matching of the COE of the primary acceleration. This approach called the single filter model, was eventually

extended to allow use of two different substitute primary system. In this "two filters model" the only difference was that a more narrow band filter was used to predict the fourth cumulant of the response.

Most of this study has considered cascade analysis, in which the response of the primary structure is assumed to be unaffected by the presence of the secondary system. Some study has also been given to noncascade analysis of P-S systems, using both analytical and simulation approaches. In these noncascade analysis the mass of the secondary structure has been taken as 0.1% and 1% of the primary mass ($\eta = 0.1\%$ and 1%).

Finally, the effects of nonnormality on the probability of failure of secondary systems have been studied for both first-passage failure and stochastic fatigue failure. A nonnormality correction factor (NCF), has been defined as the ratio of mean life to failure for a normal process to the mean life to failure for the nonnormal process. Analytical approaches have been used to approximate the NCF values. In most situations a Hermite moment series, based only on the first four cumulant functions, has been employed for representation of a non-Gaussian process. However, evaluating the fatigue failure for a COE value less than zero, required a different approach, so the non-Gaussian process was represented by a cruder nonlinear transformation of a Gaussian process.

Several observations and conclusions can be drawn based on the results of the above studies :

1. The response of the secondary system was nearly normal when the secondary frequency was much less than the primary frequency ($\omega_s/\omega_p << 1$). The

secondary COE was the same as that of the primary response acceleration when $\omega_s/\omega_p >> 1$ (called the asymptotic frequency region). In addition the secondary COE had a "tuning peak" when ω_s approximated the resonant frequency of the primary structure. The single filter model accurately approximated the COE in the low frequency and asymptotic frequency region, but completely failed to predict the tuning peak of the COE.

2. The two filters model gives quite good estimates for the COE of secondary response in most frequency regions. In particular, the empirical tuning peaks of the COE can be adequately approximated by proper choice of the bandwidth ratio. The optimal bandwidth ratio varies from 2 to 3 for the cases studies here. Using a single bandwidth ratio of $B_r = 2.5$ may be acceptable for many purposes, but sometimes gives significant errors.
3. The trispectrum of the primary acceleration is somewhat different from that of a linear system with delta correlated excitation. Based on the periodogram analysis, the trispectrum has a dominant peak at the expected location $(\omega_r, -\omega_r, \omega_r)$ but also has a nearby "donut" shaped region having a trispectrum of the opposite sign. This unexpected region of the opposite sign precludes the possibility of accurately fitting the entire secondary COE curve by any linear substitute model of the type used here. The two filters model gives reasonably good matching of the dominant peak of the trispectrum.
4. The two filters model somewhat mispredicts the COE of secondary response in an intermediate frequency range between the tuning and the asymptotic regions. This discrepancy is due to the "opposite sign" portion of the trispectrum, and is inevitable for any linear system. Fortunately, the linear system estimate is always on the conservative side for positive COE values of

secondary response, and also the largest COE values usually occur either at tuning or in the asymptotic region. Thus, the discrepancy for the intermediate frequencies may not be a problem for practical applications.

5. The interaction forces in noncascade analysis can significantly reduce the nonnormality of secondary response, especially at tuning. At other frequencies, the interaction effects are relatively small and can be neglected. The reduction of the COE of secondary response can be up to 100% for a 1% mass ratio at some tuning frequencies. The two filters model adequately approximates this effect in general.

6. The NCF for first-passage of a level four times the RMS value can be much greater than unity, indicating that neglecting nonnormality may significantly underestimate the probability of first-passage failure. In particular, the NCF is approximately 6 both at tuning and in the asymptotic frequency region for certain parameter values. Neglecting nonnormality in these situations would be unacceptable. If the exponent (m) in the fatigue law is small as 3, then the NCF of fatigue failure of the secondary response is generally less than 1.25, indicating that it may be acceptable to neglect the nonnormality effects in this situation. However, when m becomes as large as 5, the NCF can be up to 1.75, so that the effects probably should not be ignored. The influence of nonnormality in first-passage failure generally is more significant than in fatigue failure based on the cases in this study. Consideration of nonnormality effects is more critical for first-passage failure than for fatigue failure, since first-passage failure is more sensitive than fatigue failure to the probability of the extreme values.

7. Overall, it can be seen that the NCF for failure can be significant in some

situations, indicating that reliability prediction for secondary response can be greatly in error if nonnormality is ignored. The probability of failure of secondary response will generally be overestimated for small σ_x/Y values and underestimated when σ_x/Y values become large. It may also be noted that for the same yielding level, $\alpha = 0.5$ usually gives a larger nonnormality correction than $\alpha = 1/21$, and the difference is quite significant. In addition, it has been shown that the reliability effects of nonnormality are as significant in the asymptotic region as at tuning, which is particularly pertinent since secondary systems are commonly designed to operate in the asymptotic frequency region and the nonnormality effects have usually been neglected in the past.

REFERENCES

[1] Asfura, A., and Der Kiureghian, A., "Floor Response Spectrum Method for Seismic Analysis of Multiply Supported Systems,"*Earthquake Engineering and Structural Dynamics*, Vol. 14, 1986, pp. 245-265.

[2] Brillinger, D. R. and Rosenblatt, M., "Asymptotic Theory of k-Th Order Spectra," *Spectral Analysis of Time Series*, Ed. B. Harris, Wiley, New York, 1967a.

[3] Brillinger, D. R. and Rosenblatt, M., "Computation and Interpretation of k-Th Order Spectra," *Spectral Analysis of Time Series*, Ed. B. Harris, Wiley, New York, 1967b.

[4] Brinkmann, C. R., "Stochastic Dynamics of Yielding Two-story Frames," Master of Science thesis submitted to Rice University, 1980.

[5] Caughey, T. K., "Response of Nonlinear String to Random Loading ", *Journal of Applied Mechanics*, Vol. 26, 1959, pp. 341-344.

[6] Caughey, T. K., "Random Excitation of a System with Bilinear Hysteresis", *Journal of Applied Mechanics*, ASCE, Dec. 1960.

[7] Chen, D. C. K., "Nonnormality in the Seismic Response of Primary-Secondary Systems ,"Ph. D. Dissertation submitted to Rice University, 1990.

[8] Chen, D. C. K. and Lutes, L. D., "Nonnormal Accelerations due to Yielding in a Primary Structure," Technical Report NCEER-88-0030, September 1988.

[9] Choi, D., Miksad, R., Powers, E. and Fischer, F., "Application of Digital Cross-Bispectral Analysis Techniques to Model the Non-Linear Response of a Moored Vessel System in Random Seas," *Journal of Sound and Vibration*, Vol. 99(3), pp. 309-326, 1985.

[10] Cooley, J.W. and Tukey, J.W., "An Algorithm for the Machine Calculation of Complex Fourier Series ", *Mathematics of Computation*, Vol. 19, 1965, pp. 297-301.

[11] Crandall, S. H., "First-Crossing Probabilities of the Linear Oscillator," *Journal of Sound Vibration*, Vol. 12, No. 3, 1970.

[12] Crandall, S. H. and Mark, W. D., *Random Vibration in Mechanical Systems*, Academic Press, New York, 1963.

[13] Der Kiureghian, A., Sackman, J. L. and Nour-Omid, B., "Dynamic Analysis of Light Equipment in Structures: Response to Stochastic Input ," *Journal of Engineering Mechanics*, ASCE, Vol. 109, No. EM1, Feb. 1983, pp. 90-110.

[14] Grigoriu, M., "Crossing of Non-Gaussian Translation Processes," *Journal of Engineering Mechanics*, ASCE, Vol. 110, No. 4, April, 1984.

[15] Hasselman, K., Munk. W. and MacDonald, G., "Bispectrum of Ocean Waves", in *Time Series Analysis* (Ed. M. Rosenblatt), pp. 125-139, Wiley, New York, 1963.

[16] HoLung, J. A., Cai, J. and Lin, Y. K., "Frequency Response of Secondary Systems Under Seismic Excitation,"Technical Report NCEER-87-0013, 1987

[17] Hseih, J., "Higher Order Equivalent Linearization in Random Vibration," Master of Science thesis submitted to Rice University, 1979.

[18] Hu, S-L, "Fatigue Analysis for Non-Normal Stochastic Stress," Master of Science thesis submitted to Rice University, 1982.

[19] Igusa, T. and Der Kiureghian, A., "Dynamic Response of Multiply Supported Secondary Systems," *Journal of Engineering Mechanics*, ASCE, Vol. 111, No. 1, January 1985, pp. 20-41.

[20] IMSL Inc., The IMSL Library User's Manual, Version 2.0, April 1987.

[21] Iwan, W. D. and Lutes, L. D., "Response of the Bilinear Hysteretic System to Stationary Random Excitation," *The Journal of the Acoustical Society of America*, Vol. 43, No. 3, pp.545 - 552, March 1968.

[22] Kelly, J. M. and Sackman, J. L., "Response Spectra Design Methods for Tuned Equipment-Structure Systems," *Journal of Sound and Vibration*, 59(2), 1978, pp. 171 - 179.

[23] Krylov, N. and Bogoliubov N. *Introduction to Nonlinear Mechanics* , Kiev, 1931. English Translation, Princeton University Press, Princeton, New Jersey, 1943.

[24] Lin, Y. K., *Probabilistic Theory of Structural Dynamics*, Krieger, R.E., New York, 1976.

[25] Lin, J. and Mahin, S. A., "Seismic Response of Light Subsystems on Inelastic Structures," *Journal of Structural Engineering, ASCE*, February 1985, 111(2), pp.400-417.

[26] Lutes, L. D., "Approximate Technique for Treating Random Vibration of Hysteretic Systems," *The Journal of the Acoustical Society of Amercia*, Vol. 48, No. 1, pp.299 - 306, July, 1970.

[27] Lutes, L. D., Corazao, M., Hu, S-L, and Zimmerman, J. "Stochastic Fatigue Damage Analysis," *Journal of Structural Engineering*, ASCE, Vol. 110, No. 11, pp. 2585 - 2601, 1984.

[28] Lutes, L. D., and Hu, S-L, "Non-Normal Stochastic Response of Linear Systems,"*Journal of Engineering Mechanics*, ASCE, Vol. 112, No. 2, February, 1986.

[29] Lutes, L. D., and Jan, T. S., "Stochastic Response of Yielding Multistory Structures,"*Journal of Engineering Mechanics*, ASCE, Vol. 109, No. 6, December, 1983.

[30] Newmark, N. M., "Earthquake Response Analysis of Reactor Structures", *Nuclear Engineering and Design*, Vol. 20, No.2, 1972, pp. 303-322.

[31] Priestley, M. B., *Non-Linear and Non-Stationary Time Series Analysis,* Academic Press, 1988.

[32] Priestley, M. B., *Spectral Analysis and Time Series,* Volume I, Academic Press, 1981.

[33] Rice, S. O., *Mathematical Analysis of Random Noise,* in *Selected Papers on Noise and Stochastic Processes*, Edited by Wax, N., Dover, New York, 1954.

[34] Sackman, J. L. and Kelly, J. M.,"Seismic Analysis of Internal Equipment and Components in Structures," *Engineering Structures*, Vol. 1, July 1979.

[35] Scanlan, R. H. and Sachs, K., "Development of Compatible Secondary Spectra Without Time Histories," Proceedings of SMiRT-4 Conference, San Francisco, CA, paper K413, Aug. 1977.

[36] Schuster, A. "On the investigation of Hidden Periodicities with Application to a Supposed 26-day Period of Meteorological Phenomena," Terr. Mag. Atmos. Elect. Vol. 3, 1898.

[37] Shinozuka, M., "Applications of Digital Simulation of Gaussian Random Processes,"in *Random Excitation of Structures by Earthquakes and Atmospheric Turbulence*, Edited by H. Parkus, Springer-Verlag, 1977.

[38] Singh, M., "Seismic Design Input for Secondary System,"*Journal of the Structural Division*, ASCE, Vol. 106, No. ST2, Feb. 1980.

[39] Spanos, P-T. D. and Iwan, W. D., "On the Existence and Uniqueness of Solutions Generated by Equivalent Linearization,"*International Journal of Nonlinear Mechanics*, Vol. 13, No. 2, 1978, pp. 71-78

[40] Stratonovich, R. L., *Topics in the Theory of Random Noise*, Revised English edition, Gordon and Breach, New York, 1963.

[41] Suarez, L. E. and Singh, M. P., "Floor Spectra with Equipment-Structure-Equipment Interaction Effects," *Journal of Engineering Mechanics, ASCE*, Vol. 115, No. 2, Feb. 1989.

[42] Subba Rao, T. and Gabr, M. M., *An Introduction to Bispectral Analysis and Bilinear Time Series Models*, Springer-Verlag, Berlin, 1984.

[43] US Nuclear Regulatory Commission, Design Response Spectra for Nuclear Power Plants, Nuclear Regulatory Guide No. 1.60, Washington DC, 1975.

[44] Winterstein, S. R., "Non-Normal Responses and Fatigue Damage," *Journal of Engineering Mechanics*, ASCE, Vol. 111, No. 10, Oct. 1985.

[45] Winterstein, S. R., "Nonlinear Vibration Models for Extremes and Fatigue," *Journal of Engineering Mechanics*, ASCE, Vol. 114, No. 10, October, 1988.

APPENDIX A

LINEAR SUBSTITUTE PRIMARY SYSTEM

The equation of motion of a second order linear system subjected to a ground acceleration can be written as :

$$\ddot{x} + 2\beta\omega_1\dot{x} + \omega_1^2 x = -\ddot{y} \tag{A.1}$$

The transfer function of the absolute acceleration ($\ddot{z} = \ddot{x} - \ddot{y}$) can be derived from the relationships:

$$-(\ddot{x} + \ddot{y}) = 2\beta\omega_1\dot{x} + \omega_1^2 x$$

which gives

$$\begin{aligned} H_{\ddot{z}}(\omega) &= -H_x(\omega)(2\beta\omega_1(i\omega) + \omega_1^2) \\ &= \frac{-(\omega_1^2 + 2\beta\omega_1\omega i)}{(\omega_1^2 - \omega^2) + 2\beta\omega_1\omega i} \end{aligned} \tag{A.2}$$

If the excitation is delta correlated and S_0 is its constant power spectral density, then the power spectral density of absolute acceleration can be obtained as

$$S_{\ddot{z}}(\omega) = S_0|H_{\ddot{z}}(\omega)|^2 \tag{A.3}$$

The mean square response for absolute acceleration of this second order linear system has been found by Crandall and Mark [1963] as

$$\sigma_{\ddot{z}}^2 = \frac{\pi}{2}\frac{S_0\omega_1}{\beta}(1 + 4\beta^2) \tag{A.4}$$

Hence, the damping ratio which will cause matching of a given $\sigma_{\ddot{z}}$ value can be obtained from a second order algebraic equation :

$$4\beta^2 - b\beta + 1 = 0 \tag{A.5}$$

where

$$b = [\frac{\sigma_{\ddot{z}}}{\omega_0^2 Y}]^2 (\frac{\omega_0}{\omega_1})(\frac{4}{\pi})(\frac{Y}{N})^2$$

Note that ω_0 is the unyielded, undamped natural frequency of the BLH system, and Y/N is the yielding level. This gives

$$\beta = \frac{b \pm \sqrt{b^2 - 16}}{8} \tag{A.6}$$

One choice of the parameters which is valuable in the current study is to simultaneously match mean square velocity and acceleration of the second order linear system to those of the BLH system. A simple solution which gives a good approximation of this matching is to use

$$\frac{\omega_1}{\omega_0} = \frac{\sigma_{\ddot{z}}}{\sigma_{\dot{z}}} \tag{A.7}$$

and determine β from eq. A.6. The power spectral density for response absolute acceleration can be evaluated from eq. A.3 once the parameters of the second order linear system have been determined.

NATIONAL CENTER FOR EARTHQUAKE ENGINEERING RESEARCH
LIST OF PUBLISHED TECHNICAL REPORTS

The National Center for Earthquake Engineering Research (NCEER) publishes technical reports on a variety of subjects related to earthquake engineering written by authors funded through NCEER. These reports are available from both NCEER's Publications Department and the National Technical Information Service (NTIS). Requests for reports should be directed to the Publications Department, National Center for Earthquake Engineering Research, State University of New York at Buffalo, Red Jacket Quadrangle, Buffalo, New York 14261. Reports can also be requested through NTIS, 5285 Port Royal Road, Springfield, Virginia 22161. NTIS accession numbers are shown in parenthesis, if available.

NCEER-87-0001 "First-Year Program in Research, Education and Technology Transfer," 3/5/87, (PB88-134275/AS).

NCEER-87-0002 "Experimental Evaluation of Instantaneous Optimal Algorithms for Structural Control," by R.C. Lin, T.T. Soong and A.M. Reinhorn, 4/20/87, (PB88-134341/AS).

NCEER-87-0003 "Experimentation Using the Earthquake Simulation Facilities at University at Buffalo," by A.M. Reinhorn and R.L. Ketter, to be published.

NCEER-87-0004 "The System Characteristics and Performance of a Shaking Table," by J.S. Hwang, K.C. Chang and G.C. Lee, 6/1/87, (PB88-134259/AS). This report is available only through NTIS (see address given above).

NCEER-87-0005 "A Finite Element Formulation for Nonlinear Viscoplastic Material Using a Q Model," by O. Gyebi and G. Dasgupta, 11/2/87, (PB88-213764/AS).

NCEER-87-0006 "Symbolic Manipulation Program (SMP) - Algebraic Codes for Two and Three Dimensional Finite Element Formulations," by X. Lee and G. Dasgupta, 11/9/87, (PB88-219522/AS).

NCEER-87-0007 "Instantaneous Optimal Control Laws for Tall Buildings Under Seismic Excitations," by J.N. Yang, A. Akbarpour and P. Ghaemmaghami, 6/10/87, (PB88-134333/AS).

NCEER-87-0008 "IDARC: Inelastic Damage Analysis of Reinforced Concrete Frame - Shear-Wall Structures," by Y.J. Park, A.M. Reinhorn and S.K. Kunnath, 7/20/87, (PB88-134325/AS).

NCEER-87-0009 "Liquefaction Potential for New York State: A Preliminary Report on Sites in Manhattan and Buffalo," by M. Budhu, V. Vijayakumar, R.F. Giese and L. Baumgras, 8/31/87, (PB88-163704/AS). This report is available only through NTIS (see address given above).

NCEER-87-0010 "Vertical and Torsional Vibration of Foundations in Inhomogeneous Media," by A.S. Veletsos and K.W. Dotson, 6/1/87, (PB88-134291/AS).

NCEER-87-0011 "Seismic Probabilistic Risk Assessment and Seismic Margins Studies for Nuclear Power Plants," by Howard H.M. Hwang, 6/15/87, (PB88-134267/AS).

NCEER-87-0012 "Parametric Studies of Frequency Response of Secondary Systems Under Ground-Acceleration Excitations," by Y. Yong and Y.K. Lin, 6/10/87, (PB88-134309/AS).

NCEER-87-0013 "Frequency Response of Secondary Systems Under Seismic Excitation," by J.A. HoLung, J. Cai and Y.K. Lin, 7/31/87, (PB88-134317/AS).

NCEER-87-0014 "Modelling Earthquake Ground Motions in Seismically Active Regions Using Parametric Time Series Methods," by G.W. Ellis and A.S. Cakmak, 8/25/87, (PB88-134283/AS).

NCEER-87-0015 "Detection and Assessment of Seismic Structural Damage," by E. DiPasquale and A.S. Cakmak, 8/25/87, (PB88-163712/AS).

NCEER-87-0016 "Pipeline Experiment at Parkfield, California," by J. Isenberg and E. Richardson, 9/15/87, (PB88-163720/AS). This report is available only through NTIS (see address given above).

NCEER-87-0017 "Digital Simulation of Seismic Ground Motion," by M. Shinozuka, G. Deodatis and T. Harada, 8/31/87, (PB88-155197/AS). This report is available only through NTIS (see address given above).

NCEER-87-0018 "Practical Considerations for Structural Control: System Uncertainty, System Time Delay and Truncation of Small Control Forces," J.N. Yang and A. Akbarpour, 8/10/87, (PB88-163738/AS).

NCEER-87-0019 "Modal Analysis of Nonclassically Damped Structural Systems Using Canonical Transformation," by J.N. Yang, S. Sarkani and F.X. Long, 9/27/87, (PB88-187851/AS).

NCEER-87-0020 "A Nonstationary Solution in Random Vibration Theory," by J.R. Red-Horse and P.D. Spanos, 11/3/87, (PB88-163746/AS).

NCEER-87-0021 "Horizontal Impedances for Radially Inhomogeneous Viscoelastic Soil Layers," by A.S. Veletsos and K.W. Dotson, 10/15/87, (PB88-150859/AS).

NCEER-87-0022 "Seismic Damage Assessment of Reinforced Concrete Members," by Y.S. Chung, C. Meyer and M. Shinozuka, 10/9/87, (PB88-150867/AS). This report is available only through NTIS (see address given above).

NCEER-87-0023 "Active Structural Control in Civil Engineering," by T.T. Soong, 11/11/87, (PB88-187778/AS).

NCEER-87-0024 Vertical and Torsional Impedances for Radially Inhomogeneous Viscoelastic Soil Layers," by K.W. Dotson and A.S. Veletsos, 12/87, (PB88-187786/AS).

NCEER-87-0025 "Proceedings from the Symposium on Seismic Hazards, Ground Motions, Soil-Liquefaction and Engineering Practice in Eastern North America," October 20-22, 1987, edited by K.H. Jacob, 12/87, (PB88-188115/AS).

NCEER-87-0026 "Report on the Whittier-Narrows, California, Earthquake of October 1, 1987," by J. Pantelic and A. Reinhorn, 11/87, (PB88-187752/AS). This report is available only through NTIS (see address given above).

NCEER-87-0027 "Design of a Modular Program for Transient Nonlinear Analysis of Large 3-D Building Structures," by S. Srivastav and J.F. Abel, 12/30/87, (PB88-187950/AS).

NCEER-87-0028 "Second-Year Program in Research, Education and Technology Transfer," 3/8/88, (PB88-219480/AS).

NCEER-88-0001 "Workshop on Seismic Computer Analysis and Design of Buildings With Interactive Graphics," by W. McGuire, J.F. Abel and C.H. Conley, 1/18/88, (PB88-187760/AS).

NCEER-88-0002 "Optimal Control of Nonlinear Flexible Structures," by J.N. Yang, F.X. Long and D. Wong, 1/22/88, (PB88-213772/AS).

NCEER-88-0003 "Substructuring Techniques in the Time Domain for Primary-Secondary Structural Systems," by G.D. Manolis and G. Juhn, 2/10/88, (PB88-213780/AS).

NCEER-88-0004 "Iterative Seismic Analysis of Primary-Secondary Systems," by A. Singhal, L.D. Lutes and P.D. Spanos, 2/23/88, (PB88-213798/AS).

NCEER-88-0005 "Stochastic Finite Element Expansion for Random Media," by P.D. Spanos and R. Ghanem, 3/14/88, (PB88-213806/AS).

NCEER-88-0006 "Combining Structural Optimization and Structural Control," by F.Y. Cheng and C.P. Pantelides, 1/10/88, (PB88-213814/AS).

NCEER-88-0007 "Seismic Performance Assessment of Code-Designed Structures," by H.H-M. Hwang, J-W. Jaw and H-J. Shau, 3/20/88, (PB88-219423/AS).

NCEER-88-0008 "Reliability Analysis of Code-Designed Structures Under Natural Hazards," by H.H-M. Hwang, H. Ushiba and M. Shinozuka, 2/29/88, (PB88-229471/AS).

NCEER-88-0009 "Seismic Fragility Analysis of Shear Wall Structures," by J-W Jaw and H.H-M. Hwang, 4/30/88, (PB89-102867/AS).

NCEER-88-0010 "Base Isolation of a Multi-Story Building Under a Harmonic Ground Motion - A Comparison of Performances of Various Systems," by F-G Fan, G. Ahmadi and I.G. Tadjbakhsh, 5/18/88, (PB89-122238/AS).

NCEER-88-0011 "Seismic Floor Response Spectra for a Combined System by Green's Functions," by F.M. Lavelle, L.A. Bergman and P.D. Spanos, 5/1/88, (PB89-102875/AS).

NCEER-88-0012 "A New Solution Technique for Randomly Excited Hysteretic Structures," by G.Q. Cai and Y.K. Lin, 5/16/88, (PB89-102883/AS).

NCEER-88-0013 "A Study of Radiation Damping and Soil-Structure Interaction Effects in the Centrifuge," by K. Weissman, supervised by J.H. Prevost, 5/24/88, (PB89-144703/AS).

NCEER-88-0014 "Parameter Identification and Implementation of a Kinematic Plasticity Model for Frictional Soils," by J.H. Prevost and D.V. Griffiths, to be published.

NCEER-88-0015 "Two- and Three- Dimensional Dynamic Finite Element Analyses of the Long Valley Dam," by D.V. Griffiths and J.H. Prevost, 6/17/88, (PB89-144711/AS).

NCEER-88-0016 "Damage Assessment of Reinforced Concrete Structures in Eastern United States," by A.M. Reinhorn, M.J. Seidel, S.K. Kunnath and Y.J. Park, 6/15/88, (PB89-122220/AS).

NCEER-88-0017 "Dynamic Compliance of Vertically Loaded Strip Foundations in Multilayered Viscoelastic Soils," by S. Ahmad and A.S.M. Israil, 6/17/88, (PB89-102891/AS).

NCEER-88-0018 "An Experimental Study of Seismic Structural Response With Added Viscoelastic Dampers," by R.C. Lin, Z. Liang, T.T. Soong and R.H. Zhang, 6/30/88, (PB89-122212/AS).

NCEER-88-0019 "Experimental Investigation of Primary - Secondary System Interaction," by G.D. Manolis, G. Juhn and A.M. Reinhorn, 5/27/88, (PB89-122204/AS).

NCEER-88-0020 "A Response Spectrum Approach For Analysis of Nonclassically Damped Structures," by J.N. Yang, S. Sarkani and F.X. Long, 4/22/88, (PB89-102909/AS).

NCEER-88-0021 "Seismic Interaction of Structures and Soils: Stochastic Approach," by A.S. Veletsos and A.M. Prasad, 7/21/88, (PB89-122196/AS).

NCEER-88-0022 "Identification of the Serviceability Limit State and Detection of Seismic Structural Damage," by E. DiPasquale and A.S. Cakmak, 6/15/88, (PB89-122188/AS).

NCEER-88-0023 "Multi-Hazard Risk Analysis: Case of a Simple Offshore Structure," by B.K. Bhartia and E.H. Vanmarcke, 7/21/88, (PB89-145213/AS).

NCEER-88-0024 "Automated Seismic Design of Reinforced Concrete Buildings," by Y.S. Chung, C. Meyer and M. Shinozuka, 7/5/88, (PB89-122170/AS).

NCEER-88-0025 "Experimental Study of Active Control of MDOF Structures Under Seismic Excitations," by L.L. Chung, R.C. Lin, T.T. Soong and A.M. Reinhorn, 7/10/88, (PB89-122600/AS).

NCEER-88-0026 "Earthquake Simulation Tests of a Low-Rise Metal Structure," by J.S. Hwang, K.C. Chang, G.C. Lee and R.L. Ketter, 8/1/88, (PB89-102917/AS).

NCEER-88-0027 "Systems Study of Urban Response and Reconstruction Due to Catastrophic Earthquakes," by F. Kozin and H.K. Zhou, 9/22/88, (PB90-162348/AS).

NCEER-88-0028 "Seismic Fragility Analysis of Plane Frame Structures," by H.H-M. Hwang and Y.K. Low, 7/31/88, (PB89-131445/AS).

NCEER-88-0029 "Response Analysis of Stochastic Structures," by A. Kardara, C. Bucher and M. Shinozuka, 9/22/88, (PB89-174429/AS).

NCEER-88-0030 "Nonnormal Accelerations Due to Yielding in a Primary Structure," by D.C.K. Chen and L.D. Lutes, 9/19/88, (PB89-131437/AS).

NCEER-88-0031 "Design Approaches for Soil-Structure Interaction," by A.S. Veletsos, A.M. Prasad and Y. Tang, 12/30/88, (PB89-174437/AS).

NCEER-88-0032 "A Re-evaluation of Design Spectra for Seismic Damage Control," by C.J. Turkstra and A.G. Tallin, 11/7/88, (PB89-145221/AS).

NCEER-88-0033 "The Behavior and Design of Noncontact Lap Splices Subjected to Repeated Inelastic Tensile Loading," by V.E. Sagan, P. Gergely and R.N. White, 12/8/88, (PB89-163737/AS).

NCEER-88-0034 "Seismic Response of Pile Foundations," by S.M. Mamoon, P.K. Banerjee and S. Ahmad, 11/1/88, (PB89-145239/AS).

NCEER-88-0035 "Modeling of R/C Building Structures With Flexible Floor Diaphragms (IDARC2)," by A.M. Reinhorn, S.K. Kunnath and N. Panahshahi, 9/7/88, (PB89-207153/AS).

NCEER-88-0036 "Solution of the Dam-Reservoir Interaction Problem Using a Combination of FEM, BEM with Particular Integrals, Modal Analysis, and Substructuring," by C-S. Tsai, G.C. Lee and R.L. Ketter, 12/31/88, (PB89-207146/AS).

NCEER-88-0037 "Optimal Placement of Actuators for Structural Control," by F.Y. Cheng and C.P. Pantelides, 8/15/88, (PB89-162846/AS).

NCEER-88-0038 "Teflon Bearings in Aseismic Base Isolation: Experimental Studies and Mathematical Modeling," by A. Mokha, M.C. Constantinou and A.M. Reinhorn, 12/5/88, (PB89-218457/AS).

NCEER-88-0039 "Seismic Behavior of Flat Slab High-Rise Buildings in the New York City Area," by P. Weidlinger and M. Ettouney, 10/15/88, (PB90-145681/AS).

NCEER-88-0040 "Evaluation of the Earthquake Resistance of Existing Buildings in New York City," by P. Weidlinger and M. Ettouney, 10/15/88, to be published.

NCEER-88-0041 "Small-Scale Modeling Techniques for Reinforced Concrete Structures Subjected to Seismic Loads," by W. Kim, A. El-Attar and R.N. White, 11/22/88, (PB89-189625/AS).

NCEER-88-0042 "Modeling Strong Ground Motion from Multiple Event Earthquakes," by G.W. Ellis and A.S. Cakmak, 10/15/88, (PB89-174445/AS).

NCEER-88-0043 "Nonstationary Models of Seismic Ground Acceleration," by M. Grigoriu, S.E. Ruiz and E. Rosenblueth, 7/15/88, (PB89-189617/AS).

NCEER-88-0044 "SARCF User's Guide: Seismic Analysis of Reinforced Concrete Frames," by Y.S. Chung, C. Meyer and M. Shinozuka, 11/9/88, (PB89-174452/AS).

NCEER-88-0045 "First Expert Panel Meeting on Disaster Research and Planning," edited by J. Pantelic and J. Stoyle, 9/15/88, (PB89-174460/AS).

NCEER-88-0046 "Preliminary Studies of the Effect of Degrading Infill Walls on the Nonlinear Seismic Response of Steel Frames," by C.Z. Chrysostomou, P. Gergely and J.F. Abel, 12/19/88, (PB89-208383/AS).

NCEER-88-0047 "Reinforced Concrete Frame Component Testing Facility - Design, Construction, Instrumentation and Operation," by S.P. Pessiki, C. Conley, T. Bond, P. Gergely and R.N. White, 12/16/88, (PB89-174478/AS).

NCEER-89-0001 "Effects of Protective Cushion and Soil Compliancy on the Response of Equipment Within a Seismically Excited Building," by J.A. HoLung, 2/16/89, (PB89-207179/AS).

NCEER-89-0002 "Statistical Evaluation of Response Modification Factors for Reinforced Concrete Structures," by H.H-M. Hwang and J-W. Jaw, 2/17/89, (PB89-207187/AS).

NCEER-89-0003 "Hysteretic Columns Under Random Excitation," by G-Q. Cai and Y.K. Lin, 1/9/89, (PB89-196513/AS).

NCEER-89-0004 "Experimental Study of 'Elephant Foot Bulge' Instability of Thin-Walled Metal Tanks," by Z-H. Jia and R.L. Ketter, 2/22/89, (PB89-207195/AS).

NCEER-89-0005 "Experiment on Performance of Buried Pipelines Across San Andreas Fault," by J. Isenberg, E. Richardson and T.D. O'Rourke, 3/10/89, (PB89-218440/AS).

NCEER-89-0006 "A Knowledge-Based Approach to Structural Design of Earthquake-Resistant Buildings," by M. Subramani, P. Gergely, C.H. Conley, J.F. Abel and A.H. Zaghw, 1/15/89, (PB89-218465/AS).

NCEER-89-0007 "Liquefaction Hazards and Their Effects on Buried Pipelines," by T.D. O'Rourke and P.A. Lane, 2/1/89, (PB89-218481).

NCEER-89-0008 "Fundamentals of System Identification in Structural Dynamics," by H. Imai, C-B. Yun, O. Maruyama and M. Shinozuka, 1/26/89, (PB89-207211/AS).

NCEER-89-0009 "Effects of the 1985 Michoacan Earthquake on Water Systems and Other Buried Lifelines in Mexico," by A.G. Ayala and M.J. O'Rourke, 3/8/89, (PB89-207229/AS).

NCEER-89-R010 "NCEER Bibliography of Earthquake Education Materials," by K.E.K. Ross, Second Revision, 9/1/89, (PB90-125352/AS).

NCEER-89-0011 "Inelastic Three-Dimensional Response Analysis of Reinforced Concrete Building Structures (IDARC-3D), Part I - Modeling," by S.K. Kunnath and A.M. Reinhorn, 4/17/89, (PB90-114612/AS).

NCEER-89-0012 "Recommended Modifications to ATC-14," by C.D. Poland and J.O. Malley, 4/12/89, (PB90-108648/AS).

NCEER-89-0013 "Repair and Strengthening of Beam-to-Column Connections Subjected to Earthquake Loading," by M. Corazao and A.J. Durrani, 2/28/89, (PB90-109885/AS).

NCEER-89-0014 "Program EXKAL2 for Identification of Structural Dynamic Systems," by O. Maruyama, C-B. Yun, M. Hoshiya and M. Shinozuka, 5/19/89, (PB90-109877/AS).

NCEER-89-0015 "Response of Frames With Bolted Semi-Rigid Connections, Part I - Experimental Study and Analytical Predictions," by P.J. DiCorso, A.M. Reinhorn, J.R. Dickerson, J.B. Radziminski and W.L. Harper, 6/1/89, to be published.

NCEER-89-0016 "ARMA Monte Carlo Simulation in Probabilistic Structural Analysis," by P.D. Spanos and M.P. Mignolet, 7/10/89, (PB90-109893/AS).

NCEER-89-P017 "Preliminary Proceedings from the Conference on Disaster Preparedness - The Place of Earthquake Education in Our Schools," Edited by K.E.K. Ross, 6/23/89.

NCEER-89-0017 "Proceedings from the Conference on Disaster Preparedness - The Place of Earthquake Education in Our Schools," Edited by K.E.K. Ross, 12/31/89.

NCEER-89-0018 "Multidimensional Models of Hysteretic Material Behavior for Vibration Analysis of Shape Memory Energy Absorbing Devices, by E.J. Graesser and F.A. Cozzarelli, 6/7/89, (PB90-164146/AS).

NCEER-89-0019 "Nonlinear Dynamic Analysis of Three-Dimensional Base Isolated Structures (3D-BASIS)," by S. Nagarajaiah, A.M. Reinhorn and M.C. Constantinou, 8/3/89, (PB90-161936/AS).

NCEER-89-0020 "Structural Control Considering Time-Rate of Control Forces and Control Rate Constraints," by F.Y. Cheng and C.P. Pantelides, 8/3/89, (PB90-120445/AS).

NCEER-89-0021 "Subsurface Conditions of Memphis and Shelby County," by K.W. Ng, T-S. Chang and H-H.M. Hwang, 7/26/89, (PB90-120437/AS).

NCEER-89-0022 "Seismic Wave Propagation Effects on Straight Jointed Buried Pipelines," by K. Elhmadi and M.J. O'Rourke, 8/24/89, (PB90-162322/AS).

NCEER-89-0023 "Workshop on Serviceability Analysis of Water Delivery Systems," edited by M. Grigoriu, 3/6/89, (PB90-127424/AS).

NCEER-89-0024 "Shaking Table Study of a 1/5 Scale Steel Frame Composed of Tapered Members," by K.C. Chang, J.S. Hwang and G.C. Lee, 9/18/89, (PB90-160169/AS).

NCEER-89-0025 "DYNA1D: A Computer Program for Nonlinear Seismic Site Response Analysis - Technical Documentation," by Jean H. Prevost, 9/14/89, (PB90-161944/AS).

NCEER-89-0026 "1:4 Scale Model Studies of Active Tendon Systems and Active Mass Dampers for Aseismic Protection," by A.M. Reinhorn, T.T. Soong, R.C. Lin, Y.P. Yang, Y. Fukao, H. Abe and M. Nakai, 9/15/89, (PB90-173246/AS).

NCEER-89-0027 "Scattering of Waves by Inclusions in a Nonhomogeneous Elastic Half Space Solved by Boundary Element Methods," by P.K. Hadley, A. Askar and A.S. Cakmak, 6/15/89, (PB90-145699/AS).

NCEER-89-0028 "Statistical Evaluation of Deflection Amplification Factors for Reinforced Concrete Structures," by H.H.M. Hwang, J-W. Jaw and A.L. Ch'ng, 8/31/89, (PB90-164633/AS).

NCEER-89-0029 "Bedrock Accelerations in Memphis Area Due to Large New Madrid Earthquakes," by H.H.M. Hwang, C.H.S. Chen and G. Yu, 11/7/89, (PB90-162330/AS).

NCEER-89-0030 "Seismic Behavior and Response Sensitivity of Secondary Structural Systems," by Y.Q. Chen and T.T. Soong, 10/23/89, (PB90-164658/AS).

NCEER-89-0031 "Random Vibration and Reliability Analysis of Primary-Secondary Structural Systems," by Y. Ibrahim, M. Grigoriu and T.T. Soong, 11/10/89, (PB90-161951/AS).

NCEER-89-0032 "Proceedings from the Second U.S. - Japan Workshop on Liquefaction, Large Ground Deformation and Their Effects on Lifelines, September 26-29, 1989," Edited by T.D. O'Rourke and M. Hamada, 12/1/89.

NCEER-89-0033 "Deterministic Model for Seismic Damage Evaluation of Reinforced Concrete Structures," by J.M. Bracci, A.M. Reinhorn, J.B. Mander and S.K. Kunnath, 9/27/89, to be published.

NCEER-89-0034 "On the Relation Between Local and Global Damage Indices," by E. DiPasquale and A.S. Cakmak, 8/15/89, (PB90-173865).

NCEER-89-0035 "Cyclic Undrained Behavior of Nonplastic and Low Plasticity Silts," by A.J. Walker and H.E. Stewart, 7/26/89, (PB90-183518/AS).

NCEER-89-0036 "Liquefaction Potential of Surficial Deposits in the City of Buffalo, New York," by M. Budhu, R. Giese and L. Baumgrass, 1/17/89.

NCEER-89-0037 "A Determinstic Assessment of Effects of Ground Motion Incoherence," by A.S. Veletsos and Y. Tang, 7/15/89, (PB90-164294/AS).

NCEER-89-0038 "Workshop on Ground Motion Parameters for Seismic Hazard Mapping," July 17-18, 1989, edited by R.V. Whitman, 12/1/89, (PB90-173923/AS).

NCEER-89-0039 "Seismic Effects on Elevated Transit Lines of the New York City Transit Authority," by C.J. Costantino, C.A. Miller and E. Heymsfield, 12/26/89.

NCEER-89-0040 "Centrifugal Modeling of Dynamic Soil-Structure Interaction," by K. Weissman, Supervised by J.H. Prevost, 5/10/89.

NCEER-89-0041 "Linearized Identification of Buildings With Cores for Seismic Vulnerability Assessment," by I-K. Ho and A.E. Aktan, 11/1/89.

NCEER-90-0001 "Geotechnical and Lifeline Aspects of the October 17, 1989 Loma Prieta Earthquake in San Francisco," by T.D. O'Rourke, H.E. Stewart, F.T. Blackburn and T.S. Dickerman, 1/90.

NCEER-90-0002 "Nonnormal Secondary Response Due to Yielding in a Primary Structure," by D.C.K. Chen and L.D. Lutes, 2/28/90.